ATOMKI
ANNUAL REPORT
1990

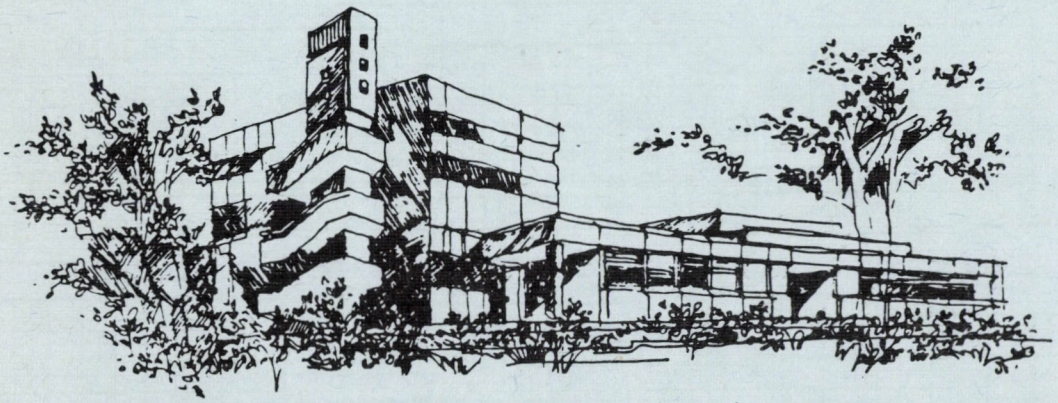

INSTITUTE OF NUCLEAR RESEARCH
OF THE HUNGARIAN ACADEMY OF SCIENCES
DEBRECEN, HUNGARY

INSTITUTE OF NUCLEAR RESEARCH
OF THE HUNGARIAN ACADEMY OF SCIENCES
DEBRECEN, HUNGARY

ANNUAL REPORT 1990

ATOMKI

Postal address:

Debrecen

P. O. Box 51
H-4001

Hungary

Edited by Z. Gácsi

HU ISSN 0231-3596

PREFACE

This report is similar to the preceding one in structure and characteristics, namely the individual contributions report on still unpublished (frequently preliminary) results. As can be seen, however, there is some change in the form of the ATOMKI Annual Report due to the development in the computerized word processing.

As regards the activity in the different research fields in ATOMKI, it is reflected fairly well in the number of individual reports in the present volume and it was not changing a lot in the last years. The number of contributions from nuclear and atomic physics amounts to about fifty percent in general, but now it is somewhat higher than the above figure. Traditionally a relatively high number of contributions come to the volume from the field of development of methods and instruments and the activity seems to be increasing on materials science and analysis, as shown by the present Annual Report.

The ECR (Electron Cyclotron Resonance Ion Source) program, which was mentioned in the last Annual Report, is still in preparation, it has not been launched yet.

At the turning of the year an important personal change happened at the head of the institute. From the 1st of January, 1991 Dr. József Pálinkás, Doctor of Physical Sciences (D.Sc.) was appointed the director of the institute by the secretary general of the Hungarian Academy of Sciences, after the expiration of the third five–year term for the preceding director (D.B.). Before the appointment the community of sciencists of the institute and independently the Division for Mathematical and Physical Sciences of the Hungarian Academy of Sciences expressed their opinion on Dr. Pálinkás' application by secret ballot according to the new procedure in this respect. Dr. Pálinkás received the overwhelming majority of the votes in both cases.

Also at this place I wish all the best to the new director. I am sure that the best traditions of this institute will be continued under the new directorship together with new initiatives and with even more outstanding results in contrary to the very difficult financial situation. When I whish the new director a similar support given to me by the scientific and the whole community of the institute, I warmly thank all the staff of the institute for the cooperation and help during my terms when I served as a director of the institute.

February 7, 1991

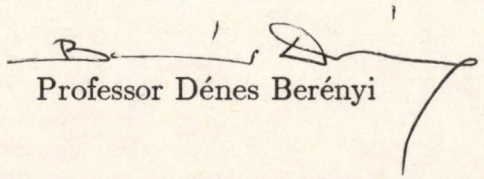

Professor Dénes Berényi

CONTENTS

PROGRESS REPORTS:

Nuclear Physics 1

Atomic Physics 49

Materials Science and Analysis 71

Earth and Cosmic Sciences, Environmental Research 90

Biological and Medical Research 95

Development of Methods and Instruments 103

PUBLICATIONS AND SEMINARS:

Papers Published in 1990 129

Conference Contributions and Talks 137

Theses Completed 147

Hebdomadal Seminars 148

Author Index 152

NUCLEAR PHYSICS

Radiative Proton Capture by the Radioactive ^{22}Ne Nucleus

S. Seuthe†, R. W. Kavanagh‡, C. Rolfs†, U. Schröder†,

W. H. Schulte†, E. Somorjai, H. P. Trautwetter†

The knowledge of reaction rates for nuclear reactions on radioactive targets is more and more important for nuclear astrophysics, considering the hot and explosive burning phases. In addition the $^{22}Na(p,\gamma)^{23}Mg$ reaction (Q=7578 keV) has a special interest connected to the so called 'Ne–E' anomaly [1].

The measurements were performed at the 4 MV Dynamitron tandem accelerator (Bochum) in the energy range of $E_p = 0.17 - 1.29 MeV$. Direct water cooled, implanted ^{22}Na–target (into Ni–backing) was used with the activity of 0.7 mCi. The implantation proved to be very important as for the background reduction.

The excitation functions were measured by a $7.6cm\varnothing \times 7.6cm$ NaI(Tl) detector (and partly a D_2O detector) with a Pb–shield of 4.6 cm. The yield curves were determined from the analysis of the NaI–spectra obtained at each proton energy. Two windows were set, one ($E_\gamma = 4.0 - 7.3 MeV$) above the triple–pile–up range from ^{22}Na and another ($E_\gamma = 7.3 - 8.4 MeV$) above the capture γ–rays from Ni–backing and ^{19}F (see Fig. 1.).

Six resonances were identified as $^{22}Na(p,\gamma)^{23}Mg$ ones in the energy region of astrophysical interest (the Gamow peak). Two of them is shown in fig. 1.

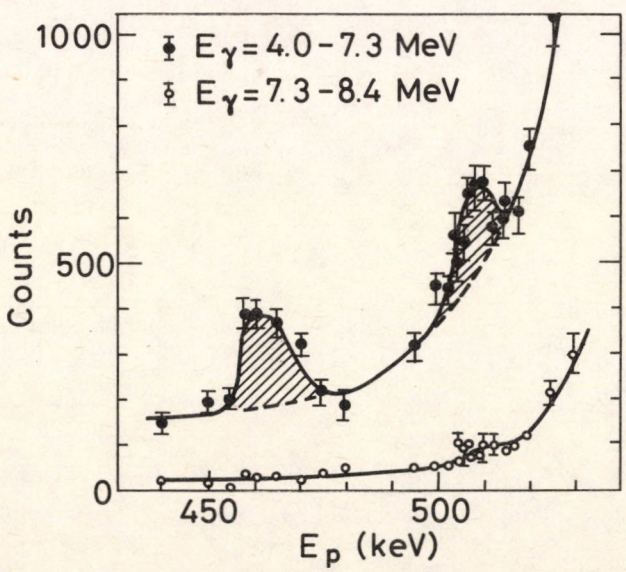

Fig. 1. A section of excitation functions with two resonances. (The steeply rising part is due to a broad resonance from ^{13}C).

The measurements were completed later (using Ge detector too) for getting the branching ratios and strengths of the resonances as well as the stellar reaction rates [2].

† Institut für Kernphysik, Universität Münster, Germany
‡ Caltech, Pasadena, California, USA

1. C. Rolfs and W. S. Rodney, Cauldrons in the cosmos. University of Chicago Press, (1988) p. 507.
2. S. Seuthe et al., Nucl. Phys. **A514** (1990) 471.

Spectroscopy of ^{25}Al via the ^{24}Mg(p,γ) Reaction

Zs. Fülöp, J. Keinonen†, Á. Z. Kiss, E. Somorjai

and P. Tikkanen†

As part of a cooperation project on the systematic study of short lifetimes in the *sd* shell region [1] mean lifetimes of levels of the ^{25}Mg-^{25}Al mirror nuclei have been measured using the Doppler shift attenuation (DSA) method in reactions $^{12}C(^{15}N,pn)^{25}Mg$ and $^{24}Mg(p,\gamma)^{25}Al$, respectively. Although in the case of ^{25}Al a few studies were already performed previously, the still missing or poorly determined branching ratio, etc. values [2] necessitated a more complex re–investigation of this latter reaction.

The $^{24}Mg(p,\gamma)^{25}Al$ reaction studies were carried out using the proton beam from the 5 MV Van de Graaff accelerator of the institute. The ^{24}Mg targets were prepared by implanting $^{24}Mg^{+}$ ions into Ta backings by the isotope separator of the University of Helsinki.

For the lifetime determinations DSA analysis has been performed using Monte Carlo calculations with the inclusion of experimental stopping power values. Lifetimes of four excited levels below the excitation energy of 4.2 MeV have been determined. The comparison of the experimentally deduced transition strengths with shell model calculations based on large–basis multi–shell wave functions is under course.

Branching ratios of gamma decay of 5 resonance and 3 bound states have been deduced. A more accurate energy of the $E_x = 4.03$ MeV excited state has also been determined.

† Accelerator Laboratory, University of Helsinki, Finland

1. P. Tikkanen, J. Keinonen, A. Kuronen, Á. Z. Kiss, E. Koltay, É. Pintye and B. H. Wildenthal, Nucl. Phys. A**517** (1990) 176.
2. P. M. Endt and C. van der Leun, Nucl. Phys. A**310** (1978) 1.

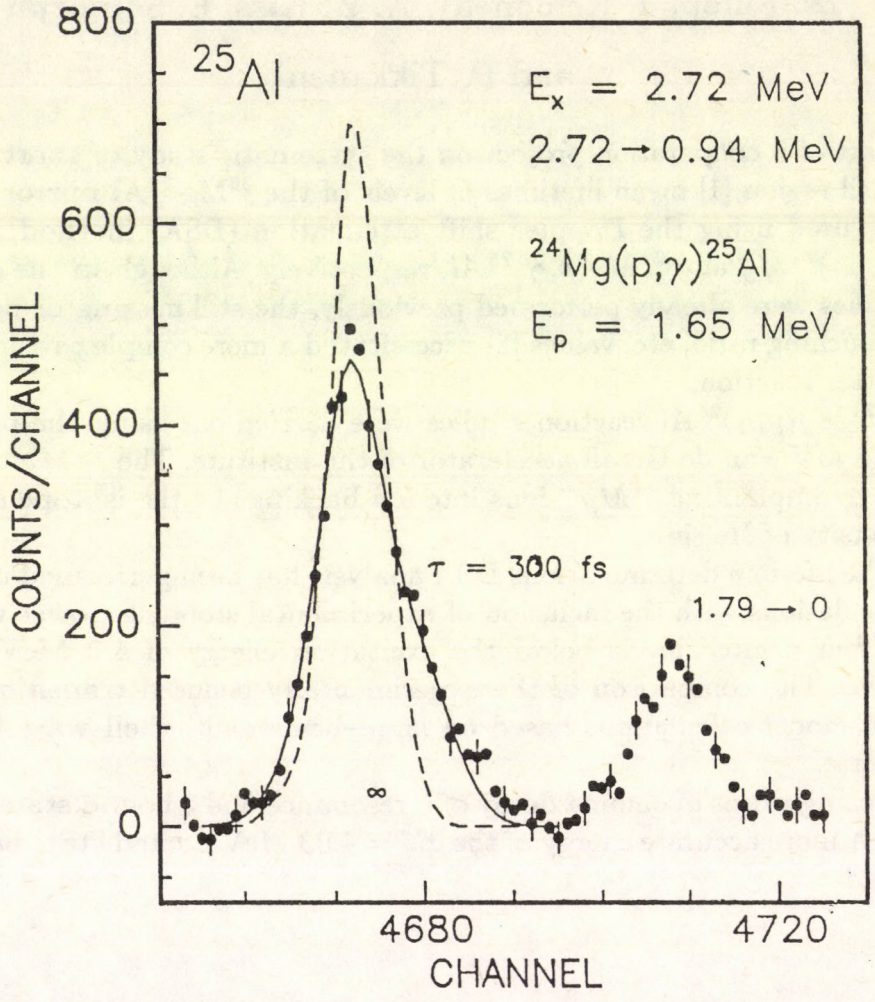

Fig. 1. Portion of γ–spectrum recorded in the DSA measurement of the 2.72 MeV ^{25}Al state. The dispersion is 0.39 keV/ch., collected charge is 0.69 C. The solid line is the Monte Carlo simulation of the γ–ray lineshape at 0°; the fit is shown for the lifetime 300 fs. As comparison, the lineshape of the ^{40}K laboratory background line ($\tau = \infty$) is shown by the dotted curve.

Excitation Function of the $^{35}Cl(\alpha,n)^{38}K$ Reaction Using Gas Targets*

F. Tárkányi, Z. Kovács, I. Mahunka, O. Solin [1], J. Bergman [1]

The positron emitting radioisotope ^{38}K ($T_{1/2}$=7.6 min) is an important tracer for myocardial blood flow measurement with PET. For routine production mainly the $^{35}Cl(\alpha,n)^{38}K$ nuclear reaction involving solid NaCl targets are used. In the frame of feasibility study of production of ^{38}K from gas target we present our results on the excitation function measured with natural chlorine gas targets.

The excitation function of the $^{35}Cl(\alpha,n)^{38}K$ reaction was measured by the activation of gas cells filled with dry chlorine gas to 1 bar. The quartz glass target cells have a polyimide foil windows and glass-teflon valves for evacuation and filling.

The cells were irradiated for 15 minutes with a collimated alpha particle beam from the Turku MGC cyclotron at 50-60 nA beam current. After the end of bombardment the cells were subjected to gamma ray measurement without separation of the ^{38}K and the target gas from the cells. The cross sections, energy degradations and their errors were calculated similarly to our previous work [1].

The measured cross section data for the formation of ^{38}K are shown in Fig. 1 in comparison with results recently obtained by Quaim et al. [2] using chlorine containing plastic target stacks. Despite the difficulties of the used techniques (low melting point of plastic, corrosive gas) the results show good agreement.

In the energy range of our cyclotron (E_α =7-21 MeV) 5 mCi/μA yield of ^{38}K could be achieved at saturation as calculated from the measured cross sections.

On the basis of the excitation function and our preli-minary experiments it seems worth-while to investigate the production of ^{38}K using gas, vapour, liquid or melted targets with high chlorine contents.

In order to examine the practicability of these methods further investigations are required for the separation of no carrier added ^{38}K from the target material and the contaminating products formed during the irradiations.

References

[1] Åbo Akademi, Accelerator Laboratory, Turku Finland

1. F. Tárkányi, S. M. Quaim, G. Stöklin: Int. J. Appl. Radiat. Isot. **39**, 135 (1988)
2. S. M. Quaim, M. S. Sutisna, H. Olligh: Appl. Radiat. Isot. **39**, 479 (1988)

*This work was supported by the Hungarian Academy of Sciences and the Academy of Finland

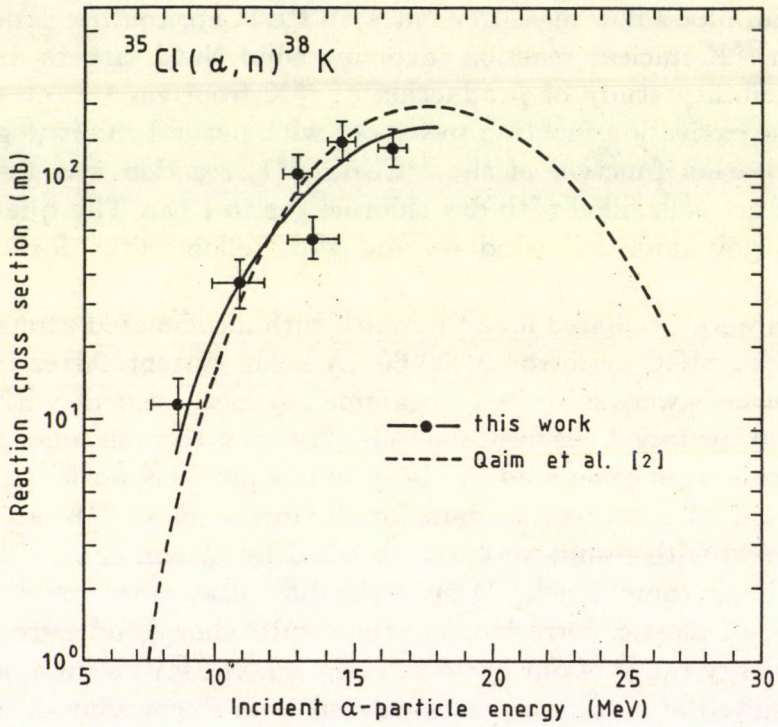

Fig. 1.. Excitation function of the $^{35}Cl(\alpha,n)^{38}K$ nuclear reaction

New Data for p, α and ^{3}He Induced Reactions on ^{nat}Ni, ^{nat}Cu and ^{nat}Ti for Monitoring the Beam Performance

F. Tárkányi, F. Szelecsényi, P. Mikecz, P. Kopecky *

For charged particle induced nuclear reactions – besides the well known primary, "absolute" methods (bending magnetic field, charge collection) – the well measured standard reactions play a very important role in monitoring the beam energy and intensity. Their use is widely spread and convenient mainly because of their simplicity and cheapness and due to the fact that the energy degradation and intesity changes could be followed in the targets.

In spite of continuing work in many laboratories around the world in the field of charged particle induced nuclear reactions for monitoring the Helium-3 and alpha beams, only very few standard reactions are available and sometimes even the proposed ones are very far from the meaning of "standard". Large systematic discrepancies are still observed between the different experiments even for well measured reactions.

This paper reports on the cross sections which have been measured in our laboratories and used as reference data for monitoring beam performance.

The exitation functions were measured by stacked-foil technique. The irradiations were carried out at the Rez U-120M cyclotron, at the Jülich CV-28 cyclotron and at the Debrecen MGC-20E cyclotron, at different incident energies to get overlapping energy regions. The total integrated charge was detected by Faraday cup measurement. The activity of the foils was determined via standard gamma ray spectro-metry. Special attention was paid to the necessary usual corrections to obtain the absolute activities. The beam energy was controlled by magnetic deflection at the Rez and Debrecen cyclotrons and by the normalization to the other monitor reactions at the Jülich experiments. The beam energy degradation was followed along the stack by a method based on flux constancy along the stack.

Exitation functions have been measured up to 30 MeV proton induced nuclear reactions on ^{nat}Ni leading to the production of ^{57}Ni, ^{57}Co, ^{56}Co and ^{55}Co; up to 40 MeV alpha and 36 MeV ^{3}He induced reaction on ^{nat}Cu leading to the production of ^{60}Cu, ^{61}Cu, ^{63}Zn, ^{65}Zn, ^{66}Ga and ^{67}Ga; up to 40 MeV alpha and 36 MeV ^{3}He induced reaction on natTi leading to the production of ^{44m}Sc, ^{48}V, ^{48}Cr, ^{49}Cr and ^{51}Cr.

The measured excitation functions were compared with the previously published data. The agreement on average is good but in some cases small systematic deviations could be observed in cross section values. on the completed data base, reference values are proposed for the above mentioned reactions.

*Dept. of Radiopharm. Nucl. Res. Ins., 25068 Rez CSFR

Excitation Function of $^{40}Ar(\alpha,p)^{43}K$ Nuclear Reaction: production of ^{43}K using Ar–Gas Target

F. Tárkányi, A. Fenyvesi, T. Molnár [1], F. Szelecsényi,

Z. Szűcs, Cs. Béres [2]

The radioactive potassium radioisotopes are widely used in the nuclear medicine. The potassium seems to be also a good tracer for studying the water transport in different plants. In the practice only three longer lived K isotopes can be used: the ^{38}K ($T_{1/2}$=7.6 min) β^+ -emitting isotope which could only be used on site of the cyclotron and the longer lived β^--emitting ^{42}K ($T_{1/2}$=12.4 h) and ^{43}K ($T_{1/2}$=22.6 h) isotopes. The last two permit transportation of the product and they are suitable for longer time investigations. The half life of ^{42}K is relatively high but energies and intensities of its principal gamma rays make it less useful for most of the applications. An other disadvantage is that its production needs medium size energy cyclotron.

The non–carrier added ^{43}K can be produced at low energy cyclotrons exclusively via the $^{40}Ar(\alpha,p)$ ^{43}K reaction (natural abundance 99.6 %). The available information on the excitation function is however unsatisfactory. Only 4 cross section value were measured below 21 MeV [1]. In connection with the optimization of production of ^{43}K for ecological purposes we have investigated these formulation cross section of (α,p) reaction in more detail. We present here also our results on a flow argon system used routinely for production and recovery of ^{43}K.

Cross sections were measured with stacked gas cell technique. Gas cells similar to those described in [2] were filled with natural Ar gas up to 0.9 bar. Irradiations were performed at the Debrecen MGC-20E cyclotron up to E_α=20 MeV bombarding energy. The activity of the produced ^{43}K were determined via standard gamma-ray spectroscopy without separation from the irradiated cell. The cross section values obtained in average are in agreement with the results of Tanaka *et al.* [1]. The study of the excitation function at higher energies is in progress.

The ^{43}K is routinely produced using a flow Ar–target–recovery system. The target system is similar to the one described by Clark *et al.* [3]. The target chamber consists of a 30 cm long 9 cm diameter nickel plated copper czlinder. The heat removal is solved by an internal water cooled spiral heat exchanger in which a copper plate serves as a beam–stop. Important difference from the gas flow system of Clark *et al.* [3] is that for shortening the deposition time of the produced ^{43}K in the target chamber, the gas inlet is performed at the beam–stop and the outlet closed to the entrance window of the target chamber. The chamber is filled to about 1 bar and a membrane compressor circulats the gas at a speed of about 50 l min^{-1}. In this way, presently cca. 60-70 % of the total activity is recovered in a glass fibre filter paper. From the filter, 95 % of the ^{43}K was washed out with 0.02 mol HCl. Several experiments have been done in a static, batch pruduction

mode and the total produced activity was washed out from the target chamber. The outwashed activities were used for investigation of water transport of different plants (Quercus petraea oak trees, Xerophyta scabrida, Zea mays).

References

[1]Biomedical Cyclotron Laboratory, Debrecen Medical University School, Nagyerdei krt. 98., H-4010 Debrecen, Hungary
[2]Ecological Institute, Lajos Kossuth University, P.O.Box 14, Debrecen, H-4010, Hungary

1. S. Tanaka *et al.*, Jour. of the Phys. Soc. of Japan, Vol.**15** No.6, p. 952 (1960)
2. F. Tárkányi, S.M. Qaim, and G. Stöcklin, Appl. Radiat. Isot. Vol.**39** No.2 pp.135-143 (1988)
3. J.C. Clark, M. L. Thakur, I.A. Watson, Int. Jour. of Appl. Rad. and Isotopes, Vol.**23** pp.329-335 (1972)

Spectroscopic Study of ^{68}Ga from (α,nγ) Reaction

J. Tímár, T. X. Quang and A. Krasznahorkay

The level structure of ^{68}Ga was studied up to 2000 keV excitation energy using 14.5 MeV bombarding alpha beam. Gamma-ray, conversion electron (fig.1), and gamma-gamma coincidence spectra (fig.2) of the ^{65}Cu(α,nγ)^{68}Ga reaction were measured with Ge(Li), Ge(HP) and superconducting magnetic lens plus Si(Li) electron spectrometer, respectively.

The energies and relative intensities have been determined for >90 (among them >60 new) gamma transitions. Internal conversion coefficients of 18 transitions have been measured.

A more complete level scheme with many new levels, gamma-ray branching ratios, level spin and parity values have been deduced.

This work was supported partly by the National Scientific Research Foundation /OTKA/.

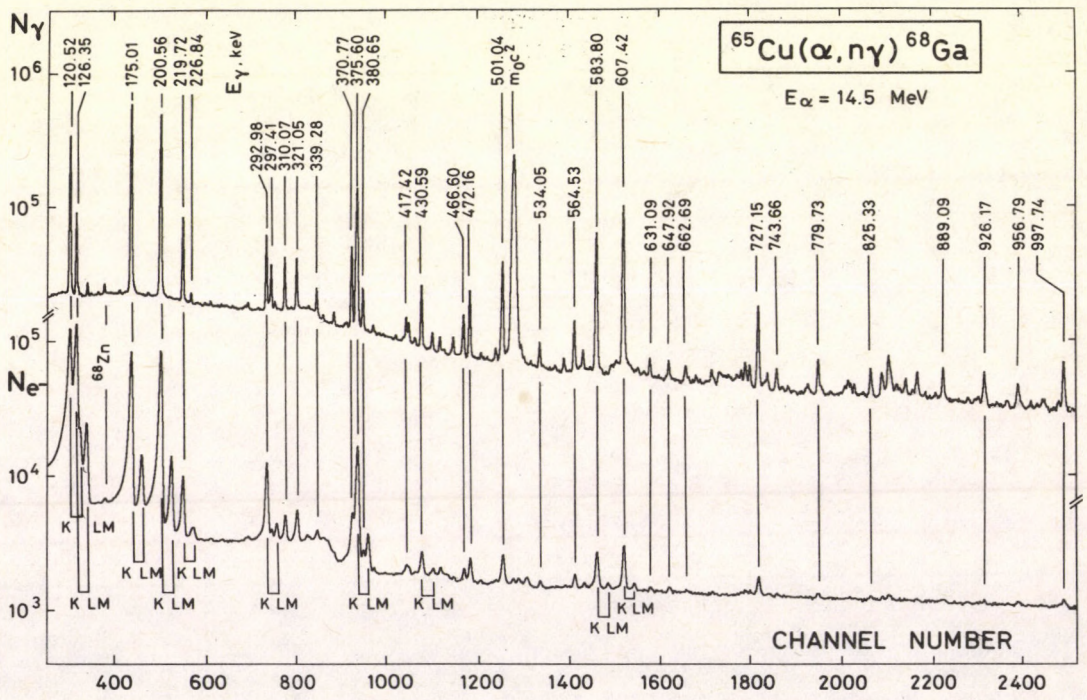

Fig. 1. Typical gamma-ray and internal conversion electron spectra of ^{68}Ga.

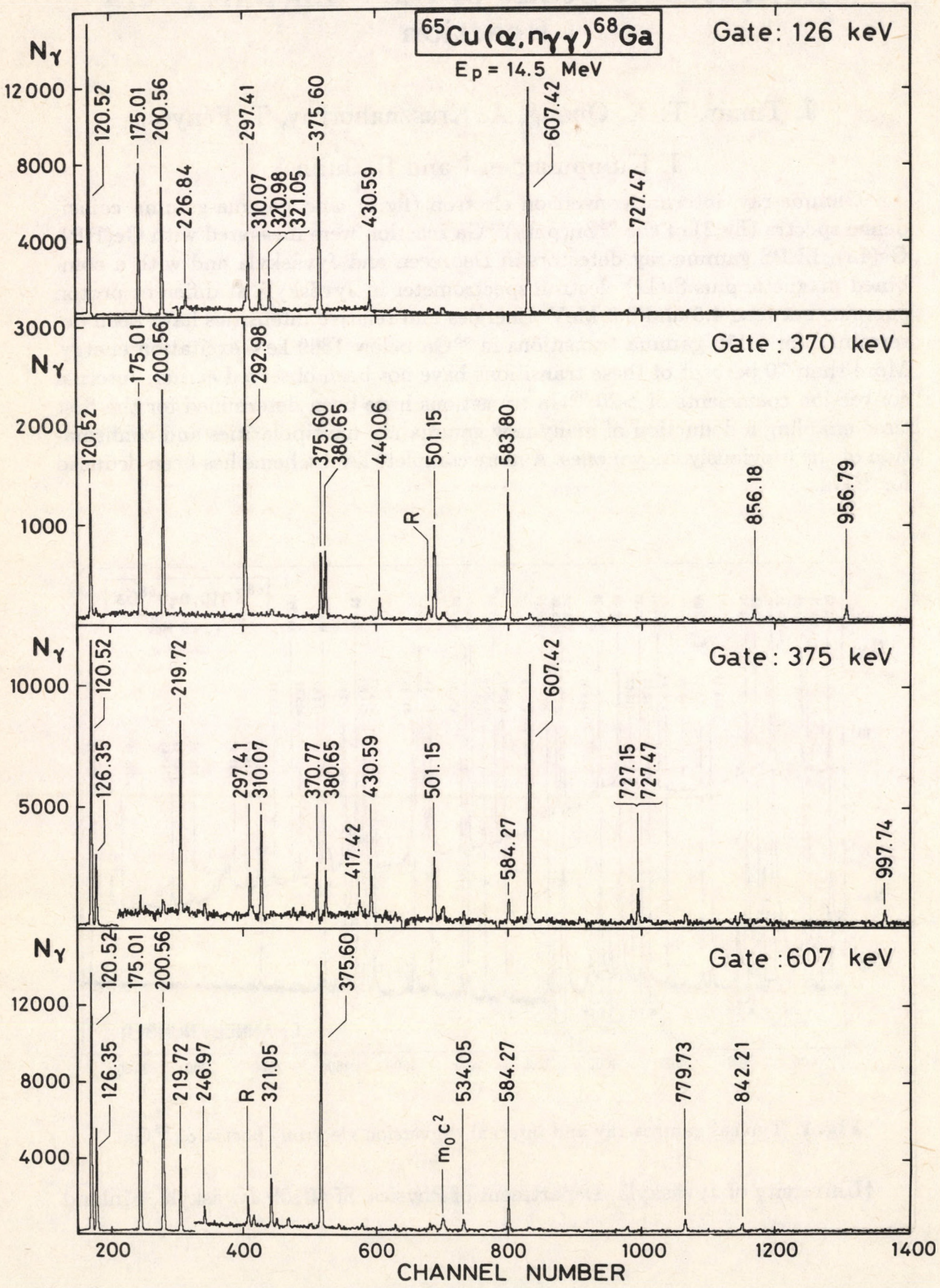

Fig. 2. Typical gamma-gamma coincidence spectra of ^{68}Ga.

Gamma and Conversion Electron Spectroscopic Study of the $^{68}Zn(p,n\gamma)^{68}Ga$ Reaction

J. Tímár, T. X. Quang, A. Krasznahorkay, T. Fényes,

J. Kumpulainen † and R. Julin †

Gamma-ray, internal conversion electron (fig.1), and gamma-gamma coincidence spectra (fig.2) of the $^{68}Zn(p,n\gamma)^{68}Ga$ reaction were measured with Ge(HP), Ge(Li), LEPS gamma-ray detectors in Debrecen and Jyväskylä and with a combined magnetic plus Si(Li) electron spectrometer in Jyväskylä at different proton energies between 4.5 and 5.3 MeV. Energies and relative intensities have been determined for >110 gamma transitions in ^{68}Ga below 1300 keV excitation energy. More than 70 percent of these transitions have not been observed earlier. Internal conversion coefficients of >20 ^{68}Ga transitions have been determined for the first time enabling a deduction of many new gamma-ray multipolarities and confirmation of the previously known ones. A more complete level scheme has been deduced for ^{68}Ga.

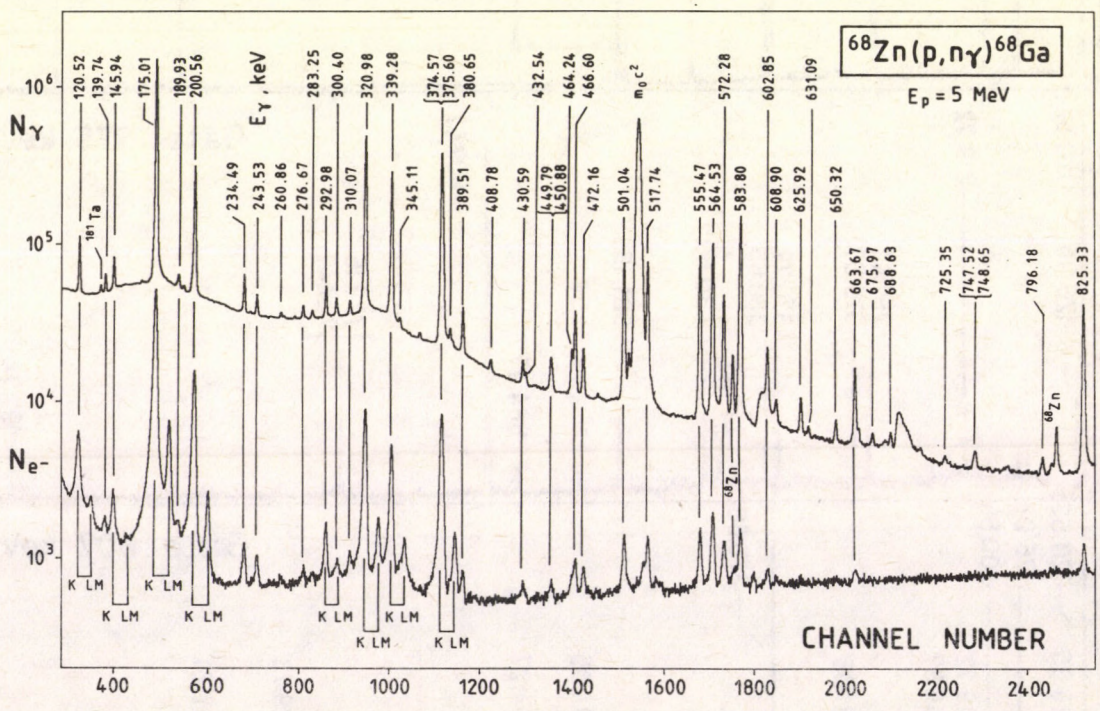

Fig. 1. Typical gamma-ray and internal conversion electron spectra of ^{68}Ga.

†University of Jyväskylä, Department of Physics, Sf-40100 Jyväskylä, Finland

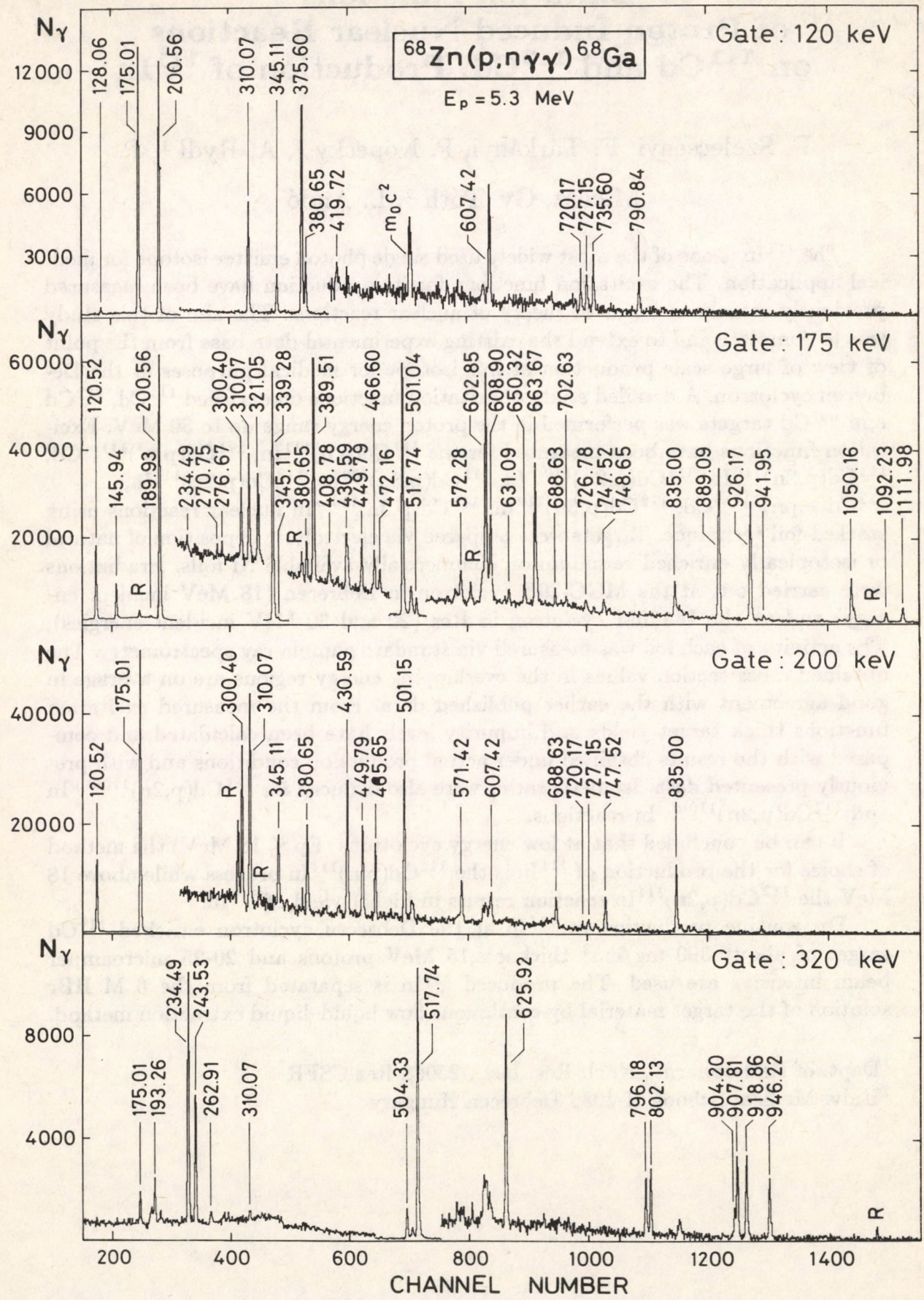

Fig. 2. Typical gamma-gamma coincidence spectra of ^{68}Ga.

Exitation Functions of Proton Induced Nuclear Reactions on ^{111}Cd and ^{112}Cd. Production of ^{111}In

F. Szelecsényi, F. Tárkányi, P. Kopecky [1], A. Rydl [1], P. Mikecz, Gy. Tóth [2], L. Andó

The ^{111}In is one of the most widely used single photon emitter isotope for medical application. The excitation functions for its production have been measured previously mainly in terms of theory of nuclear reactions. The aim of this study was to complete and to extend the existing experimental data base from the point of view of large scale production of this isotope for medical purposes at the Debrecen cyclotron. A detailed study of exitation functions on enriched ^{111}Cd, ^{112}Cd and ^{nat}Cd targets was performed in the proton energy range up to 30 MeV. Excitation functions have been measured for the ^{111}Cd(p,n)^{111}In, ^{111}Cd(p,p')^{111m}Cd, ^{111}Cd(p,2n)^{110}In, ^{111}Cd(p,2n)^{110m}In, ^{111}Cd(p,3n)^{109}In, ^{112}Cd(p,2n)^{111}In, ^{112}Cd(p,pn)^{111m}Cd, ^{112}Cd(p,3n)^{110}In, ^{112}Cd(p,3n)^{110m}In nuclear reactions using stacked-foil technique. Targets were prepared via electrolytic deposition of natural or isotopically enriched cadmium on commercially available Ni foils. Irradiations were carried out at the MGC-20E cyclotron in Debrecen (18 MeV incident energy) and at the U-120M cyclotron in Rez (22 and 30 MeV incident energies). The activity of each foil was measured via standard gamma ray spectrometry. The obtained cross section values in the overlapping energy regions are on average in good agreement with the earlier published data. From the measured excitation functions thick target yields and impurity levels have been calculated and compared with the results obtained under actual production conditions and with previously presented data. Isomeric ratios were also deduced for ^{111}Cd(p,2n)^{110m,g}In and ^{112}Cd(p,2n)^{110m,g}In reactions.

It can be concluded that at low energy cyclotrons (Ep $\leq$ 18 MeV) the method of choice for the production of ^{111}In is the ^{111}Cd(p,n)^{111}In process while above 18 MeV the ^{112}Cd(p,2n)^{111}In reaction results in higher yield of ^{111}In.

For routine production of ^{111}In at the Debrecen cyclotron enriched ^{111}Cd target of about 300 mg/cm^2 thickness,15 MeV protons and 20-25 microamper beam intensity are used. The produced ^{111}In is separated from the 6 M HBr solution of the target material by continuous flow liquid–liquid extraction method.

[1]Dept. of Radiopharm., Nucl. Res. Inst., 25068 Rez CSFR
[2]Univ. Medical School, H-4032 Debrecen Hungary

Nearly Complete Level Scheme of ^{116}Sn below 4.3 MeV

S. Raman [a], T.A. Walkiewicz [a], S. Kahane [a], E.T. Jurney [b], J. Sa [c], Z. Gácsi, J.L. Weil [c], K. Allart [d], G. Bonsignori [e], J.F. Shriner, Jr. [f]

The level scheme of ^{116}Sn has been studied by combining the results of ^{115}Sn(n,γ)^{116}Sn and ^{116}Sn(n,n'γ)Sn experiments. Both experiments were performed using isotopically enriched samples and Ge γ-ray detectors. Based on the thresholds of γ-ray excitation functions measured for the ^{116}Sn(n,n'γ) reaction and the precise γ-ray energies from the capture reaction, 100 levels were observed below 4.3 MeV excitation energy. Approximately half of these were not known previously. Forty-eight of these levels have unique or tentative spin-parity assignments, and for ten more the spin has been restricted to a single value. The spin-parity for most other levels below 4.3 MeV excitation has been restricted to a few values.These spin-parity assignments and limitations were derived mainly from (n,n'γ) angular distribution measurements, together with additional information obtained from the cross section magnitudes in both experiments. Above 4.3 MeV excitation energy, 55 additional levels are proposed, based only on the ^{115}Sn(n,γ) results. No J^π information is available for these higher-lying levels beyond the fact that they most probably all have $J \leq 4$. The level scheme below 4.3 MeV from the current work, together with known high-spin levels up to 5.4 MeV seen in other experiments, are compared to the combined predictions of the two-broken-pair model, the Interacting Boson model, and the deformed collective model. In addition, several states have been identified as proton 1p-1h and collective quadrupole-octupole two-phonon excitations. It is concluded from the good agreement between experiment and these models that all levels in ^{116}Sn with $J \leq 6$ up to an excitation of 4.0 MeV and $J \leq 3$ up to 4.3 MeV may have been experimentally identified. The nearest-neighbor spacing distribution is intermediate between that of a Gaussian orthogonal ensemble and that of a Poisson distribution, with a slight preference for the former. The neutron separation energy was determined to be 9563.47±0.11 keV.

(a) Oak Ridge National Laboratory, Oak Ridge, TN 37831, USA
(b) Los Alamos National Laboratory, Los Alamos, NM 87545, USA
(c) University of Kentucky, Lexington, KY 40506, USA
(d) Faculty of Physics and Astronomy, Free University, Amsterdam, The Netherlands
(e) Dipartmento di Fisica dell'Universita Bologna, Instituto Nazionale di Fisica Nucleare, Sezione di Bologna, Italy
(f) Tennessee Technological University, Cookville, TN 38505, USA

Nuclear Structure of ^{116}Sb

Z. Gácsi, Zs. Dombrádi, T. Fényes, S. Brant † and V. Paar †

Gamma-ray, internal conversion electron and $\gamma\gamma$-coincidence spectra of the ^{113}In(α,nγ)^{116}Sb reaction were measured, and level scheme of ^{116}Sb was deduced [1]. Multipolarities of transitions and γ-ray branching ratios were also determined. The energy spectrum (fig.1) and electromagnetic properties of the levels were calculated in the framework of the interacting boson-fermion-fermion model (IBFFM) and satisfactory agreement between the experimental and theoretical results was obtained.

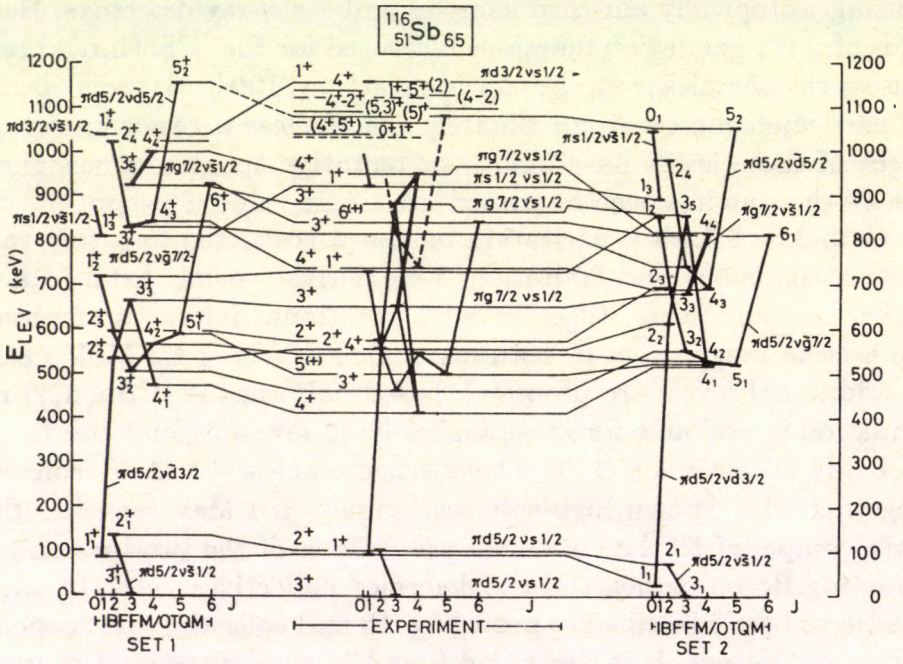

Fig. 1. IBFFM energy spectrum of ^{116}Sb in comparison with experimental data. The solid lines connect the members of the given multiplets. The experimental proton-neutron configurations are shown on the basis of (^{3}He,d) proton transfer results [2].

This work was supported partly by the National Scientific Research Foundation (OTKA).

† Prirodoslovno-Matematicki Fakultet, University of Zagreb, Zagreb, Croatia, Yugoslavia

1. Z. Gácsi, Zs. Dombrádi, T. Fényes, S. Brant, and V. Paar: ATOMKI PREPRINT 9-1990 P, 1990.

2 R. Kamermans, J. Van Driel, H.P. Blok, and P.J. Blankert: Phys. Rev. C **17**, 1555 (1978).

Proton-neutron Multiplets in ^{116}Sb

Z. Gácsi, T. Fényes and Zs. Dombrádi

On the basis of complex in-beam spectroscopic study of the ^{116}Sn(p,nγ)^{116}Sb reaction [1], new level scheme of ^{116}Sb has been proposed, which contains 38 levels and 70 γ-ray transitions among them. Multipolarities of the transitions and γ-ray branching ratios have been deduced. Calculated (p,n) level excitation cross sections were compared with experimental values, as shown in figure 1.

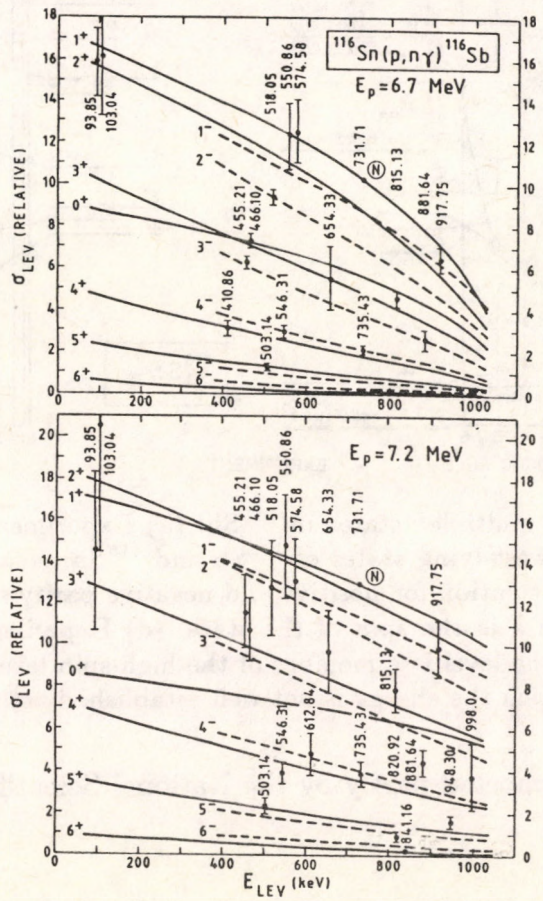

Fig. 1. Experimental relative cross sections (σ_{LEV}) of the ^{116}Sn(p,nγ)^{116}Sb reaction (dots with error bars) as a function of the ^{116}Sb level energy (E_{LEV}) at 6.7 MeV (upper part) and 7.2 MeV (lower part) bombarding proton energies. The solid and dashed curves show theoretical results obtained from the Hauser-Feshbach model. N means normalization point.

Level spins and parities were determined on the basis of Hauser-Feshbach analysis, internal conversion coefficients, and γ-ray angular distribution data. The energies of several ^{116}Sb proton-neutron multiplets were calculated using the parabolic rule [2]. The results of the calculations are presented in figure 2. Members of different multiplets have been identified.

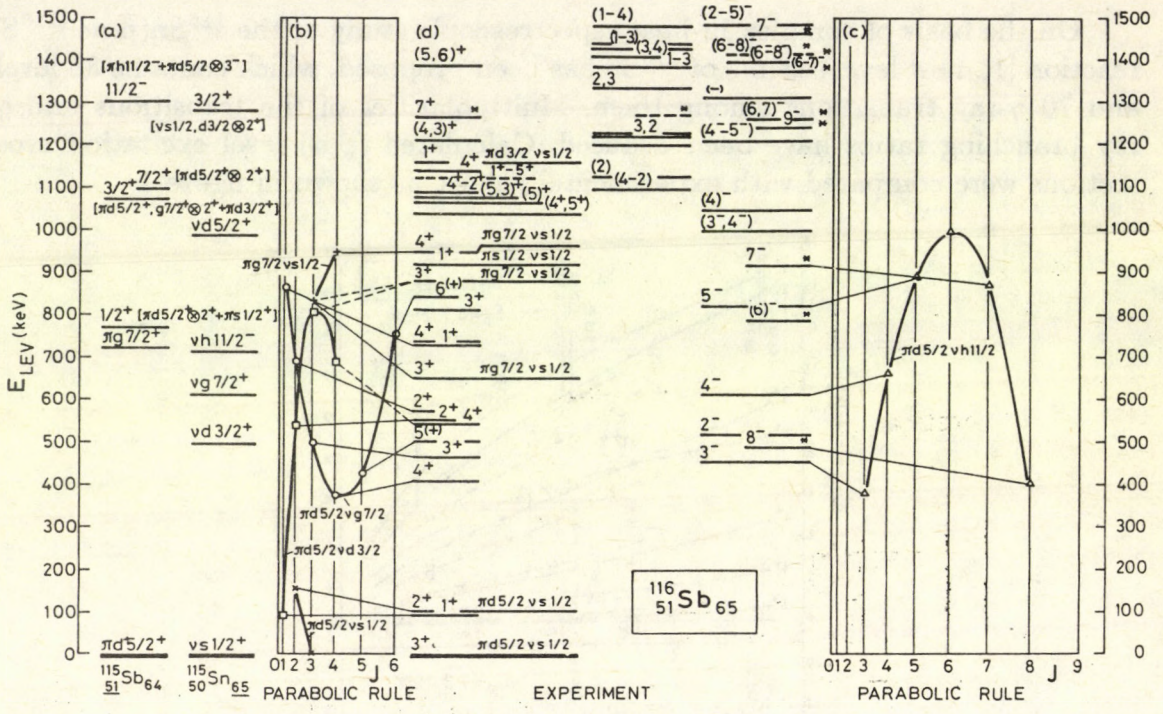

Fig. 2. Proton-neutron multiplet states in ^{116}Sb. (a) Experimental level energies and configurations of the lowest-lying states of ^{115}Sb and ^{115}Sn nuclei. (b) and (c) Results of the parabolic rule calculation for positive and negative parity states. On the abscissa J(J+1) is shown, where J is the spin of the state. (d) Experimental results on ^{116}Sb levels. * indicates that the level is a member of the high-spin level scheme based on the 8^- isomeric state for which the energy is not well established yet (383±40 keV).

This work was supported partly by the National Scientific Research Foundation (OTKA).

References

1. Z. Gácsi, T. Fényes, Zs. Dombrádi, ATOMKI PREPRINT 8-1990 P, 1990.
2. V. Paar, Nucl. Phys. **A331**, 16 (1979).

Gamma and conversion electron spectroscopic study of the ^{118}Sn(p,nγ)^{118}Sb reaction

J. Gulyás, T. Fényes, Zs. Dombrádi and T. Kibédi

The γ-ray singles and $\gamma\gamma$-coincidence spectra of the ^{118}Sn(p,n γ)^{118}Sb reaction were measured at $E_p = 5.5, 5.7, 6.0$ and 7.5 MeV bombarding energies with Ge(Li), Ge(HP) and low-energy photon spectrometers (LEPS). 134 gamma-rays (including 56 new ones, compared to ref. [1-2]) were assigned to the reaction in question. Angular distribution data have been obtained for 14 gamma-rays at $E_p = 5.6$ MeV.

Internal conversion electron spectra were measured with a superconducting magnetic lens plus Si(Li) electron spectrometer at $E_p = 6.0$ MeV. Internal conversion coefficients of 61 ^{118}Sb transitions were determined. A more complete level scheme of ^{118}Sb, multipolarities of transitions and gamma-ray branching ratios have been deduced. Spins and parities of the excited states have been determined on the basis of transition multipolarities, gamma-ray angular distribution data and Hauser-Feshbach analysis.

This work was supported partly by the National Scientific Research Foundation /OTKA/.

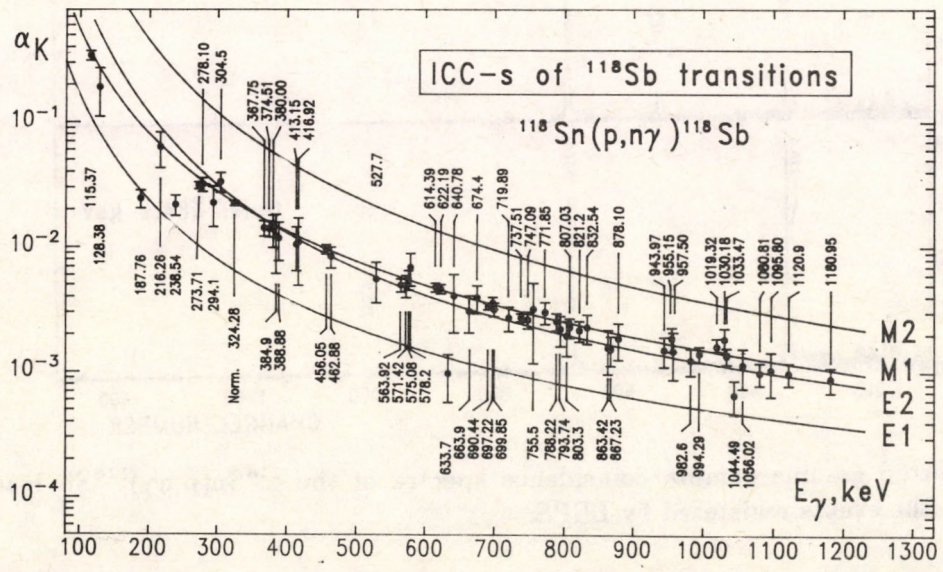

Fig. 1. Experimental (dots with error bars) and theoretical [3] (solid lines) α_K internal conversion coefficients of ^{118}Sb transitions as a function of gamma-ray energy.

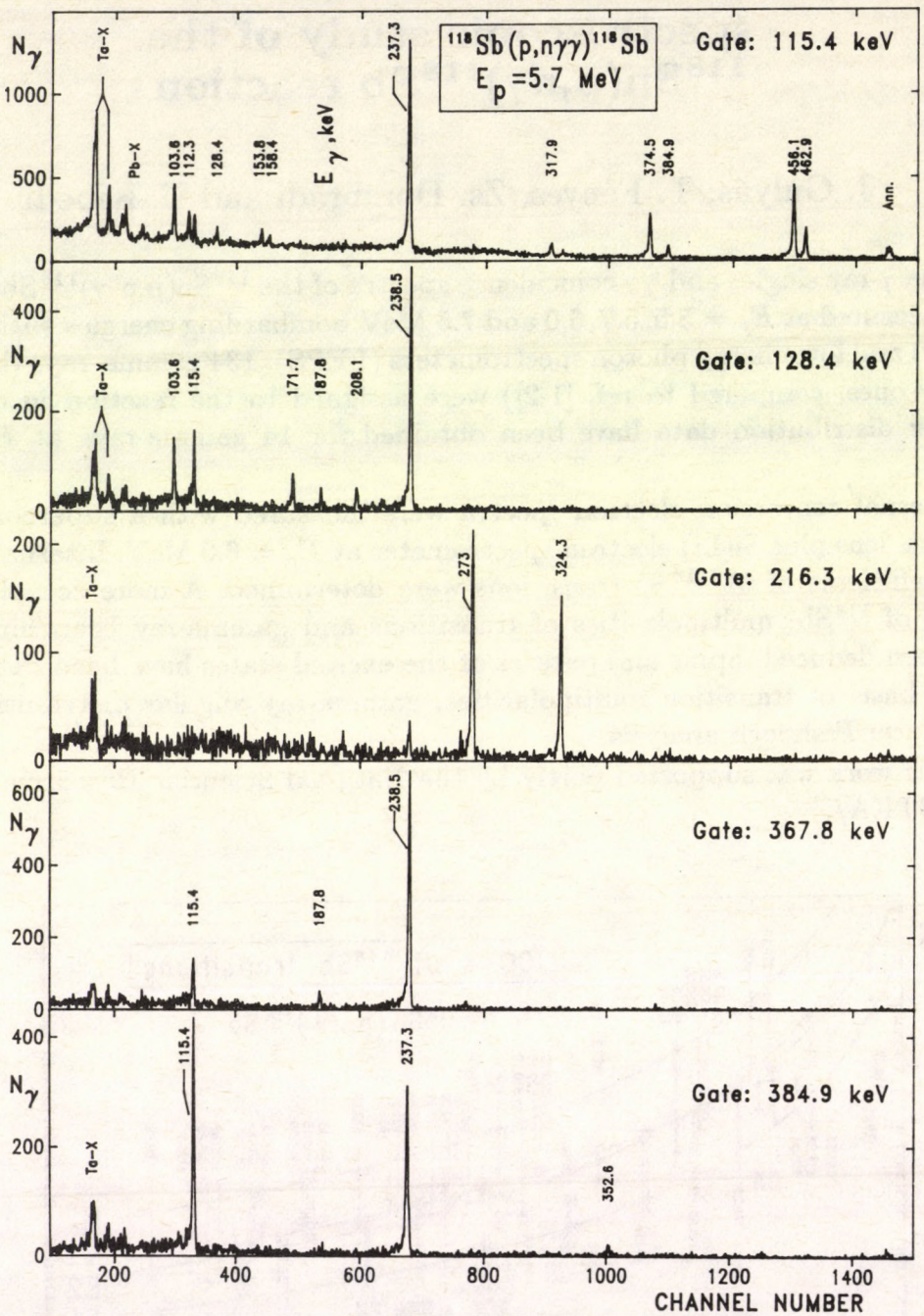

Fig. 2. Selected gamma-gamma coincidence spectra of the ^{118}Sn(p,nγ)^{118}Sb reaction sorted from the events registered by LEPS.

References

1. Ch. W. Bacon, The levels of the odd-odd nucleus antimony-118 below 1200 keV, Ph.D. Dissertation, Michigan State University, 1974
2. T. Tamura, K. Miyano and S. Ohya, Nucl. Data Sheets **51** (1987) 329.
3. F. Rösel, H. M. Fries, K. Alder and H. C. Pauli, Atomic Data and Nuclear Data Tables **21** (1978) 91.

Study of ^{118}Sb from (α,n γ) reaction

J. Gulyás, J. Kumpulainen † and R. Julin †

†University of Jyväskylä, Department of Physics

The γ-ray and internal conversion electron spectra of the ^{115}In(α,nγ)^{118}Sb reaction were measured at E_α = 14.5 MeV bombarding α-particle energy with Ge(HP), Ge(HP,LEPS) gamma and superconducting magnetic lens plus Si(Li) electron spectrometers. Internal conversion coefficients of 30 ^{118}Sb transitions were determined from the electron and gamma-ray intensities. Gamma-gamma coincidences were also measured at E_α = 14.5 MeV. Level scheme, complementing the previous [1] and our (p,n) [2] data, as well as multipolarities of transitions and gamma-ray branching ratios have been deduced. Level spins and parities have been determined mainly on the basis of internal conversion coefficients and the results of our (p,n) data.

This work was supported partly by the National Scientific Research Foundation /OTKA/.

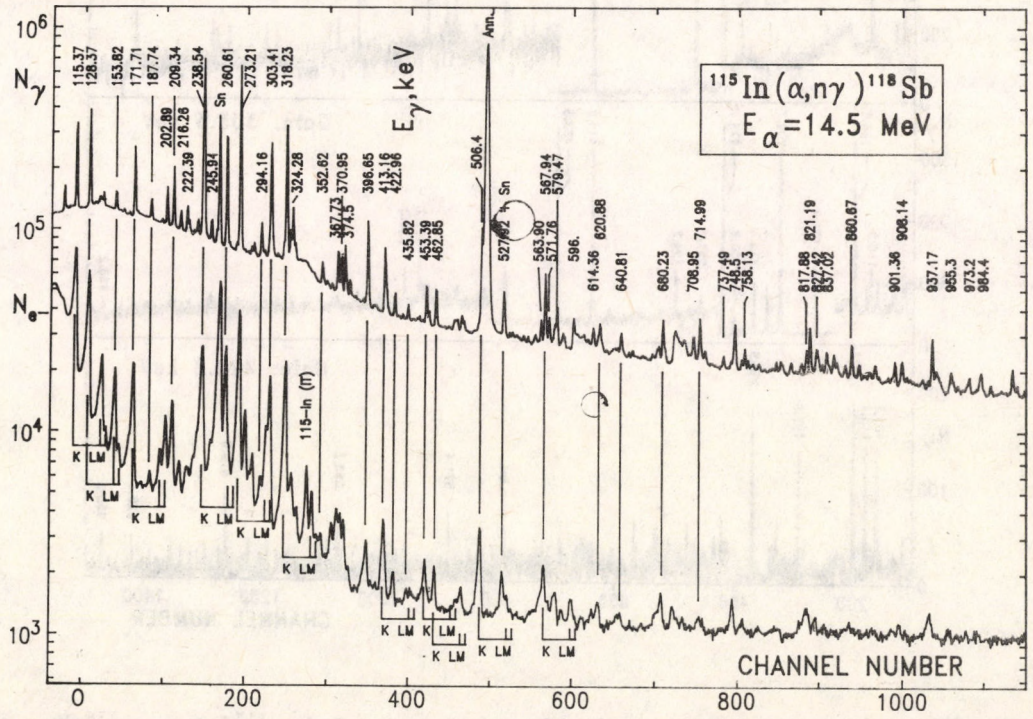

Fig. 1. Typical gamma-ray and internal conversion electron spectra. Gamma-ray energies are given only for the strongest ^{118}Sb lines. K,L,M denote the corresponding conversion electron lines.

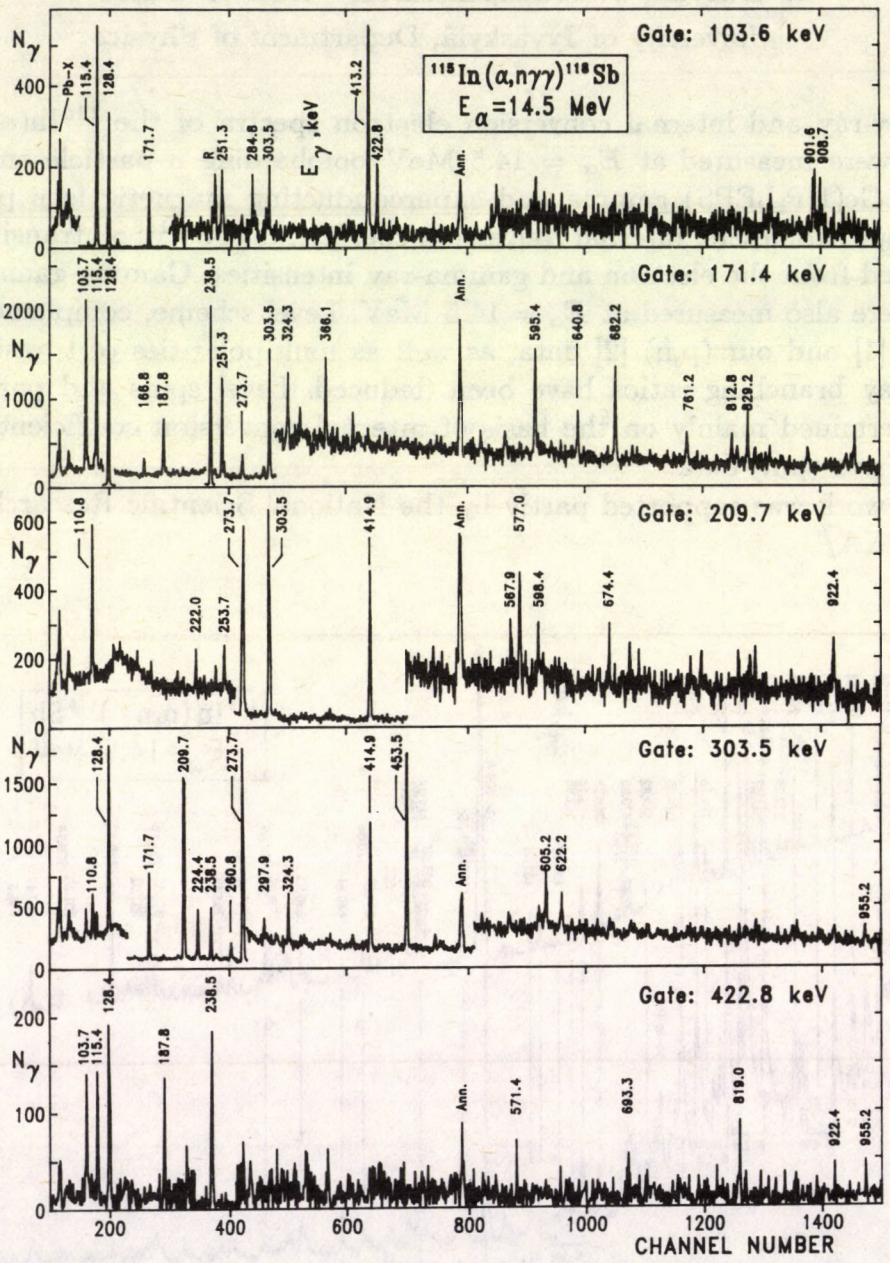

Fig. 2. Selected gamma-gamma coincidence spectra of the ^{115}In(α,nγ)^{118}Sb reaction. The background was subtracted using the adjacent continuum parts of the spectra.

References

1. T. Tamura, K. Miyano and S. Ohya, Nucl. Data Sheets **51** (1987) 329.
2. J. Gulyás, T. Fényes, Zs. Dombrádi and T. Kibédi, in this volume

NUCLEAR STRUCTURE OF ^{120}Sb

T. Fényes and Zs. Dombrádi

The low-lying levels of ^{120}Sb nucleus have been studied mainly from (p,n γ) and (d,p) reactions [1-5]. Although the quantum characteristics of many states have been determined, a theoretical description of the ^{120}Sb was missing. In the present work we have calculated the energy levels and electromagnetic properties of the low-lying levels of ^{120}Sb within the framework of the interacting boson-fermion-fermion model (IBFFM).

The hamiltonian of the IBFFM and the computer code, used in the calculations, are described in refs. 6 and 7, respectively. The single-proton and the quasineutron energies, as well as the strength parameters of the nucleon-core interaction were fitted to the level energies and electromagnetic moments of ^{119}Sb and ^{119}Sn by IBFM [8] calculations, and finally they were slightly adjusted to the level energies and electromagnetic properties of ^{120}Sb. The occupation probabilities of neutron states were taken from the systematics of experimental data. The strength of the residual interaction, as well as the effective proton and neutron charges and gyromagnetic ratios were close to the values used in the case of ^{116}Sb [9].

The energy spectrum of the ^{120}Sb states is presented in fig. 1. As the figure shows, the main features of the energy spectrum have been well reproduced by the model calculations.

The known experimental and calculated IBFFM electromagnetic moments of ^{120}Sb (table 1) as well as the δ^2 mixing and the gamma ray branching ratios agree reasonably well.

This work was supported partly by the National Science Foundation (OTKA).

Table 1. Magnetic dipole (μ in μ_N) and electric quadrupole (Q in eb) moments of some ^{120}Sb states.

Moments	1_1^+ (ground) $\pi d_{5/2}\nu d_{3/2}$	3_1^+ (78 keV) $\pi d_{5/2}\nu s_{1/2}$	8_1^- ($T_{1/2}$=5.76 d) $\pi d_{5/2}\nu h_{11/2}$
μ_{exp} [5]	±2.34(22)	+2.584(6)	±2.34(4)
μ_{IBFFM}	+2.32	+2.64	+2.51
Q_{exp} [5]		±0.41(4)	
Q_{IBFFM}		−0.47	

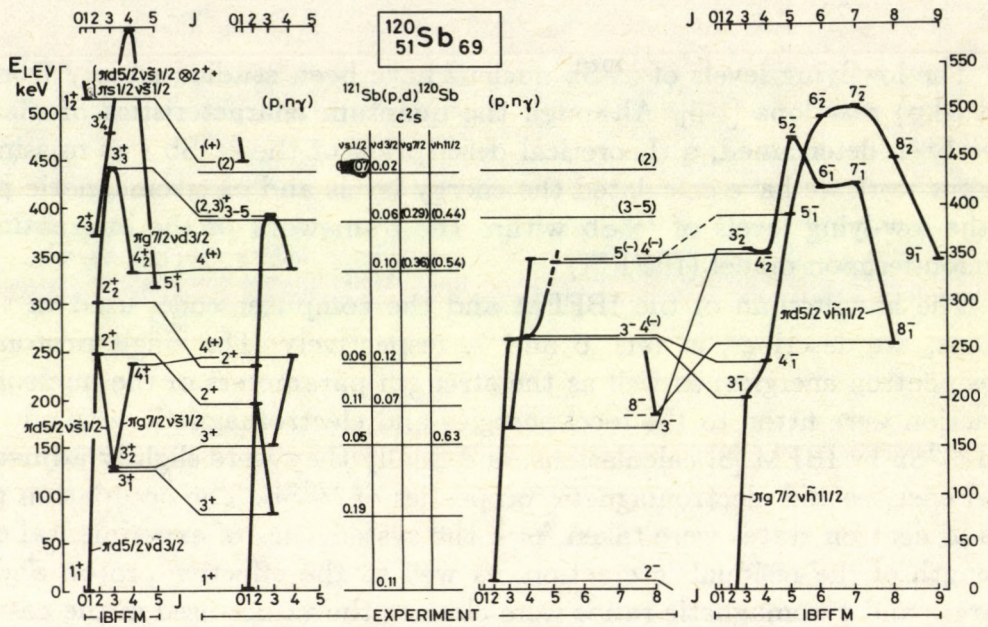

Fig. 1. The IBFFM energy spectrum of ^{120}Sb in comparison with the experimental data [2,3]. The solid lines connect levels, for which the main components of the wave functions belong to the same p-n multiplet. The abscissa is scaled according to J(J+1), where J is the spin of the state.

References

1. M.Adachi et al., Nucl.Phys. **A314** (1979) 80
2. R. A. Emigh et al., Z. Phys. A **308** (1982) 173
3. R. A. Emigh et al., Z. Phys. A **308** (1982) 165
4. A. Hashizmue et al. Nucl. Data Sheets **52** (1987) 641
5. P. Raghavan, Atomic Data and Nuclear Data Tables **42** (1989) 189
6. V. Paar, in In-Beam Nuclear Spectroscopy, ed. Zs. Dombrádi and T. Fényes, vol. 2 (Akad. Kiadó, Budapest, 1984) p. 675
7. S.Brant, V. Paar, D. Vretenar, Computer code IBFFM/OTQM (Institut für Kernphysik, KFA, Jülich, 1985) unpublished
8. F. Iachello and O. Scholten, Phys Rev. Lett. **43** (1979) 679; V. Paar et al., Nucl. Phys. **A378** (1982) 41
9. Z. Gácsi et al., ATOMKI Preprint 9-1990 (MTA Atommagkutató Intézet, Debrecen, 1990)

STRUCTURE OF THE ^{122}Sb NUCLEUS

T. Fényes and Zs. Dombrádi

It has been shown that the interacting boson- fermion-fermion model(IBFFM) is able to give account of the main features of the structure of ^{116}Sb [1] and ^{120}Sb [2] low-lying levels. In the present work we have extended the IBFFM calculations on ^{122}Sb.

The structure of the ^{122}Sb nucleus has been studied earlier in refs. 3-7. The present calculations have been performed in a similar way, using the same computer program as in the case of ^{116}Sb [1] and ^{120}Sb [2]. The energy level spectrum is presented in fig.1. As the figure shows, reasonable agreement has been obtained between experimental and theoretical results.

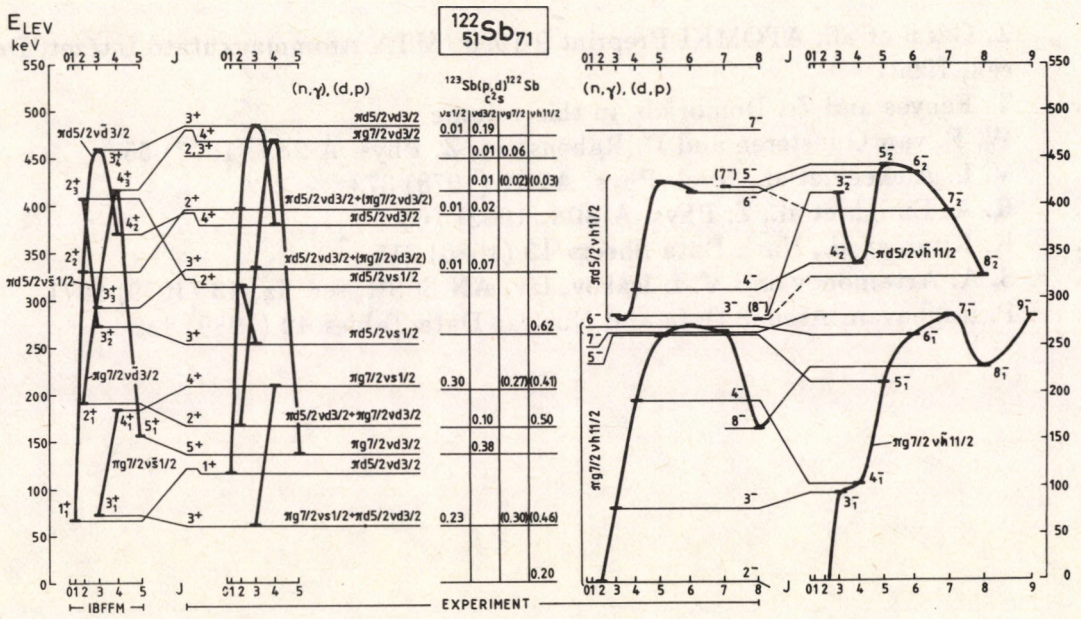

Fig. 1. The low-lying levels of ^{122}Sb. The experimental data have been taken from refs 4,5. The abscissa is scaled according to J(J+1), where J is the spin of the state.

The experimental and calculated electromagnetic moments are presented in table 1.

This work was supported partly by the National Science Foundation (OTKA). We are indepted to Prof. Dr. V. Paar, as well as to Drs. S. Brant and D. Vretenar for useful discussions.

Table 1. Magnetic dipole (μ in μ_N) and electric quadrupole (Q in eb) moments of some ^{122}Sb states.

Moments	2_1^- (ground) $\pi g_{7/2}\nu h_{11/2}$	3_1^+ (61 keV) $\pi g_{7/2}\nu s_{1/2}$	5_1^+ (137 keV) $\pi g_{7/2}\nu d_{3/2}$
μ_{exp} [8]	−1.905(20)	+2.983(12)	+3.05(10)
μ_{IBFFM}	−2.37	+3.09	+3.03
Q_{exp} [8]	+0.85(11)	±0.41(4)	
Q_{IBFFM}	−0.12	−0.48	

References

1. Z. Gácsi et al., ATOMKI Preprint 9-1990 (MTA Atommagkutató Intézet, Debrecen, 1990)
2. T. Fényes and Zs. Dombrádi, in this volume
3. W. F. van Gunsteren and D. Rabenstein, Z. Phys. A **282** (1977) 55
4. V. L. Alexeev et al., Nucl. Phys. **A297** (1978) 373
5. R. A. Emigh et al., Z. Phys. A **308** (1982) 165
6. K. Kitao et al., Nucl. Data Sheets **49** (1986) 315
7. S. A. Artamonov and V. I. Isakov, Izv. AN SSSR, ser. fiz. **43** (1979) 2071
8. P. Raghavan, Atomic Data and Nuclear Data Tables **42** (1989) 189

IBFFM DESCRIPTION OF ^{124}Sb

T. Fényes and Zs. Dombrádi

The level scheme of the ^{124}Sb has been studied formerly mainly from (p,nγ), (n,γ) and (d,p) reactions [1-4]. As a result of earlier works more then 60 excited states have been observed at this nucleus and also the spins and parities have been determined for many states. In the present work we have calculated the energy spectrum and electromagnetic moments of ^{124}Sb in the framework of the interacting boson-fermion-fermion model (IBFFM). The calculations have been performed in a similar way as in the case of ^{116}Sb [5]. The energy spectrum is presented in fig. 1.

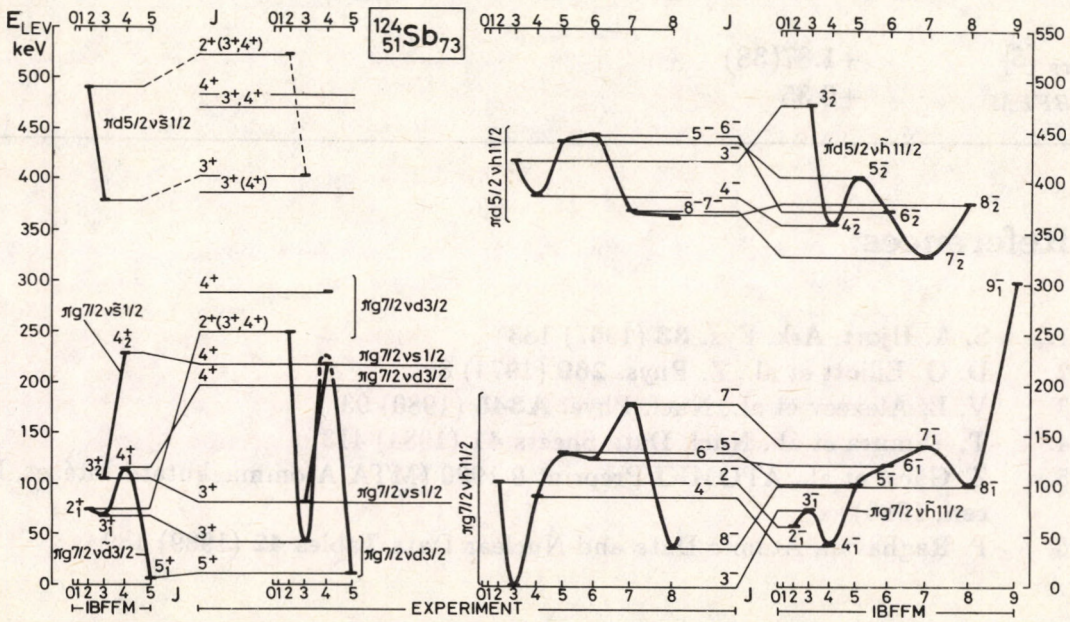

Fig. 1. The IBFFM and experimental [3] energy spectrum of the low lying states of ^{124}Sb. The abcissa is scaled according to J(J+1), where J is the spin of the state.

The wave functions are in general very complex, nevertheless in the low-lying states usally one of the proton-neutron components is dominating. The energy splitting of the $\pi g_{7/2}\nu s_{1/2}$ and $\pi d_{5/2}\nu s_{1/2}$ doublets shows a quite regular systematic behavior in ^{116,120,122,124}Sb nuclei. At the same time the splitting of the ^{124}Sb $\pi g_{7/2}\nu d_{3/2}$, $\pi g_{7/2}\nu h_{11/2}$ and $\pi d_{5/2}\nu h_{11/2}$ multiplets is far from the pure parabolic form, which is characteristic for the (quasi)particle-core dynamical interaction. The occupation probability of the $\nu d_{3/2}$ and $\nu h_{11/2}$ neutron subshells in ^{124}Sb is

close to 0.5. In this case the exchange interaction plays an important role. The reasonable agreement of the experimental and theoretical level schemes shows, that the IBFFM is capable for the description of this irregular energy splitting, too.

The electromagnetic moments are given in table 1.

Table 1. Magnetic dipole (μ in μ_N) and electric quadrupole (Q in eb) moments of some ^{124}Sb states.

Moments	3_1^- (ground) $\pi g_{7/2}\nu h_{11/2}$	3^+ (41 keV)	6_1^- (125 keV) $\pi g_{7/2}\nu h_{11/2}$
μ_{exp} [6]	$\pm 1.20(2)$	$+2.970(33)$	$+0.384(12))$
μ_{IBFFM}	-1.23	$+2.32\ \pi g_{7/2}\nu d_{3/2}\ 3_1^+$	$+0.35$
		$+2.91\ \pi g_{7/2}\nu s_{1/2}\ 3_2^+$	
Q_{exp} [6]	$+1.87(38)$		
Q_{IBFFM}	$+0.35$		

References

1. S. A. Hjort, Ark. Fys. **33** (1967) 183
2. D. O. Elliott et al., Z. Phys. **269** (1974) 89
3. V. L. Alexeev et al., Nucl. Phys. **A345** (1980) 93
4. T. Tamura et al., Nucl. Data Sheets **41** (1984) 413
5. Z. Gácsi et al., ATOMKI Preprint 9-1990 (MTA Atommagkutató Intézet, Debrecen, 1990)
6. P. Raghavan, Atomic Data and Nuclear Data Tables **42** (1989) 189

Collective Bands in ^{128}Ce *

B.M.Nyakó[1,2], G.Cata-Danil[2,3], J.Gizon[2], S.André[2], V.Barci[2], D.Bucurescu[3],

D.Curien[4], C.Foin[2], J.Genevey[2], A.Gizon[2], L. Hildingsson[5],

W.Klamra[5], J.C.Merdinger[2], L.Zolnai[1]

The knowledge of the level structure of ^{128}Ce was fragmentary since only the yrast band and some additional side-levels were determined [1]. Preliminary results from an experiment performed to identify further collective states in this nucleus are reported here.

The nucleus ^{128}Ce was produced in the reaction ^{94}Mo(^{37}Cl,p2n) at 158 MeV with the MP Tandem accelerator at CRN Strasbourg using two stacked self-supporting targets (0.62 mg·cm^{-2} thickness each.) Gamma-rays were detected by means of the "Chateau de Cristal" array equipped with eight 70% and three 20% coaxial Ge-detectors and a planar diode. $3\cdot10^6$ γ-γ fold-sum energy coincidence events have been recorded.

Five collective bands have been observed (see figure). The yrast band (2) is seen up to 28^+ with a crossing at $\hbar\omega = 0.315$ MeV. This frequency and an aligned angular momentum of i≈8.5 $\hbar$ associated with the alignment of a pair of $h_{11/2}$ quasi-protons. Bands (3) and (5) have tentatively assigned bandheads of 5^- and 4^-, respectively and could be based on two-quasiproton configurations. The frequency ($\hbar\omega$=0.43 MeV) at which a peak appears on the $J^{(2)}(\hbar\omega)$ plot of band (3) is consistent with the alignment of two $h_{11/2}$ quasi-neutrons.

Two more bands feeding to yrast at 4^+ and one feeding to 10^+ are under further studies.

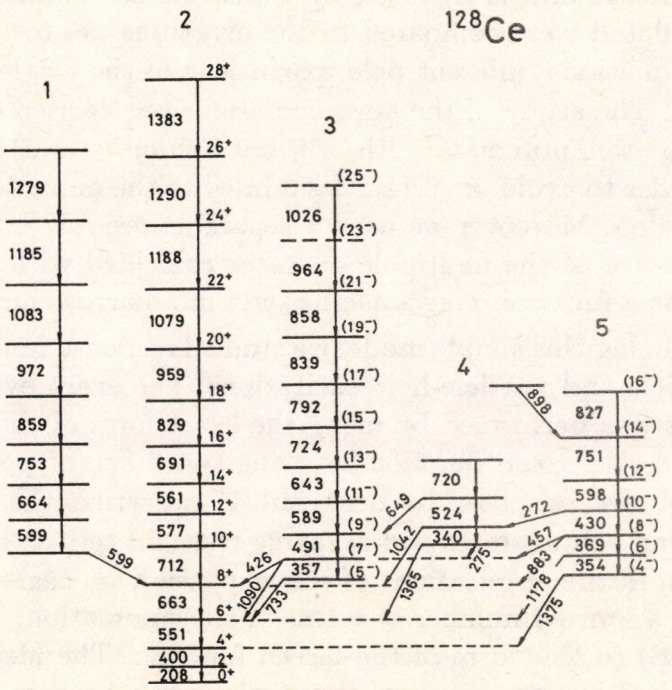

Partial decay scheme of ^{128}Ce

Reference:

* Contribution to the International Conference on High Spin Physics and Gamma-Soft Nuclei, Pittsburg (USA) September 1990

1. Institute of Nuclear Research, Debrecen, Hungary
2. Institut des Sciences Nucléaires, Grenoble, France
3. Institute of Atomic Physics, Bucharest, Romania
4. Centre de Recherches Nucléaires, Starsbourg, France
5. Manne Siegbahn Institute of Physics, Stockholm, Sweden

[1] J.L.S. Carvalho et al., Phys. Rev. C31 (1985) 1049

Approximations in calculating response functions

T. Vertse, P. Curutchet *, R.J. Liotta *

The effect of an external field on a nucleus can be characterized by the response function which is a complex function constructed from the operator of the field and the Green function of the system concerned. The particle-hole response functions has crutial importance in the theoretical description of the particle decay of the giant resonances which raised considerable attention recently. Continuum effects play important role in these processes and in their usual continuum RPA (CRPA) description the resolvent has to be calculated at many energy values. In order to speed up the calculations we have studied different approximations where the continuum is replaced by a discrete set of states and the response function calculated were compared to the exact one i.e. to the CRPA result. In these approximations different pole expansions of the single-particle Green function were used. The study of the approximations was carried out in a very simple model. A square well potential (with/without Coulomb term) was used as diagonal potential in order to avoid uncertainties related to the numerical solution of the Schrödinger equation. Moreover we used a separable residual interaction where the radial dependence of the multipole operator coincided with that of the external field and it was a function nonvanishing only in a narrow surface region.

Using this simple model we studied response functions corresponding to single-particle and particle-hole excitations. The exact evaluation of the response functions was performed by using the exact form of the Green function and we evaluated the Green function by using two different pole expansions. In one of them which was proposed by Berggren [1] one writes the Green function as a sum containing bound states and decaying resonant terms plus an integral along a complex path. In the applications of this expansion we neglected the integral and included only a limited number of terms in the summation. We call "Berggren expansion" (BGE) to this form of the Green function. The idea behind the BGE is that the physical resonances, i. e. those which can be seen in the response function, are narrow. Therefore if one chooses the integration path far enough from the real axis its contribution would only affect the continuous background. The attractive feature of the BGE is that it provides a set of linear equations for the complex energies of the particle-hole resonances in a similar way as done in the RPA. The resulting formalism was called resonant RPA in ref.[2]. In the Mittag–Leffler expansion (MLE) which is the other expansion we used one also writes the Green function as an infinite sum of terms corresponding to its all possible poles on the complex k-plane (bound, antibound and both type of resonant states). There is not any integral contribution to the MLE, which is a great convenience. But its validity has been proved only for potentials of a finite range, thus excluding the important Coulomb potential.

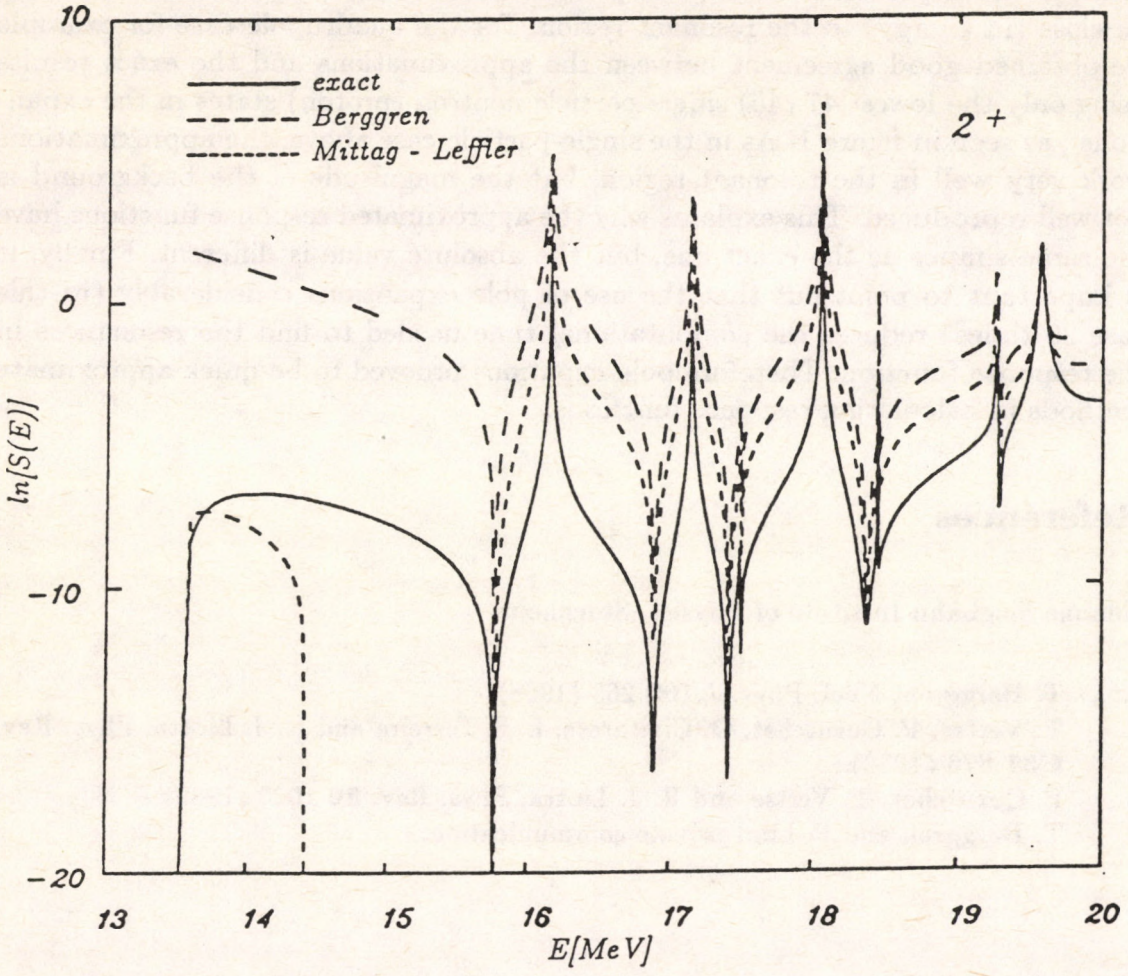

Fig. 1. Quadrupole particle-hole strength function calculated exactly and within the Berggren and Mittag-Leffler expansions.

We applied both expansions to calculate single-particle and particle-hole response functions. For the single-particle case we found that for positive energies the results of these two expansions agree well with the corresponding exact results if a large number of terms is used in the expansions. Moreover we found that in the resonant region using only one term in the expansions one gets an excellent agreement with the exact result. For negative energies the BGE did produce a false non-zero imaginary part while the MLE did not. We also observed that the MLE reproduces the exact results not only for neutrons but for protons too. This gave a hint that this type of expansion might be valid for the case of the long range Coulomb interaction as well [3]. Using the experience we gained in the studies of the single-particle response function we performed an analysis of particle-hole response functions. In the corresponding BGE and MLE approximations we used the single-particle propagator of the CRPA as in the single-particle case. Since the main goal was to investigate the possibility of obtaining the energies of the resonances fast and with reasonable accuracy we used a very limited number of

terms in the expansions. We kept only those terms in the expansions which would be close (in energy) to the resonant region. For the quadrupole case for example we obtained good agreement between the approximations and the exact results using only the lowest 47 (45) single-particle neutron (proton) states in the expansions , as seen in figure 1. As in the single-particle case above, the approximations work very well in the resonant region, but the magnitude of the background is not well reproduced. This explains why the approximated response functions have the same shapes as the exact one, but the absolute value is different. Finally, it is important to point out that the use of pole expansions considerably (in this case 26 times) reduces the computational time needed to find the resonances in the response function. Therefore pole expations prooved to be quick approximate methods in calculating response functions.

References

*Manne Siegbahn Institute of Physics, Stockholm

1. T. Berggren, Nucl. Phys. **A109** 265 (1968).
2. T. Vertse, P. Curutchet, O. Civitarese, L. S. Ferreira and R. J. Liotta, Phys. Rev. **C37** 876 (1988).;
   P. Curutchet, T. Vertse and R. J. Liotta, Phys. Rev. **39** 1020 (1989).
3. T. Berggren and P. Lind private communication.

Cluster model of few-nucleon systems

A. Csótó, A. T. Kruppa, R. G. Lovas, K. F. Pál and K. Varga

In recent years we have done extensive work on the description of the ground state of the nucleus ^{6}Li [1–4]. We treat all nucleonic degrees of freedom explicitly and the Pauli principle as well as the centre-of-mass motions exactly. Our most realistic model depicts ^{6}Li as a pair of excitable α and deuteron clusters interacting. We use a central effective nucleon–nucleon force. Within this framework the approximation consists in truncations of the state spaces of the clusters and of the intercluster relative motion. We describe the α and deuteron clusters as superpositions of translationally invariant 0s harmonic-oscillator shell-model states of different size parameters. For the ground state of the deuteron this amounts to an exact treatment considering that a central force can only produce a spherically symmetrical deuteron ground state. A central force does not give rise to angular momentum mixing in the relative α–d motion either. So the ^{6}Li ground state can be characterized by orbital momentum $L = 0$ and summed nucleon spin $S = 1$.

We have calculated the electromagnetic and fragmentation properties. The known values of these properties are reproduced reasonably well, with a few notable exceptions. In particular, we have shown that a gross discrepancy in the α+d spectroscopic factor between the macroscopic α+p+n three-particle approaches and our microscopic model is mainly caused by the ill-treatment of the Pauli effects in the spectroscopic factor formula of the three-particle models [4]. The agreement with experiment is least convincing in the spectral function for the ^{6}Li $\rightarrow ^5$He +p disintegration in the ^{5}He energy region below the t+d threshold [3]. We concluded that, to reproduce the ^{5}He+p spectral function deduced from the ^{6}Li(e, e'p)^{5}He experiment, we need to include the ^{5}He+p clusterization explicitly. Furthermore, we have to use a non-central force and allow for L and S mixing.

We have, however, obtained good agreement in the spectral function over the t+d threshold, especially in the region of the famous $J^\pi = \frac{3}{2}^+$ resonance [3]. This is surprising because in our model this resonance is purely of t+d structure with $S = \frac{3}{2}$, $L = 0$, while the well-known extremely large t+d $\rightarrow$ α+n cross section in this resonance seems to indicate a strong coupling with the α+n ($S = \frac{1}{2}$, $L = 2$) channel.

To understand these observations and to broaden the scope of our study, we have developed a general formalism for two interacting clusters, of 0s and 0p nucleons, bound to or colliding with each other. We are also working on a microscopic α+p+n model for the bound states of these three clusters. These

formalisms allow to use tensor as well as spin–orbit interactions. Applications to the problems outlined above are forthcoming.

References

1. K. Varga and R. G. Lovas, ATOMKI Ann. Report, 1989, p. 15;
R. G. Lovas, A. T. Kruppa and R. G. Lovas, ATOMKI Ann. Report, 1989, p. 17
2. R. Beck, F. Dickmann and A. T. Kruppa, Phys. Rev. **C30** (1984) 1044;
R. Beck, F. Dickmann and R. G. Lovas, Nucl. Phys. **A446** (1985) 703;
A. T. Kruppa, R. G. Lovas, R. Beck and F. Dickmann, Phys. Lett. **179B** (1986) 317;
R. Beck, F. Dickmann and R. G. Lovas, Ann. Phys. (N.Y.) **173** (1987) 1;
R. G. Lovas, A. T. Kruppa, R. Beck and F. Dickmann, Nucl. Phys. **A474** (1987) 451;
A. T. Kruppa, R. Beck and F. Dickmann, Phys. Rev. **C36** (1987) 327
3. J. B. J. M. Lanen, R. G. Lovas, A. T. Kruppa, H. P. Blok, J. F. J. van den Brand, R. Ent, E. Jans, G. J. Kramer, L. Lapikás, E. N. M. Quint, G. van der Steenhoven, P. C. Tiemeyer and P. K. A. de Witt Huberts, Phys. Rev. Lett. **63** (1989) 2793;
R. G. Lovas, A. T. Kruppa and J. B. J. M. Lanen, Nucl. Phys. **A516** (1990) 325
4. K. Varga and R. G. Lovas, Phys. Rev. C, in press

Alpha decay in a mixed shell-and-cluster model

R. J. Liotta †, R. G. Lovas, K. Varga and T. Vertse

†Manne Siegbahn Institute of Physics, Stockholm

We cannot say that we understand the dynamics of α decay until we are able to predict absolute α decay rates without any open or hidden assumption on the probability of α-particle pre-formation. Obviously, such a model should treat the valence nucleons of the parent nucleus microscopically. Notwithstanding a long history of the microscopic models of α decay, the problem is still unsettled.

Of course, we know a lot of the α-particle formation. For instance, it is very likely that the major part of the correlation that causes the α-particle formation comes from the proton–proton and neutron–neutron pair correlations [1]. A really fundamental approach should, however, not use such fragments of knowlegde as input. Rather, it should reproduce them if they are correct. A fundamental approach thus calls for the shell model. The shell-model techniques are, however, challenged by the description of α decay very severely. The matter is that the model wave function of the parent nucleus should be correct in the region of the configuration space in which the α cluster is far enough from the residual nucleus for the nuclear interaction as well as Pauli exchanges to be negligible. This can only be achieved in a pure shell model with bases of extremely large dimensions. It is for this reason that even the best existing shell-model calculations tend to underestimate the decay rate [2].

We improve on the shell model by complementing its basis by cluster-model basis states of the type of α particle plus residual nucleus. With the core assumed to be infinitely heavier than the α particle, the cluster-model states look like shell-model states that involve single-particle orbits not orthogonal to those occupied by the core nucleons and partially occupied by the valence nucleons. This makes it possible to reformulate the cluster model in conformity with the shell model. It is only the valence nucleons that are to be treated explicitly, and the Pauli principle can be incorporated in an orthogonality condition exactly.

Our approach can be said to be unbiassed in favour of α decay inasmuch as the shell-model basis is large enough. We will use as large a shell-model basis as we can. We hope that the cluster-model states will not become overpopulated as a result of the lack of certain shell-model configurations. Our approach differs from that of Steinmayer, Sünkel and Wildermuth just in this respect [3]. In that work the ordinary shell-model configurations are very much underrepresented. Moreover,

none of the cluster-model basis elements is a decaying single-particle state by itself. Unlike Okabe [4], we do not assume the existence of a single-particle model state near the position of the physical decaying state. Nevertheless, if such a model state is realistic, it will emerge as a combination of our model states.

An actual application of the model to the decay of ^{212}Po is under way.

References

1. G. Dodig-Crnković, F. A. Janouch, R. J. Liotta and L. J. Sibanda, Nucl. Phys. **A444** (1985) 419;
   A. Insolia, R. J. Liotta and E. Maglione, Europhys. Lett. **7** (1988) 209
2. I. Tonozuka and A. Arima, Nucl. Phys. **A323** (1979) 45
3. T. Steinmayer, W. Sünkel and K. Wildermuth, Phys. Lett. **125B** (1983) 437
4. S. Okabe, Proc. 5th Int. Conf. on Cluster ing Aspects in Nucl. and Subnucl. Systems, J. Phys. Soc. Japan **58** (1989) Suppl. p. 516

New Classes of Solvable Potentials

G. Lévai

The application of supersymmetric quantum mechanics (SUSYQM) [1] to solvable potentials of nonrelativistic quantum mechanics turned out to be remarkably successful. It helped to view old potential problems from a new angle and stimulated further study of this seemingly exhausted field. The introduction of the concept of shape–invariance [2] was another remarkable development. Potentials satisfying the shape–invariance requirement proved to be soluble, practically without explicit reference to the Schrödinger equation. It was found that the most well–known potentials are shape–invariant, nevertheless the question whether there are any other shape–invariant potentials besides the known ones, is still unanswered [3].

In a previous publication [4] we have performed a search for shape–invariant potentials using a simple method of finding solvable potentials [5] and linking it with the formalism of SUSYQM. This method proved to be successful in identifying and classifying shape–invariant potentials. Each potential class was associated with a simple differential equation of the function $g(x)$, which we used to transform the Schrödinger equation (in one dimension) into the differential equation of some special function of mathematical physics. This method can be used to generate non–shape–invariant, but solvable potentials as well. Recently we have investigated [6] a potential class of this kind related to the Jacobi polynomials.

This family of potentials (called the *PIII* class) depends on three parameters, one of which (C) is a scaling parameter of the energy (and the coordinate), while the two others (p and q) define the shape of the potential:

$$V(x) = C\left(-q(2p-1) + g(x)\left(p^2 - \frac{1}{16}\right) + g^{-1}(x)\left(q^2 - p + \frac{5}{8}\right) - \frac{5}{16}g^{-3}(x)\right).$$

Here the internal function $g(x)$ is implicitly defined by the inverse $x(g)$ function:

$$x(g) = C^{-1/2}\left(tanh^{-1}(g^{1/2}) - tan^{-1}(g^{1/2})\right).$$

The coordinate x is restricted to positive values only, so the *PIII* potentials can be interpreted as the radial part of central potentials in three dimensions. A characteristic feature of these potentials is their behaviour near the origo. Independently of the parameters they tend to $-\infty$ as $V(x) \simeq -5x^{-2}/36$. This numerical constant is not strong enough for the particle to "fall" into the attractive potential [7]. It was shown that these potentials can support only a finite number of bound states. Characteristic shapes (minima and maxima) of the potentials depending on the parameters p and q have been identified. The energy spectrum and the corresponding wave functions have been determined (for $l = 0$).

The supersymmetric partner of the general *PIII* potential has also been studied, and it was shown that it does not belong to the *PIII* potential family. (This is due to the structure of the wave functions, which contain the linear combinations

of two Jacobi polynomials in this case.) As an illustrative example, in Figure 1. we present $V_-(x) \equiv V(x)$ and its supersymmetric partner $V_+(x)$ for the parameters $p = 36$, $q = 20$ and $C = 1$, together with the squared modulus of the corresponding wave functions.

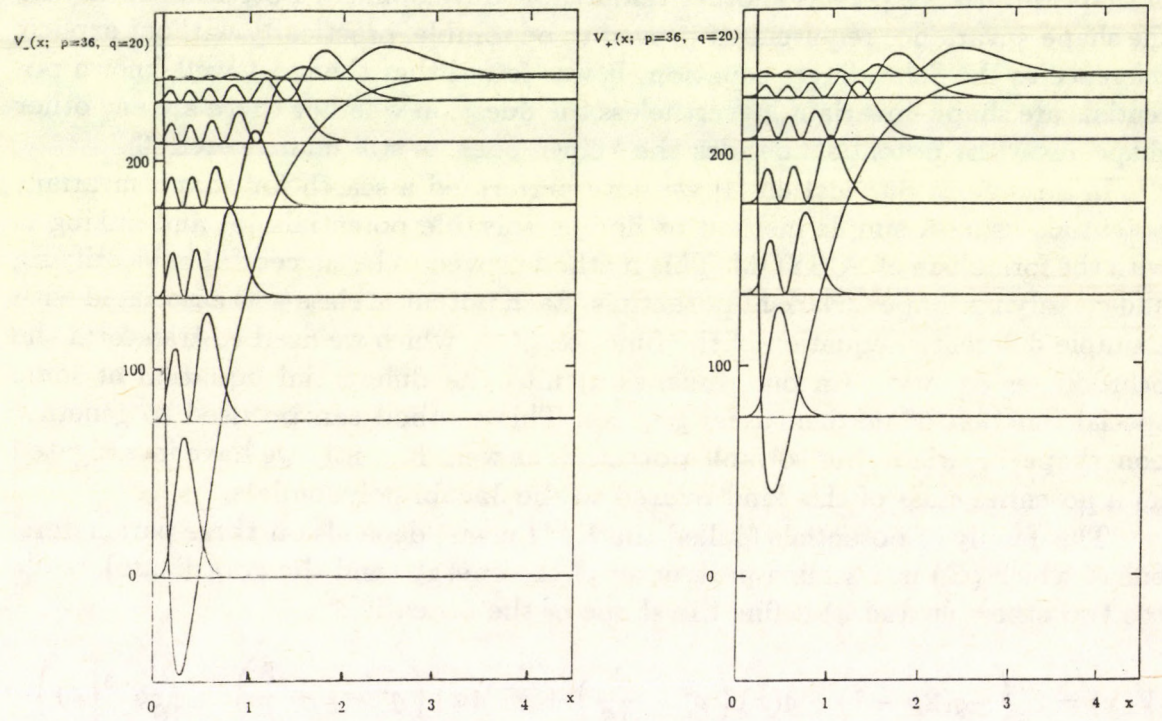

Fig. 1. The *PIII* potential and its supersymmetric partner for the parameters $p = 36$, $q = 20$ and $C = 1$, displayed together with the squared modulus of the wave functions. (The true behaviour of $V_-(x)$ can not be seen near the origo. $V_-(x)$ has a maximum at $x = 0.0077$ and tends to $-\infty$ in the $x \to 0$ limit.)

It was shown that the *PIII* potentials form a special subclass of the six parameter Natanzon potential class [8], similarly to the (two parameter) Ginocchio class potentials [9]. We have also pointed out similarities and differences between these two potential families. These considerations may help us to identify further subclasses of the Natanzon potentials and may serve as an aid for further investigations concerning the relationship between shape–invariance and solvability.

Without further discussion we also sketched a procedure by which further solvable potentials can be introduced in a similar fashion.

1. E. Witten: Nucl. Phys. **B188** 513 (1981)
F. Cooper, B. Freedman: Ann. Phys. (N. Y.) **146** 262 (1983)
A. A. Andrianov, N. V. Borisov, M. V. Ioffe: Phys. Lett. **105A** 19 (1984)
2. L. Gendenshtein: Zh. Eksp. Teor. Fiz. Pis. Red. **38** 299 (1983); (*JETP Lett.* **38** 356 (1983))
3. F. Cooper, J. N. Ginocchio, A. Khare: Phys. Rev. D **36** 2458 (1987)
4. G. Lévai: J. Phys. A:Math. Gen. **22** 689 (1989)
5. A. Bhattacharjie, E. C. G. Sudarshan: Nuovo Cim. **25** 864 (1962)
6. G. Lévai: J. Phys. A:Math. Gen. **24** 131 (1991)
7. L. D. Landau, E. M. Lifshitz: Quantum Mechanics, Oxford: Pergamon, 1977
8 G. A. Natanzon: Vest. Leningrad Univ. **10** 22 (1971); Teor. Mat. Fiz. **38** 146 (1979)
9. J. N. Ginocchio: Ann. Phys. (N. Y.) **152** 203 (1984); **159** 467 (1985)

Independent and Consistent Parametrization of Energy Eigenvalues and Cluster Spectroscopic Factor in the Vibron Model

J. Cseh†, G. Lévai and K. Katō‡

Recently we have introduced cluster spectroscopic factor in the vibron model [1]. Similarly to other physical quantities its operator (S_L) was obtained as a series expansion of the boson operators. In fact, S_L has a form similar to that of the Hamiltonian.

One of the consequences of obtaining the physical quantities in the interacting boson models by series expansions is that the number of free paarameters can be large. When the same two or more operators appear in the expression of two different quantities, it is possible and advantageous to use them with the same relative weights. This question has been discussed in relation with the quadrupole operator appearing in the Hamiltonian and in the electric transition operator $T(E2)$ of the IBM–1 [2]. That parametrization, called consistent–Q formalism, reduces the number of parameters by one.

Here we can raise a similar question addressed to the relative weights of the zeroth, first and second order operators of H and S_L. Specifically, when the $U(3)$ dynamical symmetry holds, the eigenvalues of these operators in the corresponding basis are

$$E = \beta L(L+1) + \gamma n_\pi + \delta n_\pi^2 + \epsilon \qquad (1.a)$$

and

$$S_L = \beta_2 L(L+1) + \alpha_1 n_\pi + \alpha_2 n_\pi^2 + \alpha_0. \qquad (1.b)$$

We have considered the 0_1^+, 0^- and 0_4^+ bands of ^{20}Ne, as an example of core–plus–alpha–particle system, and applied equations $(1.a)$ and $(1.b)$ with independent and with consistent parametrization. In the latter case the

$$\frac{\alpha_0}{\alpha_1} = \frac{\epsilon}{\gamma}, \qquad \frac{\alpha_2}{\alpha_1} = \frac{\delta}{\gamma} \qquad (2)$$

constraints have been used. The experimental data seem to support the consistent parametrization, as shown in Figure 1.

† Alexander von Humboldt fellow; present address: Institut für Theoretische Physik, Justus–Liebig Universität, Giessen, Germany

‡ Department of Physics, Hokkaido University, Sapporo, Japan

1. J. Cseh, G. Lévai, K. Katō: ATOMKI Ann. Rep. 1989 p. 24
2. D. D. Warner and R. F. Casten: Phys. Rev. C **28** 1798 (1983)
3. J. Cseh, G. Lévai, K. Katō: Phys. Rev. C, in press

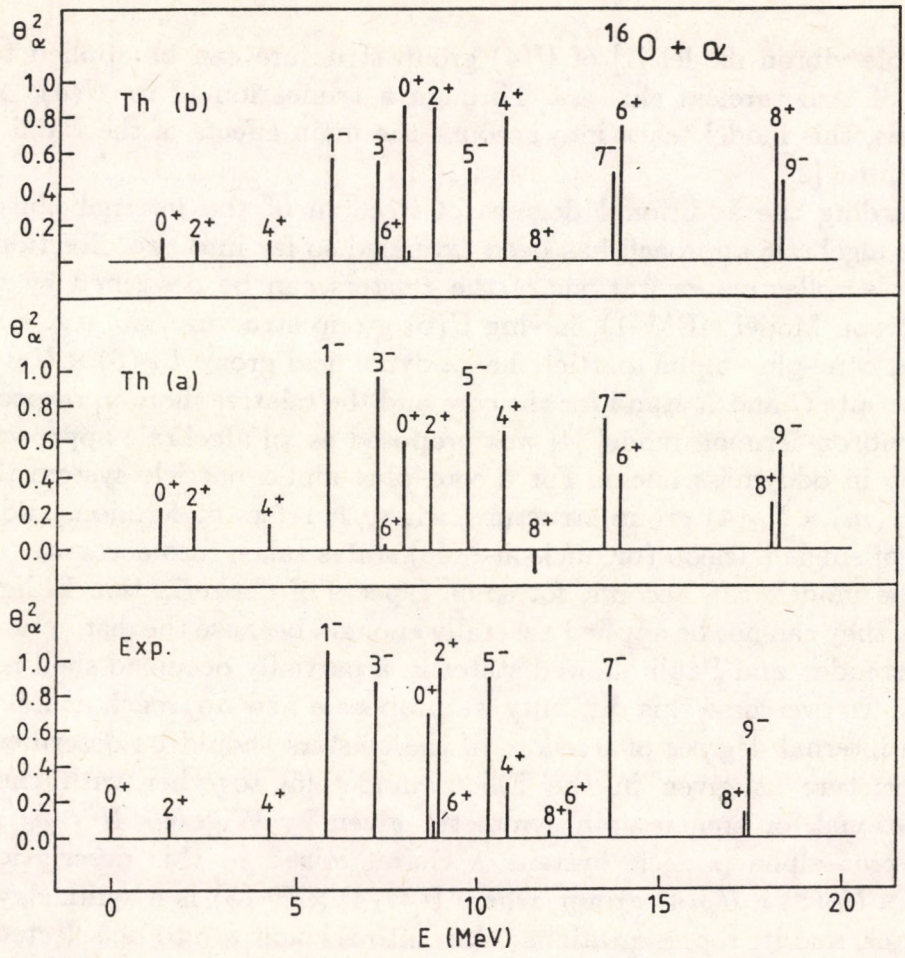

Fig. 1.. Energy spectrum and alpha–particle spectroscopic factors of cluster states in ^{20}Ne. Experimental data for the 0^+_1, 0^- and 0^+_4 bands, and vibron model calculation with independent (a) and consistent (b) patrametrization.

Non–closed–shell Clusters in Light Nuclei: An Algebraic Treatment

J. Cseh†

The simple vibron model [1] of $U(4)$ group structure can be applied to nuclear systems of structureless clusters. Through a truncation of its $U(4) \supset U(3) \supset O(3)$ basis, this model takes into account the main effects of the Pauli exclusion principle, too [2].

Regarding the additional degrees of freedom of the internal cluster structure, the algebraic approach has been extended so far into two directions. *i)* The quadrupole collective excitations of the clusters can be described by the Interacting Boson Model (IBM–1), having $U(6)$ group structure. So, e.g. a system of deformed core–plus–alpha–particle has a dynamical group $U_C(6) \times U_R(4)$, where the subscripts C and R stand for the core and the relative motion, respectively [3]. *ii)* The vibron–fermion model [4] was proposed as an algebraic approach to clusterization in odd–mass nuclei. For a core–plus–alpha–particle system this model has a $U_F(m) \times U_R(4)$ group structure, where F refers to fermion, and m is the number of single nucleon (or nucleon–hole) states taken into account.

These models can account for some aspects of clusterization in light nuclei, however, they can not be applied generally enough, because the distinction between Pauli forbidden and Pauli allowed states in a partially occupied shell is not done properly. To overcome this difficulty we propose a new approach as follows.

The internal degrees of freedom of the clusters should be described by their $U(3)$ structure as given in the Elliott model [5] together with their proper permutational, or spin–isospin symmetry given by Wigner's $U^{ST}(4)$ group [6]. A core–plus–alpha–particle system is characterized in this description by the $U_C^{ST}(4) \times U_C(3) \times U_R(4)$ group, where $U_C^{ST}(4) \times U_C(3)$ is a symmetry group of the cluster, and its representations taken into account are to be selected by physical arguments. The $l = 1$ bosons here (both in $U_C(3)$ and in $U_R(4)$) represent harmonic oscillator excitation quanta.

The allowed states of the model space are selected by the requirement of a matching condition between the cluster model basis and the shell model basis. In other words we keep only those states in this cluster model which appear also in a properly antisymmetrized shell model basis. Specifically, we take into account only those states, for which the representation labels of the $U_C^{ST}(4)$ and $U(3)$ groups of the group chain

$$U_C^{ST}(4) \times U_C(3) \times U_R(4) \supset U_C^{ST}(4) \times U_C(3) \times U_R(3) \supset U_C^{ST}(4) \times U(3)$$

match with those of the shell model configurations having the same number of oscillator quanta.

The shell model states are contaminated with the center of mass motion. In the $U(3)$ basis, however, it can be separated [7], so our model space can also be built up in such a way that it is free from the spurious motion.

The physical operators of this model are to be constructed in a similar way as in other interacting boson models of coupled degrees of freedom.

Occasionally this model can give the same description as the $U_C(6) \times U_R(4)$ or the $U_F(m) \times U_R(4)$ model, but it has a larger range of applicability.

† Alexander von Humboldt fellow; present address: Institut für Theoretische Physik, Justus–Liebig Universität, Giessen, Germany

1. F. Iachello: Phys. Rev. C **23** 2778 (1981);
F. Iachello, R. D. Levine: J. Chem. Phys. **77** 3046 (1982)
2. J. Cseh, G. Lévai: Phys. Rev. C **38** 972 (1988);
J. Cseh: J. Phys. Soc. Jpn. Suppl. **58** 604 (1989);
J. Cseh, G. Lévai, K. Katō: Phys. Rev. C, in press
3. H. J. Daley, F. Iachello: Ann. Phys. (N. Y.) **167** 73 (1986)
4. G. Lévai, J. Cseh: Phys. Rev. C, accepted for publication
5. J. P. Elliott: Proc. Roy. Soc. **A245** 128 (1958); 562 (1958);
M. Harvey: Adv. Nucl. Phys. **1** 67 (1968)
6. E. P. Wigner: Phys. Rev. **51** 106 (1937)
7. D. M. Brink, G. F. Nash: Nucl. Phys. **40** 608 (1963);
K. T. Hecht: Nucl. Phys. **A170** 34 (1971)

Some Group Theoretical Aspects of the Vibron–Fermion Model

G. Lévai and J. Cseh†

A straightforward generalization of the interacting boson models is their extension towards fermionic degrees of freedom. This allows the coupling of collective (bosonic) and single particle (fermionic) excitations by means of algebraic manipulations. This treatment was first applied to the Interacting Boson Model, and the Interacting Boson–Fermion Model was introduced in a series of publications [1].

The similar fermionic extension of the Vibron Model [2] was carried out only for one of its dynamical symmetries (the $O(4)$ limit), and the Vibron–Electron Model was introduced [3] as an algebraic approach to electronic, vibrational and rotational excitations of diatomic molecules. Recently we have introduced [4] the fermionic extension of the $U(3)$ limit of the Vibron Model and proposed its application to the cluster structure of some odd–mass nuclei. We have also proposed the name Vibron–Fermion Model (VFM) for the general fermionic extension of the Vibron Model, involving both the Vibron–Electron Model and our approach (with $O(4) \times U(2)$ and $SU(3) \times U(2)$ group structure, respectively). Here we make a comparison of the dynamical symmetries of the IBFM and the VFM and discuss some group theoretical considerations concerning the fermionic generalization of the interacting boson models.

The mathematical formulation of the boson–fermion models is based on bosonic and fermionic operators, which are constructed as bilinear products of creation and annihilation operators written as spherical tensors: $B^{(L)}_{\kappa}(k,k') = [b^{\dagger}_{k} \times \tilde{b}_{k'}]^{(L)}_{\kappa}$ and $A^{(L)}_{\kappa}(j,j') = [a^{\dagger}_{j} \times \tilde{a}_{j'}]^{(L)}_{\kappa}$. These operators generate the $U^B(M)$ (bosonic) and $U^F(m)$ fermionic groups, respectively. (Here k, k' and j, j' are the angular momenta of the single particle states available for the bosons and fermions respectively, while M and m are the total number of these states.) Whenever the same groups appear in the bosonic and fermionic group chains, one can introduce boson–fermion dynamical symmetries by combining the corresponding bosonic and fermionic group generators. The fermionic group chain generally contains the product group $U^F_l(m/2) \times U^F_s(2)$, (which corresponds to the decomposition of j into orbital (l) and spin ($s = 1/2$) parts), and it is usually the fermionic orbital group to which the bosonic groups are coupled. With the exception of some more general cases to be mentioned later, the generators of the boson–fermion groups are written as $G^{(L)}_{\kappa}(l,l') = B^{(L)}_{\kappa}(l,l') + K^{(L)}_{\kappa}(l,l')$, where $K^{(L)}_{\kappa}(l,l')$ is a special linear combination of the operators $A^{(L)}_{\kappa}(j,j')$.

In Table 1. we presented the dynamical symmetries of the IBFM and the VFM and the formal mathematical analogies between them. These analogies are based on the similar structure of the group generators. We also displayed the set of generators associated with the analogous dynamical symmetries of two models. In the general $SU(3) \times U(2)$ case (for both the IBFM and the VFM) and in the

general $O(4)\times U(2)$ case (for the VFM,) the fermionic group generators are formed as linear combinations of the $K_\kappa^{(L)}(l,l')$ operators with $L=1$ and $L=2$.

Table 1. Summary of the dynamical symmetries of the IBFM and the VFM.

Generators	IBFM ($\lambda=2$)	VFM ($\lambda=1$)
$G^{(L)}(r,r')$	$U^B(6)\times U_l^F(6)\supset U(6)$	$U^B(4)\times U_l^F(4)\supset U(4)$
$r,r'=0,\lambda$	$j=\frac{1}{2},\frac{3}{2},\frac{5}{2};\quad l=0,2$	$j^\pi=\frac{1}{2}^+,\frac{1}{2}^-,\frac{3}{2}^-;\quad l^\pi=0^+,1^-$
General case	$SU^B(3)\times SU_l^F(3)\supset SU(3)$	$SU^B(3)\times SU_l^F(3)\supset SU(3)$
	$j=\frac{1}{2},\frac{3}{2},\ldots n+\frac{1}{2};$	$j^\pi=\frac{1}{2}^\pi,\frac{3}{2}^\pi,\ldots(n+\frac{1}{2})^\pi;\ \pi=(-)^n$
	$l=0$ or $1,\ldots n-2,\ n$	$l^\pi=0^\pi$ or $1^\pi,\ldots(n-2)^\pi,\ n^\pi$
$G^{(L)}(\lambda,\lambda)$	$U^B(5)\times U_l^F(5)\supset U(5)$	$U^B(3)\times U_l^F(3)\supset U(3)$
	$j=\frac{3}{2},\frac{5}{2};\quad l=2$	$j^\pi=\frac{1}{2}^-,\frac{3}{2}^-;\quad l^\pi=1^-$
General case		$O^B(4)\times O_l^F(4)\supset O(4)$
		$j^\pi=\frac{1}{2}^+,\frac{1}{2}^-\ldots(n-\frac{1}{2})^\pi;$
$G^{(L)}(\lambda,0)+$		$l^\pi=0^+,1^-,\ldots(n-1)^\pi;\ \pi=(-)^l$
$(-)^\lambda G^{(L)}(0,\lambda)$,	$O^B(6)\times O_l^F(6)\supset O(6)$	$O^B(4)\times O_l^F(4)\supset O(4)$
$G^{(L=odd)}(\lambda,\lambda)$	$j=\frac{1}{2},\frac{3}{2},\frac{5}{2};\quad l=0,2$	$j^\pi=\frac{1}{2}^+,\frac{1}{2}^-,\frac{3}{2}^-\quad l^\pi=0^+,1^-$

There are further possible ways of boson–fermion couplings. Some of these involve no decomposition of the fermionic angular momenta j; some others use "artifical" values for the spin s and therefore have a larger fermionic spin group; or, (in case of the IBFM) originate from the isomorphisms of some algebras (e.g. $o(5)\simeq sp(4)$ or $o(6)\simeq su(4)$). Since these are less important from the point of view of physical applications, we neglected them here, similarly to the dynamical symmetries involving the trivial angular momentum coupling.

† Alexander von Humboldt fellow; present address: Institut für Theoretische Physik, Justus–Liebig Universität, Giessen, Germany

1. F. Iachello, S. Kuyucak: Ann. Phys. (N. Y.) **136** 19 (1981);
R. Bijker, V. K. B. Kota: Ann. Phys. (N. Y.) **156** 110 (1984);
R. Bijker, F. Iachello: Ann. Phys. (N. Y.) **161** 360 (1985);
R. Bijker, V. K. B. Kota: Ann. Phys. (N. Y.) **187** 148 (1988);
2. F. Iachello: Phys. Rev. C **23** 2778 (1982);
F. Iachello, R. D. Levine: J. Chem. Phys. **77** 3046 (1982)
3. A. Frank, R. Lemus, F. Iachello: J. Chem. Phys. **91** 29 (1989)
4. G. Lévai, J. Cseh: Phys. Rev. C, accepted for publication;
G. Lévai, J. Cseh: submitted to the Phys. Rev C

Multi–level Model of the Structure of the Elementary Particles

E. Vatai

A multi–level model of elementary particles and interactions was developed [1], which is consistent with existing observations. Accepted theories of gravitation, electromagnetism and quantum mechanics are used only. The particles belonging to different levels are assumed to be similar in the sense that the change of the particle parameters, e.g., of the Planck constant ($\hbar_i$), charge (e_i), particle mass (m_i), etc., can be described as regular functions of the level number i. The existence of many particle levels allows us to bring the gravitational and Coulomb interaction of the proton to the same strength, if suitable change of the ratio e_i/m_i is chosen. The following level dependence of parameters was found in zeroth-order approximation: (a) $\alpha_i = e_i/\hbar_i c \sim 1/137 \sim$ const.; (b) $e_i/e_{i+1} \sim 137$ const.; (c) from (a) and (b) follows $\hbar_i/\hbar_{i+1} \sim 137^2 \sim$ const.; $e^{1+\gamma}/m_i \sim$ const.; where $1 \gg \gamma > 0$, in order to have $e_i^2/G_N m_{p,i} \sim 1$ when $i \to i_{lim}$; the dimension of the particles is determined by their Compton wave length: $\lambda_i = \hbar_i/m_i c \propto e_i$.

Basic entity of the model is the *yangyin*, which is a black hole formed by two black holes consisting of higher level photons polarized in opposite phase, each having the energy $E_{ph} = m_{ph}c^2$, where $m_{ph} = \sqrt{2/3}\, m_{pl}$ and $m_{pl} = 2.15 \times 10^{-5}$g is the Planck mass, and which are orbiting around their common c. m. with the speed of light (fig.1).

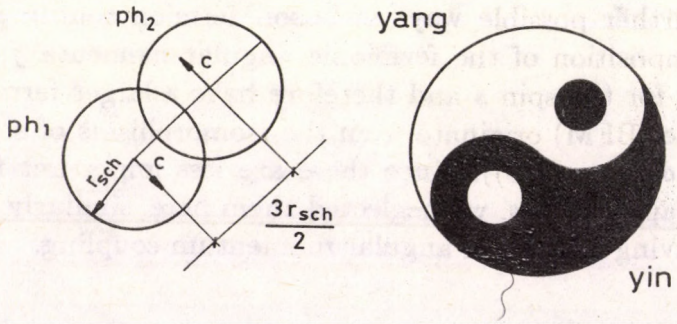

Fig. 1. The yangyin

Yangyins with synchronous or Planck frequency of photons ($r_{sch} = \lambda_{ph} = c/\upsilon_{ph}$) are pulsating dipoles. Three of such yangyins with phase delay $\pm 2\pi/3$ can give permanent or Coulomb field, therefore the *quark* is assumed to consist of three yangyins with total spin zero ($s_q = 0$), because the yangyins' spin $0 \leq s_{yy} \leq 4\hbar$ makes it difficult to form spin $\hbar/2$ in a symmetrical structure (fig. 2).

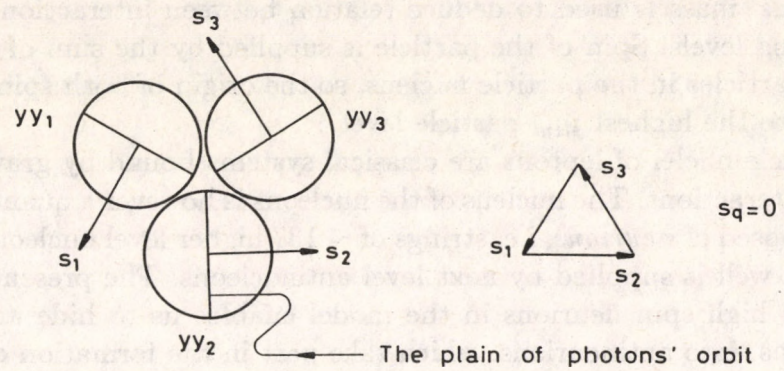

Fig. 2. The quark

The charge of quarks in an elementary particle is required to be asymmetric as in the standard model, e.g., 2/3, -1/3, -1/3 for the neutron. Strong or weak interactions are induced by photons with frequency lower or higher than the synchronous frequency. Frequencies higher than the Planck one are possible due to the existence of higher level photons.

Binding energy of gravitational and electromagnetic interactions between the yangyins does not compensate their large mass, therefore the particle nucleus is introduced (fig. 3).

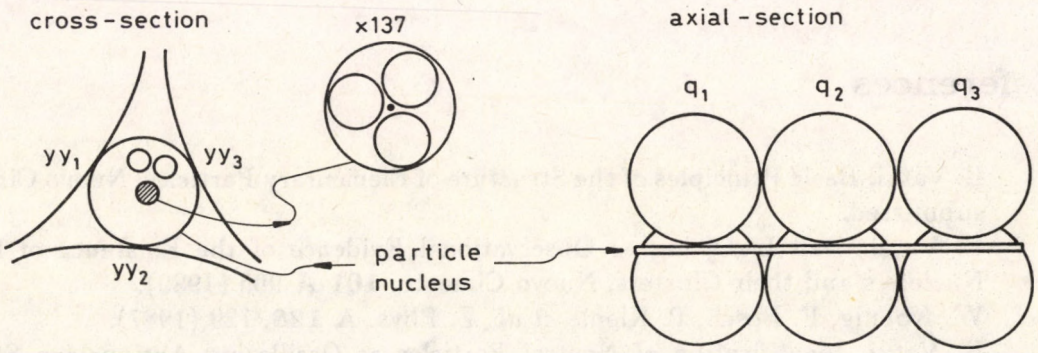

Fig. 3. The particles nucleus

Interactions between the *particle nucleus* and yangyins contribute into the compensation of the rest mass, and at the same time electromagnetic interaction compensates the inner permanent polarization of the quarks, which makes possible the existence of monopole charges. Similarity of the inner and outer polarizations of the quark envelope suggests that the particle nucleus is composed of higher level quarks or particles of the same kind as the outer quarks are. Charge independence

of the nucleons' mass is used to deduce relation between interaction frequencies of neighbouring levels. Spin of the particle is supplied by the sum of the spins of higher level particles in the particle nucleus, so the origin of both spin and charge is pushed up to the highest i_{lim} particle level.

The particle nuclei of leptons are classical systems bound by gravitation and higher level interactions. The nucleus of the nucleons is however a quantum system, which is composed of *neurions*, i.e. strings of ~ 137 higher level nucleon structures. The potential well is supplied by next level antinucleons. The presence of stable, low mass and high spin neurions in the model enables us to hide antimatter, i. e., antinucleons, into antineurions, which take part in the formation of the atmospheric net named *vata*, on which the ball-lightning is moving [2]. Neutral particles observed in Darmstadt [3] are interpreted as string oscillations of neurions and/or neurisons [4].

Particle structures, the dimension of which is of the order of the Planck length (1.6×10^{-33} cm), induce around themselves universal field structures [5], consisting of a large number of string structures parallel with the spin of the particle structure. Universality of field structures means that they can be transformed into either particle or antiparticle structures depending on the polarization of the quarks, therefore e.g., nucleon structures, nucleon-antinucleon (meson) structure, neurion and neurion-antineurion (*neurison*) structures are able to move non-locally [6] in the same nucleon field. Strange fields are overwritten during the movement of nucleon, virtual meson and neurison structures, so particle fields are dynamical entities, making possible the coexistence of numerous kind of fields in the same physical volume. Physical volume of a particle can be defined as the Compton wavelength ($\lambda \sim \hbar/mc$) of the particle or/and that of virtual particles moving in the same field.

References

1. E. Vatai, Basic Principles of the Structure of Elementary Particles, Nuovo Cimento, submitted.
2. E. Vatai, Ball Lightning as Observational Evidence of the Existence of Lepto-Nucleons and their Clusters, Nuovo Cimento, **101 A** 905 (1989).
3. W. Koenig, F. Bosch, P. Kienle *et al.*, Z. Phys. **A 128**, 129 (1987).
4. E. Vatai, Identification of Neutral Particles as Oscillating Antinucleon Strings. Phys. Lett. B, submitted.
5. E. Vatai, On the Structure of Particle Fields. Phys. Lett. A, submitted.
6. E. Vatai, J. Phys. **B20** L731 (1987).

ATOMIC PHYSICS

ECC peak asymmetry in $H^+ \rightarrow$ He collision

L. Gulyás, Á. Kövér, Gy. Szabó, T. Vajnai†, D. Berényi

It is nearly ten years that Meckbach et al. proposed a method for analyzing the distribution of electrons ejected from electron transfer to the projectile's continuum (ETC) processes [1]. On the basis of the method the measured electron yield $Q(v, \vartheta)$ (v *and* ϑ are the velocity and ejection angle of the electron) are parametrized in the following:

$$Q(v, \vartheta) = \sum_{n,j} B_{nj} \int (v')^{(n-1)} P_j(cos\vartheta') S(v, \Omega) d\bar{v} \qquad (1)$$

where P_j is the Legendre polynomials, the prime labels the quantities in the projectile frame. B_{nj} are the fitting parameters and $S(v, \Omega)$ is the transmission function of the spectrometer. It can be seen from Eq. 1 that the B_{nj} parameters are independent on the experimental conditions. In spite of this, in most cases the deviations among the B_{nj} values determined from different experiments are much higher than the experimental errors [2].

Last time we measured the ECC peak (electron capture to the projectile's continuum) in the 200-300 keV $H^+ \rightarrow He$ collision system at 0^o ejection angle, at different angular acceptance angles: $\vartheta_o = 0.3^o, 0.6^o, 1.1^o, 1.4^o, 2.0^o$, [3].

Analyzing the measured spectra we used different approximations in determining the $S(v, \Omega)$ transmission function. It was found that the evaluated B_{nj} parameters were independent on the experimental conditions if the determination of the $S(v, \Omega)$ function was improved, relatively to that ones used before [3]. In this case the parameters of $S(v, \Omega)$ were free within its estimated errors in the fitting. Fig. 1 shows the asymmetry parameter $\beta_1 = B_{01}/B_{00}$ as a function of the impact energy.

References

† On leave from the University of Miskolc, H-3515 Miskolc

1. W. Meckbach, I.B. Nemirovsky and C.R. Garibotti: Phys. Rev. A **24** 1793 (1981)
2. D. Berényi, L. Gulyás, Á. Kövér: J. de Phys. **48** C9-231 (1987)
3. L. Gulyás, Á Kövér, Gy. Szabó, T. Vajnai, D. Berényi: 4th Workshop on High-Energy Ion-Atom Collision Processes Debrecen 1990, Lecture Notes in Physics, eds D. Berényi and G. Hock (Springer, Berlin 1991) to be published
4. P. Dahl: J. Phys. B: At. Mol. Phys. **18** 1181 (1985)
5. L.H. Andersen, K. E. Jensen and H. Knudsen: J. Phys. B: At. Mol. Phys: **19** L161 (1986)
6. B. L. Moiseiwitsch: 4th Workshop on High-Energy Ion-Atom Collision Processes Debrecen 1990, Lecture Notes in Physics, eds D. Berényi and G. Hock (Springer, Berlin 1991) to be published

7. J. Burgdörfer: Phys. Rev. A **33** 1578 (1986)
8. D.S.F. Crothers and J.F. McCann: J. Phys. B: At. Mol. Phys. **20** L19 (1987)

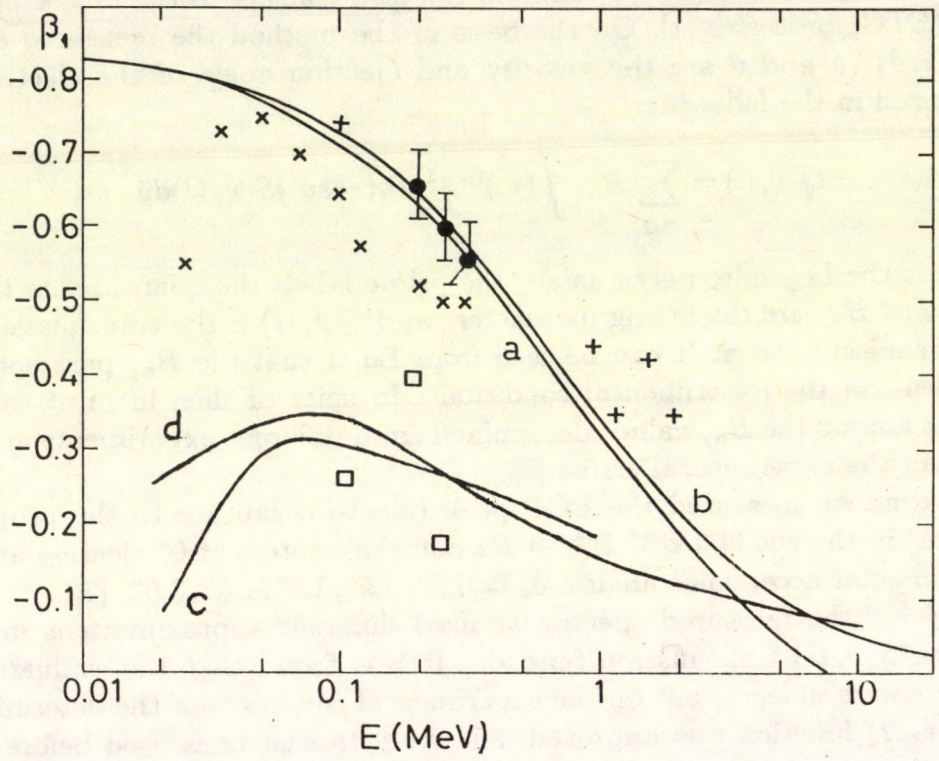

Fig. 1. β_1 parameter for H^+-He collision. Experiment: □, Meckbach et al [1]; ×, Dahl [4]; +, Andersen et al [5]; •, present result. Theory, solid lines: a,b two different version of OBK2 approximations [6]; c CDW approximations [7]; d CDW approximations [8]

Systematic Study of the Anisotropy of Ne K Auger Satellites in Ion-Atom Collisions

E. Takács, S. Ricz, J. Végh, I. Kádár, B. Sulik, T. Papp, I. Török, J. Pálinkás, B. Tóth and D. Berényi

Our group previously investigated the angular distribution of the target Ne K Auger satellite lines [1] by means of a special triple-pass electrostatic electron spectrometer ESA-21 built in the Institute [2]. This spectrometer can take electron energy spectra under 13 different angles from 0 to 180 degrees simultaneously. In the above mentioned systematic study the velocity of the projectile was constant and the projectile charge was varied from 2 to 10 [3].

In the present study we examine the impact energy dependence of the angular distribution of the O-like Ne K Auger satellite lines using proton as projectile. The measurements have been performed on the beamlines of the MGC cyclotron and the 5 MV Van de Graaff generator of ATOMKI. The electron spectrometer ESA-21 was used to take the spectra as in our earlier studies.

During the data evaluation procedure an asymmetric line shape [4] was used due to the non-negligible role of post collision interaction in the investigated projectile energy region. The evaluation was carried out by the EWA computer code [5]. Fig 1. shows a typical spectrum under investigation.

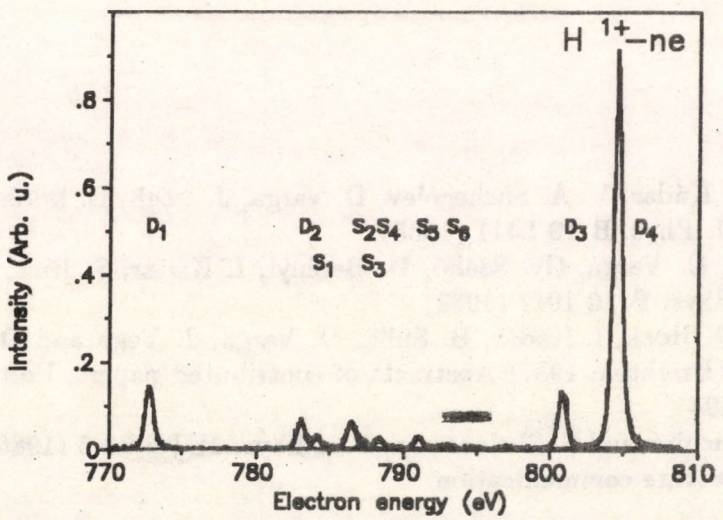

Fig. 1. Part of the investigated Ne K Auger spectrum. (Diagram lines: D1: 126 ^{2}S - 215 ^{1}P, D2: 126 ^{2}S - 215 ^{3}P, D3: 126 ^{2}S - 224 ^{1}S, D4: 126 ^{2}S - 224 ^{1}D, Satellite lines: S1: 125 ^{3}P - 223 ^{2}P, S2: 125 ^{3}P - 223 ^{2}D, S3: 116 ^{3}S - 214 ^{2}D, S4: 116 ^{3}S - 223 ^{2}P, S5: 125 ^{1}P - 223 ^{2}D, S6: 116 ^{1}S - 214 ^{2}D. (126 = 1s,2s^2,2p^6))

In the present study the angular distribution of three satellite lines (125 ^{3}P - 223 ^{2}P, 125 ^{1}P - 223 ^{2}P and 125 ^{1}P - 223 ^{2}D) were analysed. For the determination

of the alignment parameter the angular coupling coefficients of ref. [3] were used. Fig. 2 depictes the obtained alignment parameter values as a function of the projectile energy. The evaluation of further experimental data and comparison with theories are under work.

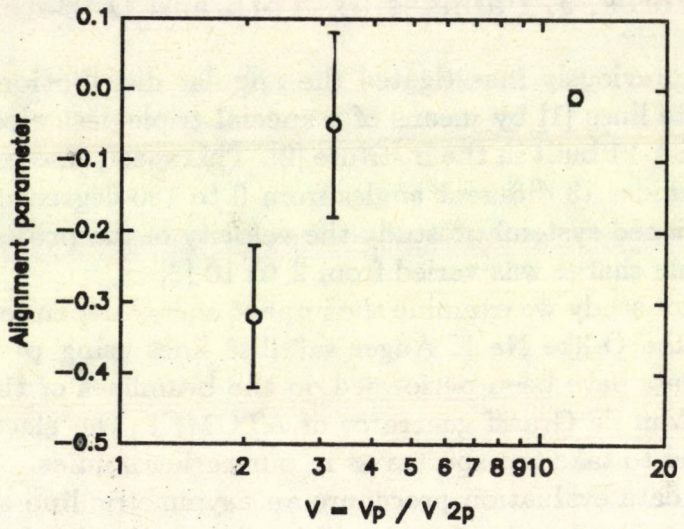

Fig. 2. Alignment parameter for the vacancy production of the 2p subshell of neon simultaneously with the production of a K-shell vacancy as a function of the scaled velocity of the bombarding proton.

References

1. S. Ricz, I. Kádár, V. A. Shchegolev, D. Varga, J. Végh, D. Berényi, G. Hock and B. Sulik: J. Phys. B **19** L411 (1986)
2. A. Kövér, D. Varga, Gy. Szabó, D. Berényi, I. Kádár, S. Ricz, J. Végh and G. Hock: J. Phys. B **16** 1017 (1983)
3. S. Ricz, G. Hock, I. Kádár, B. Sulik, D. Varga, J. Végh and D. Berényi: XVth ICPEAC (Brighton, 1987) Abstracts of contributed papers, Edited by J. Geddes et al., p. 494
4. M. Yu. Kuchiev and S. Sheinerman: Sov. Phys.-JETP **63** 5 (1986)
5. J. Végh: private communication

Measurement of Post-Collision Interaction effects for p on Ne collisions

E. Takács, L. Sarkadi, S. Ricz, B. Sulik and L. Tóth

With the help of the Auger-electron spectroscopy we have investigated the change (shape and position) of the Ne K-$L^2_{2,3}(^1D_2)$ (804.5 eV) Auger line as a function of the projectile energy. The projectile was proton with energy from 700 keV to 2 MeV. The change is caused by the interaction of the Auger electron with the outgoing projectile after the Auger decay (post-collision interaction, PCI). With the variation of the bombarding energy the relative velocity of the two particles and consequently, the average interaction between them changes. The most interesting energy region from this point of view is that region where the velocities of the two charged particles are almost the same. In our case it occurs at 1477 keV bombarding energy. As we have shown in ref. [1] the asymmetry of the shape of the Auger line is in close connection with the shift of the peak maximum. If we fit the peak with the line shape of van der Straten et al [2] and Kuchiev and Sheinerman [3]:

$$P(\epsilon) = \frac{\Gamma}{2\pi} \frac{1}{(\epsilon - \epsilon_0)^2 + \Gamma^2/4} \frac{\pi\xi}{\sinh(\pi\xi)} \exp\left(2\xi \arctan \frac{2(\epsilon - \epsilon_0)}{\Gamma}\right) \quad (1)$$

the PCI shift will be:

$$\Delta\epsilon = \Gamma\xi/2, \quad (2)$$

where ϵ is the energy of the detected electron, ϵ_0, Γ are the transition energy and width of the Auger line, respectively and ξ is the asymmetry parameter.

The measurements were performed by the ESA-21 triple-staged electrostatic spectrometer [4]. With the help of this spectrometer one can record high energy resolution (0.7 eV at 804.5 eV) electron spectra at 13 different observation angles (0 to 180 degrees) relative to the beam direction. The target pressure was $1.5\text{x}10^{-3}$ mbar with $3\text{x}10^{-5}$ mbar overall pressure in the target chamber. The base pressure without gas target was $8\text{x}10^{-7}$. The proton beam was produced by the 5 MeV Van de Graaf generator of our institute. The average beam current was 0.8 μA. The measurement was performed at 12 different energies from 700 keV to 2 MeV.

We evaluated the data with the help of the EWA spectrum evaluation computer program [5]. We fitted the Ne K-$L^2_{2,3}(^1D_2)$ peak with a five parameter function which was the convolution of eq. (1) with the spectrometer function. During the fitting the Γ Lorentzian width was kept constant, 0.27 eV [6] and the other four parameters were free. The ξ asymmetry parameter was converted to energy shift according to eq. (2).

Part of the obtained results have been plotted in figure 1. They show the energy dependence of the PCI line shifts at three different observation angles. The solid curve is the theoretical line shift from the van der Straten and Morgenstern's theory [2]. The theory considers a constant velocity projectile and describes its interaction

with the Auger electron classically. At observation angles around 0° this theory is very sensitive to the angular region of integration, because the line shape changes very sharply with the angle around 0°. The best fit has been obtained assuming a circular shape for the entrance slit of the spectrometer with acceptance angle ± 3.5°, which is a good approximation of the real geometry. The maximal line shifts have been found at 0° at all the bombarding energy, and from 45° to 180° the shift is constant and small. The maximal shift appears as a function of the energy at the value where the velocity of the projectile is approximately equal to that of the Auger electron. The theory can describe the asymmetry of the shift values below and above this bombarding energy (see [1]).

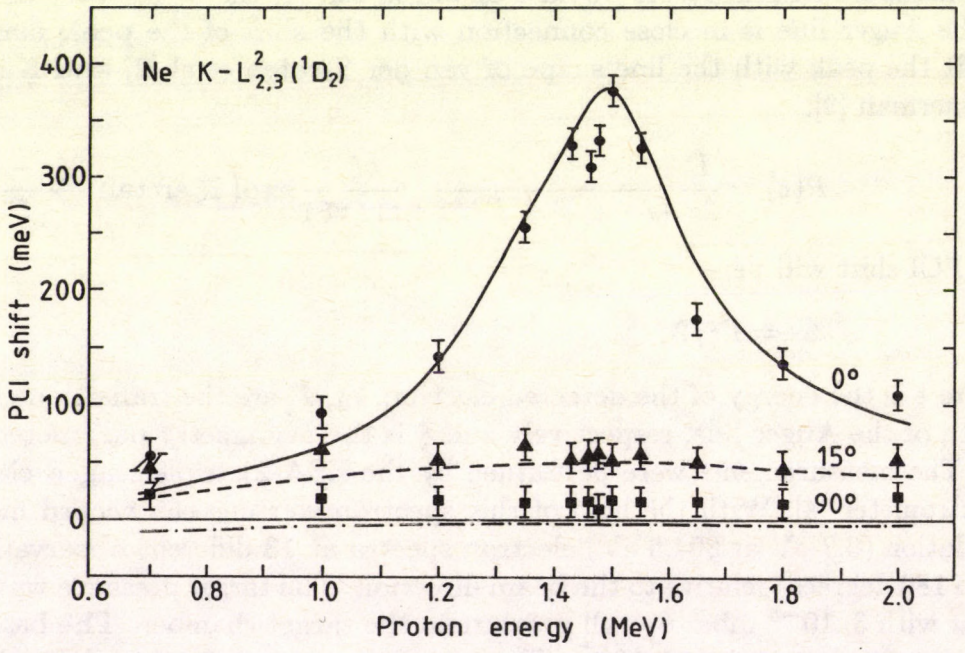

Fig. 1. Energy dependence of the PCI lineshifts at three different observation angles.

References

1. Sarkadi L, Vajnai T, Végh J and Kövér Á: Submitted to J. Phys. B. (1990)
2. van der Straten P, Morgenstern R and Niehaus A: Z.Phys. D **8** 35 (1988)
3. Kuchiev M Yu and Sheinerman S: Sov. Phys.-JETP **63** 986 (1986)
4. Kövér Á, Varga D, Szabó Gy, Berényi D, Kádár I, Végh J and Hock G: J. Phys. B: At. Mol. Phys. **B16**, 1017 (1983)
5. Végh J: Private communication
6. Sandner W and Völkel M: Phys. Rev. Letters **62** 885 (1989)

e^- impact energy dependence of the L_3 subshell alignment of Ar

K. Tőkési, S. Ricz, E. Takács, B. Sulik, L. Tóth, and N. Takada†

† Waseda University, School of Science and Engineering

Experiment.

We have investigated the projectile energy dependence of the angular distribution of the Ar LMM Auger lines induced by electron impact. The spectra were measured under the observation angles 30°, 45°, 60°, 75° and 90° by using a triple-staged electrostatic electron spectrometer ($ESA-21$,(ref 1.)). The slits of the spectrometer were set to $1.7mm$ that made possible to measure with a high energy resolution.

Evaluation.

The theoretical work shows (ref 2.) that the effect of PCI can not be neglected in our energy range. During the evalution, the PCI effect was taken into account by using distorted line shapes (ref 3.). The fitting of the spectra was made by a computer code (ref 4.) specifically developed.

Results.

Fig. 1. shows the energy dependence of the anisotropy parameters of the various L_3 peaks. The energy dependence of the anisotropy parameter of the $L_3 - M_{23}^2(^1S_0)$ line agrees with the dependence measured by DuBois and Rødbro (ref 5.). In Fig. 3. one can see the data for the anisotropy parameters of the $L_3 - M_{23}^2(^1D_2)$, $L_3 - M_{23}^2(^0P_{012})$, too.

References

1. Á. Kövér et al. J. Phys. B: **16** 1017 (1983)
2. G.B. Armen et al. Phys. Rev. A **36** No. 12 5606 (1987)
3. W. Sandner and M. Völkel Phys. Rev. Lett. **62** No. 8 885 (1989)
4. J. Végh, Theses, 1990 (unpublished)
5. R. DuBois and M. Rødbro J. Phys. B: **13** 3739 (1980)
6. B. Cleff and W. Mehlhorn Phys. Lett. **37A** 3 (1971)
7. M. Rødbro at al. J. Phys. B: **11** L551 (1978)
8. W. Sandner and W. Schmitt J. Phys. B: **11** 1833 (1978)

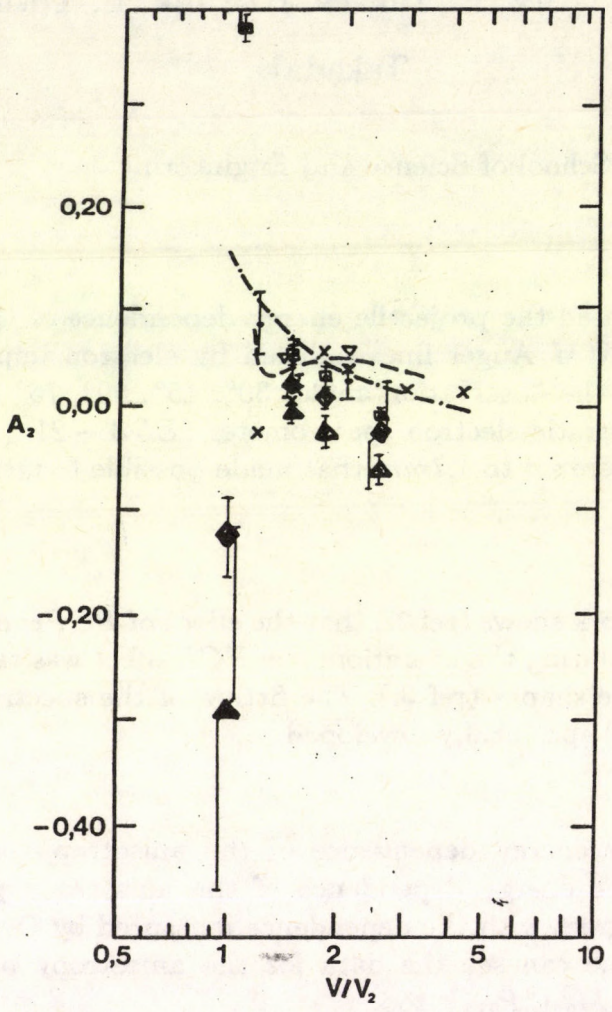

Fig. 1. Anisotropy parameter of the different L_3 peaks as a function of the relative collision velocity. ◘ present data for $L_3 - \frac{1}{3}M_{23}^2(^1S_0)$; ◆ present data for $L_3 - M_{23}^2(^1D_2)$; . ▲ present data for $L_3 - M_{23}^2(^3P_{012})$; • DuBois and Rødbro (1980); ∇ Cleff and Mehlhorn (1971); × Sandner and Schmitt (1978); —·— theory of Sandner and Schmitt (1978), — — A_2 for Mg from Rødbro at al (1978)

Measurement of Post-Collision Line Distortion of Auger Electrons Applying Coincidence Technique

L. Sarkadi, T. Vajnai†, J. Végh and Á. Kövér

Assuming that the excitation and decay of an atomic resonance state are independent processes, the Auger line shape can be described by a Lorentzian function. In the case of ion-atom collisions the outgoing charged particles of the excitation process interact with the Auger electrons (post-collision interaction, PCI) even at asymptotically high impact energies, because the Coulomb potential has long range. The result of this continuum interaction is that the measured energy distribution of the Auger electrons is asymmetrically broadened and shifted.

In PCI studies the determination of the distortions with use of a reference line shape (which is not disturbed) is more reliable than the direct measurement of the effect. Our method for obtaining such a reference line is based on the assumption that the excitation of Auger transition by electron capture at impact of singly charged ion is not influenced by PCI in lack of charged outgoing particles, because in this case only a neutral outgoing projectile can act upon the Auger electron, which causes only a negligible effect.

We have measured the L_3-$M^2_{2,3}(^1S_0)$ Auger line of argon ejected in the forward direction from 0.7 Mev p-Ar collisions in coincidence with the neutralized H^0 atoms and without it. The non-coincidence spectrum (originating dominantly from direct ionization) shows a considerable shift and asymmetry of the peak compared to the peak of the coincidence spectrum (see the Fig. 1.).

We assumed that the PCI line shape distortions can be well represented by the analytical asymmetric function suggested by Kuchiev and Sheinerman [1] and van der Straten et al. [2]. Fitting the spectrum with this function (convolving it with the spectrometer function) we observed that the asymmetry of the line shape was proportional to the PCI energy shift which we obtained from the coincidence measurement.

Further non-coincidence measurements determining the asymmetry of the $L_{2,3}$-$M^2_{2,3}$ Auger lines as a function of the proton energy and observation angle have also been made. The obtained PCI shifts and line line shapes have been found in a qualitative agreement with the semi-classical theory of van der Straten and Morgenstern [3]. This theory considers PCI only between the Auger the electron and the outgoing projectile.

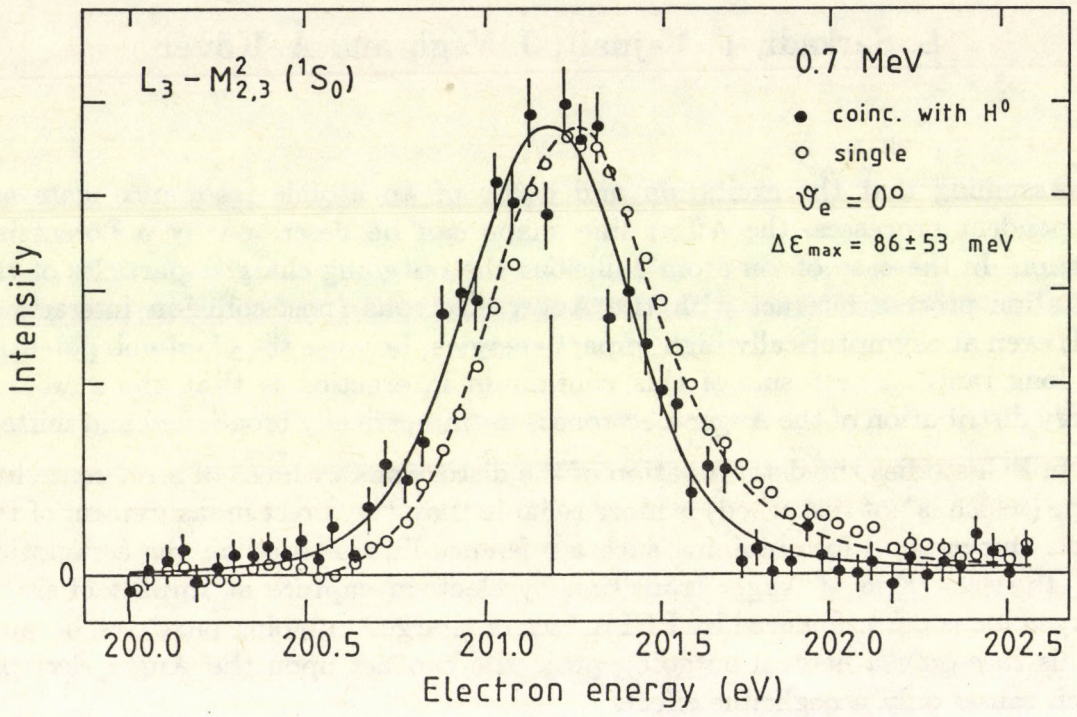

Fig. 1. Energy spectra of the L_3-$M^2_{2,3}(^1S_0)$ Auger line of argon. The notations are: •, coincidence data; ○, non-coincidence data.

References

† On leave from the University of Miskolc, H-3515 Miskolc

1. Kuchiev M Yu and Sheinerman S A: Sov. Phys.-JETP **63** 986 (1986)
2. van der Straten P, Morgenstern R and Niehaus A: Z.Phys. D **8** 35 (1988)
3. van der Straten P and Morgenstern R: J.Phys. B **19** 1361 (1986)

Measurement of the Polarization of Ti K_α X-Ray Satellites

V. P. Petukhov [1], S. M. Blokhin [2], I. Török, J. Pálinkás,

L. Sarkadi, T. Papp, B. Sulik, E. Takács.

An x-ray polarimeter, based on a crystal spectrometer using flat analyzer crystal and Soller slits collimator, designed and manufactured at the Moscow State University [1], has been installed at the 5 MV Van de Graaff generator of the ATOMKI. Some blocks were borrowed from the x-ray crystal spectrometer of the ATOMKI [2]. After matching the two system, aligning and calibrating the polarimeter, the first x-ray polarization measurements were performed.

Using pure Ti target the Ti K_α region was scanned to measure the polarization of the $K_\alpha L^n$ satellite groups. The Ti target was a 2 mm thick Ti metal disk. In a further measurement targets of $BaTiO_3$ and $PbTiO_3$ in a form of pressed powder disks were also used. The compounds were chosen because of their piezo- and ferroelectric properties, and because of their perovskite structure, now widely investigated from many aspects. The different electron densities seen by the Ti atoms in the neighbourhood of Ti, Ba, and Pb atoms, may manifest in differences of polarization of the satellite lines. 1 MeV proton and 3.5 MeV helium ion beams were used as projectiles. The present measurements are direct extensions of former ones in Moscow on the same target materials, using 0.5 MeV proton projectiles [3].

The obtained spectra are under processing, i. e. the spectra are being checked against instability and the acceptable ones of a series of scans are being summed, to obtain the resulting spectra. All measurements were carried out at two polariser positions: parallel and perpendicular relative to the direction of the incoming beam. The EWA spectrum evaluating software [4] will be used to analyze the spectra, and the polarization of the satellite lines will be determined.

The results with the present energy resolution can be regarded only as the first pilot experiment to notice the possible polarization differences. An improved Soller slit is planned for the next series of measurements, and the higher resolution will make it possible to resolve not only the diagram line and the KL^1, KL^2, KL^3, etc. satellite groups, but also the strongest distinct transitions, e. g. the $K_{\alpha 3}$ and $K_{\alpha 4}$ satellite lines in the KL^1 group.

Future measurements will be carried out on $SrTiO_3$ targets and on the present targets using also heavier ions.

References

[1]Moscow State University, Institute of Nuclear Physics, Moscow, USSR.
[2]State University, Rostov-on-Don, USSR.

1. V. P. Petukhov: Prib. Tech. Expt., No.1, p. 195 (1990) *(in Russian)*
2. I. Török, B. Tóth: J. de Physique, **46** suppl. to No.12, p. C9-79 (1987)
3. S. M. Blokhin, V. P. Petukhov: ATOMKI REP., 1990/1-R, p.22, abstract H.3.1.
4. J. Végh: *Thesis*, 1990, ATOMKI, Debrecen

The Intensity Distribution of Ion-Induced $K_\alpha L^n$ X-Ray Satellites and the Geometrical Model of Ionization

B. Sulik, I. Török, A. Ágoston and I. Kádár

Light element (Mg, Al, Si, Ti) $K_\alpha L^n$ x-ray satellites have been measured by a crystal spectrometer. The x-rays were induced by p and He^+-ion bombardment at several energies (0.8-3.2MeV). Thick targets have been used at about 1 μA target currents. In addition to our measured relative satellite intensity values, further data have been collected from the literature, covering a wide energy range, and a variety of bombarding particles. In some cases more than two orders of magnitude of projectile energy has been covered. There are available experimental relative satellite intensity data for the following projectiles+target pairs: He,C,O,Ne+Al; He,C,O,Ne+Si; He+Cl; H,He,Li,C,N,O+Ti.

The experimental satellite intensity distributions were compared with the predictions of a recently developed ionization model, the so called geometrical model [1-3]. In the present study an attempt was made to extend the use of this model to lower velocities. The model calculations use an effective binding energy of the electron involved in the process, which can be chosen by different ways. We tried to use three variations: i) I_1 i. e. the experimental value of the first ionization potential of the given subshell (2s or 2p); ii) I_{av} the "average" binding energy of the given subshell, taking into account the screening constant, determined by Hartree-Fock calculations; and iii) I_{12} the average of the first ionization potential for a 2s or 2p electron in a neutral atom, and the first ionization potential of it in an atom, where a K-shell electron has been removed. All three types of average binding energy give good agreement with the experiments at bombarding energies higher than 1 MeV/u for He+Al collisions. The I_1 gave a prediction of the maximum of multiple ionization at a lower bombarding energy than the experiments, I_{av} gave it at higher energy (Fig. 1. a.), I_{12} gave the position of maximum multiple ionization at about the proper position, and the relative intensity values were in better agreement with experiment, than in the two former cases (Fig. 1. b., and Fig. 2.).

Our results were partly presented at the Eleventh International Conference on the Application of Accelerators in Research and Industry, Denton, Nov. 1990. Detailed discussion will be given in the conference proceedings.

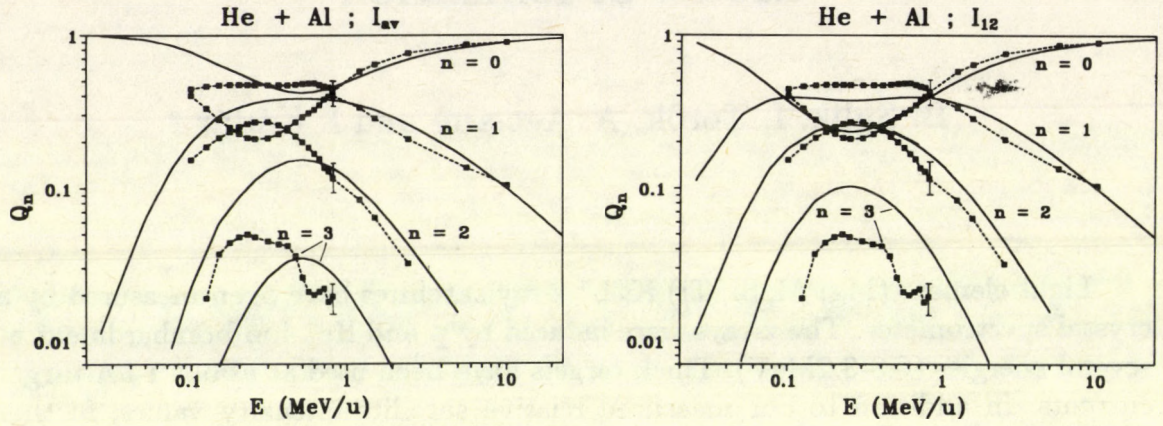

Fig. 1. The relative intensities of the Al $K_\alpha L^n$ satellites Q_n as a function of bombarding He-ion energy. Experiment: squares, dashed lines, stars: our measurements; theory: solid lines. a, Using the "average" binding energy (I_{av}) of the subshell in question. The maximum of multiple ionization is predicted to higher bombarding energies, than it was measured. b, Using I_{12} type average binding energy.

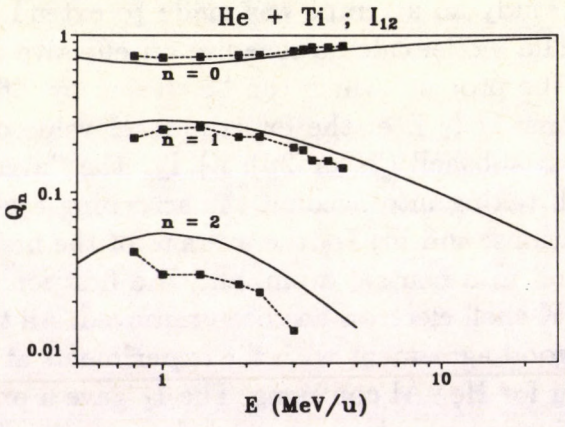

Fig. 2. The relative intensities of the Ti $K_\alpha L^n$ satellites Q_n as a function of bombarding He-ion energy. Experiment: squares, dashed lines, full circles - our measurements, theory: solid lines - geometrical model with I_{12} type average binding energy.

References

1. B. Sulik, G. Hock, D. Berényi: J. Phys. B: At. Mol. Phys., **B17** 3239 (1984)
2. B. Sulik, I. Kádár, S. Ricz, D. Varga, J. Végh, G. Hock, D. Berényi: Nucl. Instrum. Meth. **B28** 509 (1987)
3. A. Berinde, C. Ciortea, A. Enulescu, D. Fluerasu, G. Hock, I. Piticu, L. Sarkadi, B. Sulik, V. Zoran: J. Phys. B: At. Mol. Phys., **B20** L481 (1987)

Classical Trajectories during Atomic Collisions

K. TŐKÉSI and G. HOCK

We have developed a computer code [1] for simulating pure 3-body atomic collisions in terms of the Classical Trajectory Monte Carlo (CTMC) method, last year. As a practical application to this code classical trajectories of atomic particles are visualized by means of live pictures on screen. The demonstrational CTMC computer code [2], which runs on IBM PC-s (AT-286/386 with coprocessor, CGA/EGA/VGA display), includes samples of natural atomic and exotic creatures, bombarded by other particles under various classical initial conditions and exposed in different reference frames of observation. The program is provided with about 70 examples of collisions of different kind at various collision circumstances. The above program may serve as an educational tool for the subject concerned, as well.

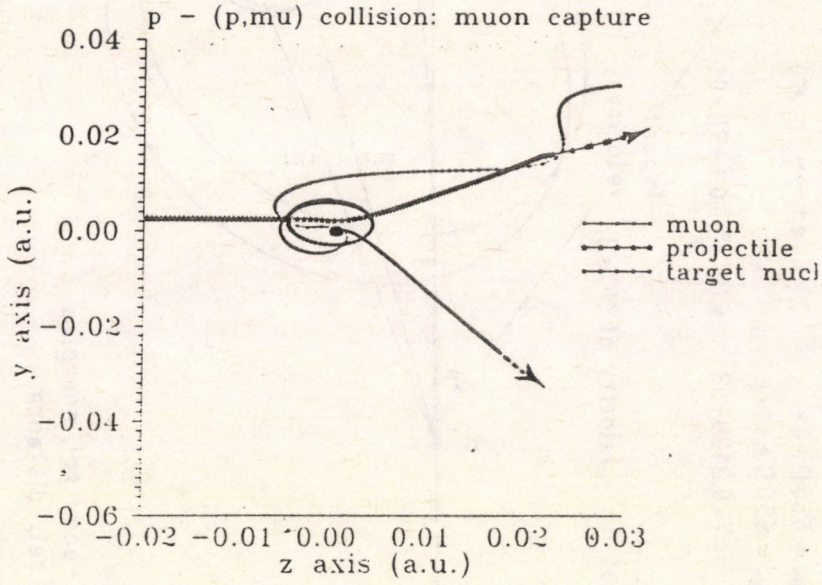

Fig. 1. A particular collisional system: atomic muon capture by a proton.

References

1. K. Tőkési and G. Hock: ATOMKI Ann. Rep. **1989** 49 (1990)
2. K. Tőkési and G. Hock: ATOMKI Report. **1990**/1-R 7 (1990)

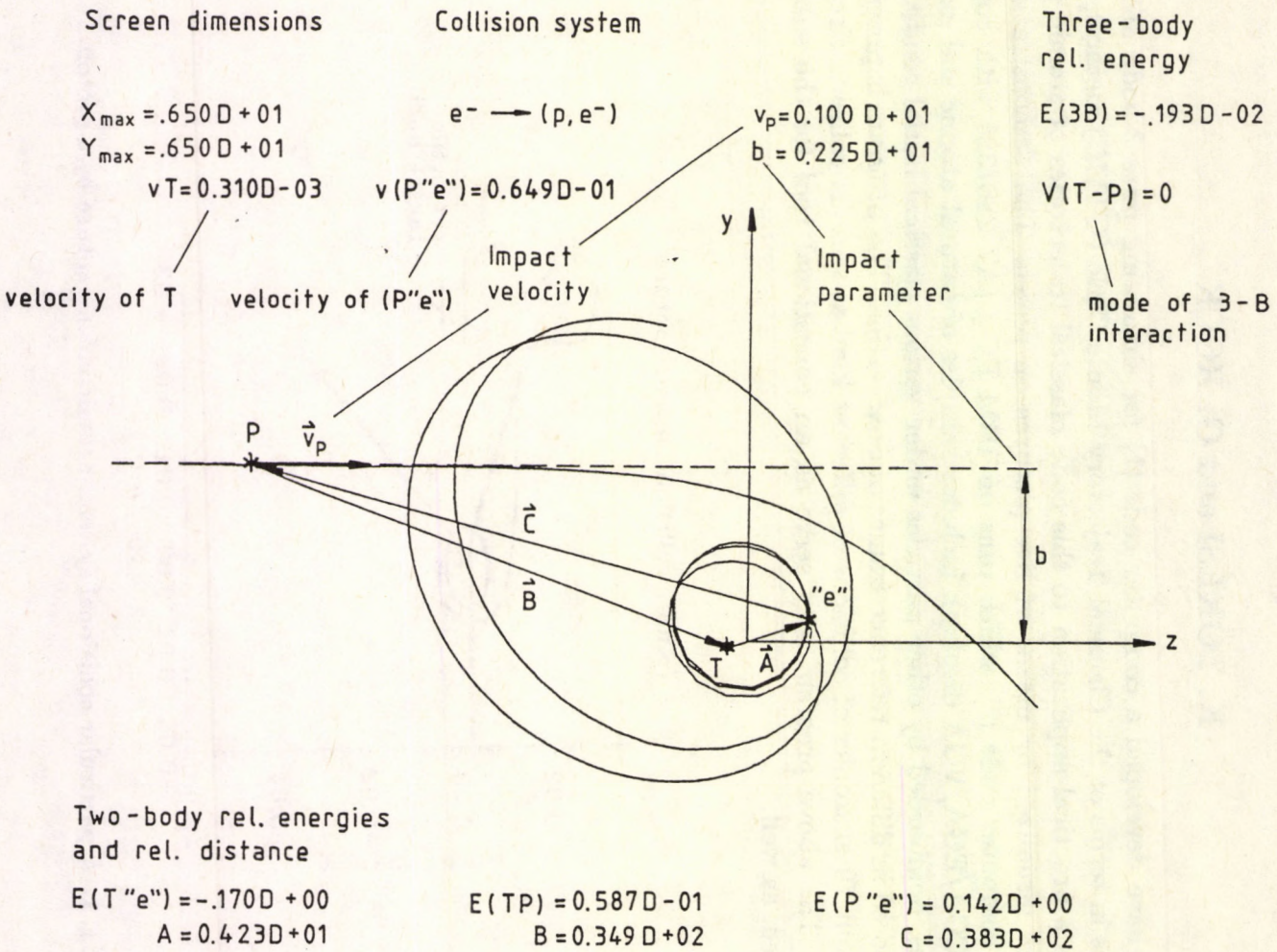

Fig. 2. Schematic plot of a collision event with explanatory items showing the collision system, the mode of the 3-body collision, impact parameter b, the *temporary* particle velocities (`vp, vT, v(P''e'')`), relative 2-body energies and separations (`E(T''e''), A`, etc.), all the quantities are given in atomic units.

CTMC Studies of $e^{\pm}, p^{\pm} + H$ Collisions

K. TŐKÉSI and G. HOCK

The collision systems $e^{\pm}, p^{\pm} + H$ are treated in the 3-body Classical Trajectory Monte Carlo (CTMC) [1] and the traditional (2-body) first Born approximations. The total cross sections of direct, breakup, transfer, exchange and/or binding processes (if any), simultaneously obtained in the CTMC calculations [2], are determined with (full 3-body) and without (restricted 3-body) the inclusion of the projectile– target potential. This latter case simulates the "plain wave"-Born approximation. Comparison is made for the total ionization cross sections of the above collisions among the CTMC, plane wave and Coulomb corrected 1st Born [3] approximations.

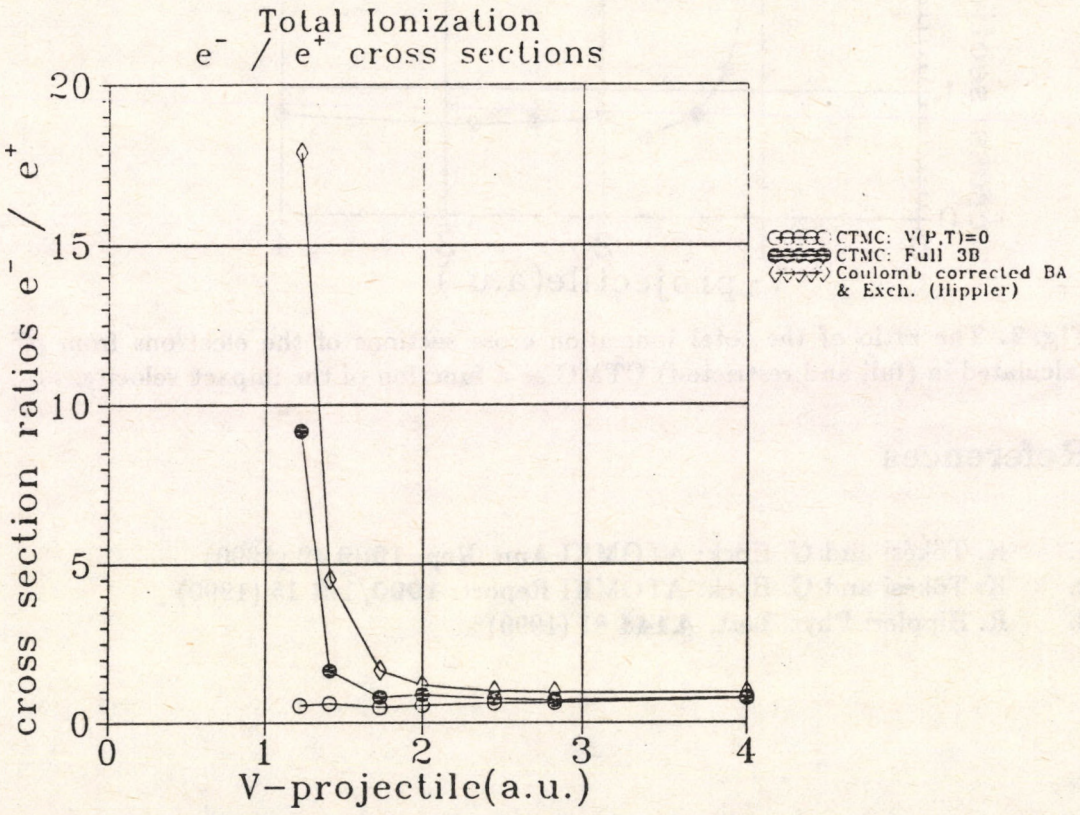

Fig. 1. The ratio of the total ionization cross sections of the electrons from $e^{\pm} + H$ calculated in (full and restricted) CTMC and Coulomb corrected 1st Born approximations as a function of the impact velocity.

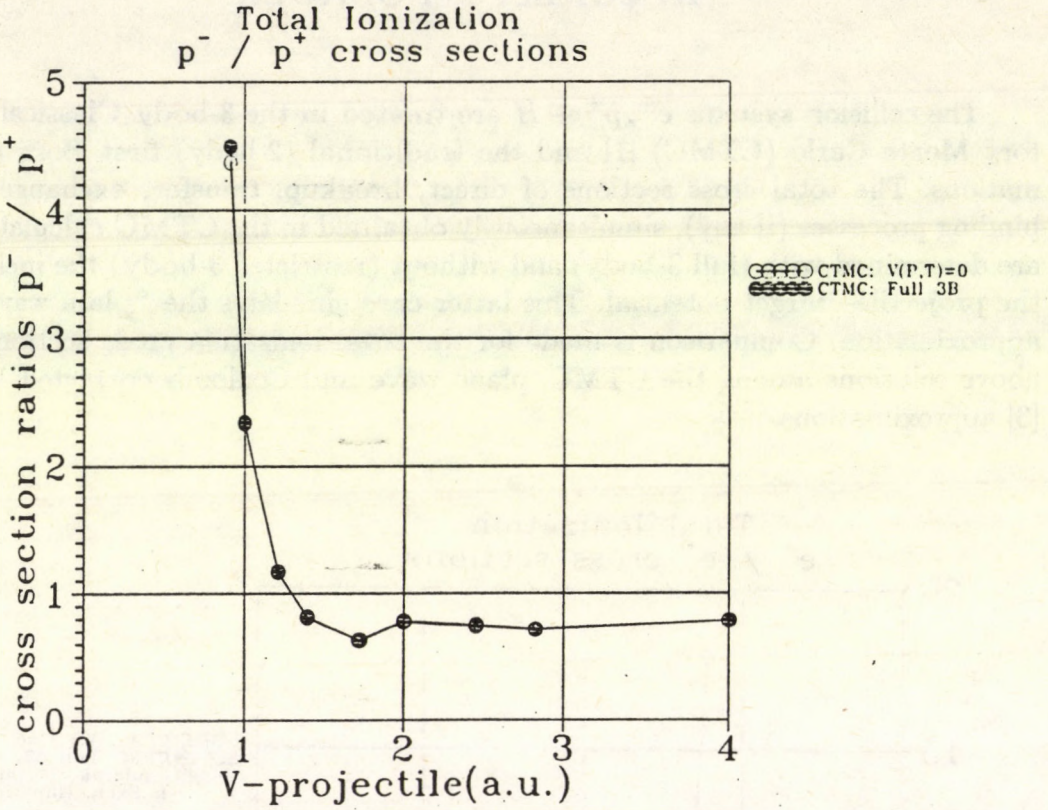

Fig. 2. The ratio of the total ionization cross sections of the electrons from $p^{\pm} + H$ calculated in (full and restricted) CTMC as a function of the impact velocity.

References

1. K. Tőkési and G. Hock: ATOMKI Ann. Rep. **1989** 49 (1990)
2. K. Tőkési and G. Hock: ATOMKI Report. **1990**/1-R 15 (1990)
3. R. Hippler: Phys. Lett. **A144** 81 (1990)

Dynamic Screening in Ion-Atom Collisions

B. Sulik, V. C. Montemayor†, N. Stolterfoht†, I. Kádár, G. Schiwietz† and S. Ricz

In ion-atom collision experiments the interest is often focussed to only one of the collision partners, i. e. the final states of only one of the partners are observed. This may be equally the target atom or the projectile ion. The other partner is handled in such cases as only a source of physical perturbation which may be characterized by an effective perturbation potential. However, if this latter one is an atom or non-bare ion its electrons may also become ejected, excited or captured. Usually the final states of the above electrons are not observed.

This situation is essential in projectile X-ray or Auger spectroscopy [1] where - from the point of view of the investigated process - the ionizing or exciting partner is the neutral atom, but it becomes strongly ionized during the collision, especially when the other partner is a highly charged heavy ion. Therefore, the perturbation potential is time dependent and roughly asymmetric from the point of view of the incoming and the outgoing projectile wich results in breaking up symmetries connected to a central potential, even in first order calculations.

From the theoretical point of view it is necessary to make assumptions both about the shape of the perturbation potential and about the change of it during the collision. In most cases the nuclear charge, the ionic charge or some kind of effective charges are used as the central charge of a static Coulomb field. [2,3] At a higher level time-independent static screened potentials or adiabatically changing time-dependent potentials can be applied. [3] In the case of using a static screened potential in the time-dependent perturbation theory, the simplest way to take into account screening in calculation of matrix elements is to approximate $Z(|\mathbf{R}-\mathbf{r}|)$ by Z(R) [4].

Recently we calculated non-adiabatic time-dependent perturbation potentials with extended dCTMC codes [5] for the helium atom colliding with different ions. We defined in this model the effective charge of the target atom at the place of the projectile nucleus taking into account the actual charge distribution of the target developing in time. Similar calculations were done within a coupled-channel model [6] resulting in a quantitative agreement with the dCTMC data. We found a strongly asymmetric behaviour of the effective charge before and after the collision correspondingly to a strong target polarisation.

Furthermore, a simplified model has been worked out to extend the results to more complicated atoms in order to handle time dependent perturbations in ion-atom collisions in general. On the basis of the results of dCTMC calculations, extracting the average motion of the center of charge of the electrons, we could construct a model, in wich the ionized fraction of the electrons has an 'artificial' motion during the collision but only along the z axis. The model is free of any fitting parameters. All quantities are calculated from the primary data of the collision i. e. the velocities and charges of the collision partners. For the determination of

the ionization probabilities the geometrical model [7] was applied. In its present form, the above mentioned model can reproduce all the results of the dCTMC calculations wich has been applied for the following systems:

110 and 180 MeV Ar^{7+} - He
10 and 20 MeV O^{5+} - He
170 MeV Ne^{7+} - He
332 keV H^{+} - He.

The extension of the present model to more complicated target atoms needs some additional efforts, because in these cases dCTMC calculations can not be used so easily as reference. On the experimental side, the study of double exitation (1s-2p and 2s-2p) of Li-like ions seems to be a sensitive test of the validity of the above picture. Preliminary data [1] show an enhancement in the double exitation cross section in qualitative agreement with the present model but they have too pure statistics for a quantitative comparison. Further measuremens on a beamline of the heavy-ion cyclotron VICKSI, HMI, Berlin are under preparation.

This work has been done within the frame of the collaboration between the German and Hungarian Academies of Sciences.

References

† HMI, Berlin

1. Stolterfoht N, Miller P D, Krause H F, Yamazaki Y, Swanson J K, Bruch R, Dittner P F, Pepmiller P L and Datz S: Nucl. Instr. Meth. B **24** 168 (1987)
2. Bates D R and Griffing G: Proc. Phys. Soc. **66** 961 (1953) Toburen L H, Stolterfoht N, Ziem P and Schneider D: Phys. Rev. A **24** 1741 (1981)
3. Brandsen B H, Atmic Collision Theory, W A Benjamin Inc., New York, 1970
4. Végh L and Sarkadi L, J. Phys. B **16** L727 (1983)
5. Montemayor V and Schiwietz G, Phys. Rev. A **40** 6223 (1989)
6. Schiwietz G, Phys. Rev. A **42** 296 (1990)
7. Sulik B, Kádár I, Ricz S, Varga D, Végh J, Hock G and Berényi D, Nucl. Instr. Meth. B bf28509 (1987)

Calculation of ELC in case of projectiles having one electron in arbitrary quantum state

Gy. Szabó, J. Burgdörfer†, L. Gulyás

Cross sections for electron emission in inelastic ion-atom collisions show a peak-like, so-called cusp structure at electron velocities approximately equal to the projectile velocity in the forward direction. This cusp is the result of two different processes: target ionization (i.e., electron capture to continuum, ECC) and projectile ionization (i.e., electron loss to continuum ,ELC).

Multipole expansion in terms of Legendre polynomials [1] is widely used to investigate this phenomenon

$$v_e \frac{d\sigma}{d\bar{v}_e} = \sum_{i=0}^{\infty} B_i(v_e) P_i(cos\Theta_e) = B_0(v_e) \sum_{i=0}^{\infty} \beta_i(v_e) P_i(cos\Theta_e)$$

where $\bar{v}_e(v_e, \Theta_e, \phi_e)$ is the velocity vector of the electron in the frame of the projectile and $\beta_i = B_i/B_0$. The expansion coefficients can be written in the form:

$$B_0(v_e) = 1/2 \int v_e \frac{d\sigma}{d\bar{v}_e} dcos\Theta_e \quad ; \quad \beta_i(v_e) = \frac{2i+1}{2B_0} \int v_e \frac{d\sigma}{d\bar{v}_e} P_i(cos\Theta_e)\, dcos\Theta_e.$$

In this case the cross section of ELC was calculated in PWBA approximation. The bound-free transition form factors for projectile in arbitrary quantum states are expressed in terms of Appell functions [2]. The elastic and inelastic form factors of the target atom of a noble gas are calculated by the help of Roothaan-Hartree-Fock wave functions, their values reproduce the results of Hubbell [3] within a few percent. In case of other atoms these Hubbell data are used. Furthermore the inelastic processes of the target are calculated by the usual closure approximation (the C1 rule by Day [4]). Note that the values of the β_i coefficients do not change essentially if other closure approximations [4,5] are used.

The theoretical basis of the multipole expansion coefficients and results of the calculations for n$\leq$ 2 cases by $v_e = 0$ are to be found in [6].

The program system built upon the principles described above can be used for calculation for single and double differential cross sections in projectile and laboratory frame and total cross section besides for the calculation of B_0 and β_i parameters. The figure shows the values of the β_i(=BETA(I)) parameters as a function of v_e/v_p for He+H collision at v_p=10 au projectile velocity if the projectile atom is in 8S state. Similiar results indicate the role of the coefficients used in the fitting procedure for examining the experimental data [6,7].

The above results can also be used to examine the ELC process and processes of states with high quantum number in ion-solid collisions.

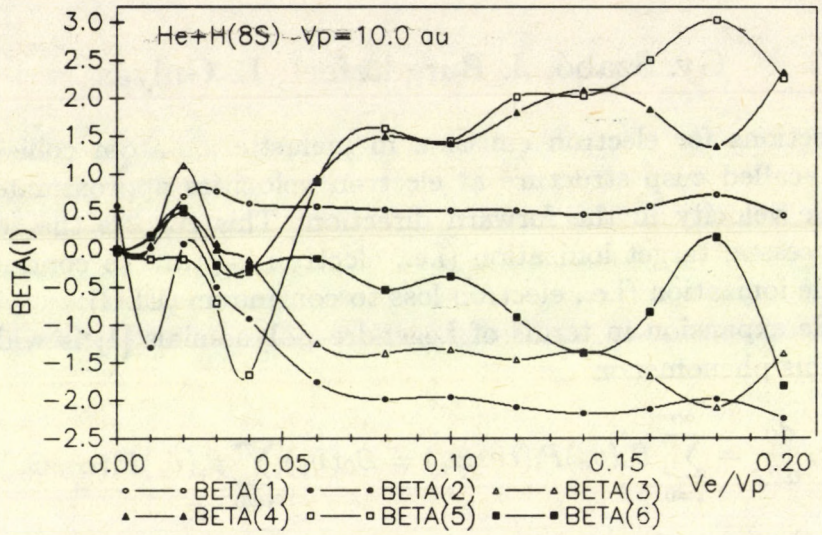

References

† Oak Ridge National Laboratory, Oak Ridge, USA

1. W. Meckbach, I.B. Nemirowski, C.R. Garibotti: Phys. Rev. **A24** 1793 (1981)
2. Dz. Belkic: J.Phys B: At. Mol. Phys. **14** 1907 (1981)
3. J.H. Hubbell, V.J. Veigele, E.A. Briggs, R.T. Brown, D.T. Cromer, R.J. Howerton: J.Phys. Chem. Ref. Data **4** 471 (1975)
4. M.H. Day: J.Phys B: At. Mol. Phys. **14** 231 (1981)
5. H.M. Hartley, H.R. Walters: J.Phys. B: At. Mol. Phys. **20** 1983 (1987)
6. J. Burgdörfer, M. Breing, S.B. Elston, I.A. Sellin: Phys. Rev. **A28** 3277 (1983)
7 L. Gulyás, L. Sarkadi, Á Köver, T. Vajnai, D. Berényi and S.B. Elston: ATOMKI Annual Report 35 (1989)

MATERIALS SCIENCE AND ANALYSIS

Photon induced Auger-electron spectroscopy of solid surfaces using bremsstrahlung radiation

L. Kövér, D. Varga, I. Cserny, J. Tóth, K. Tőkési

X-ray excited Auger-electron spectroscopy (XAES) of solid surfaces is a valuable tool for studying chemical and solid state effects on Auger transition energies and probabilities or to increase the chemical resolution of other surface analytical methods [1,2].

For excitation of photon induced Auger-electron lines either characteristic or continuous X-rays can be used. Continuous energy distribution X-rays obtainable from synchrotron photon sources or from bremsstrahlung radiation can provide an efficient Auger-electron production close to the respective ionization thresholds, in a very broad energy range. This possibility is especially important in the case of high (several keV) energy core-valence-valence Auger transitions where the number of the available optimum energy X-ray lines is rather limited.

Bremsstrahlung induced high-energy Auger-electron spectra on Fig. 1 and Fig. 2, measured by our new electron spectrometer [3] illustrate the attainable resolution and the considerable gain in peak intensity relatively to the case of using an excitation source conventional for X-ray photoelectron spectroscopy.

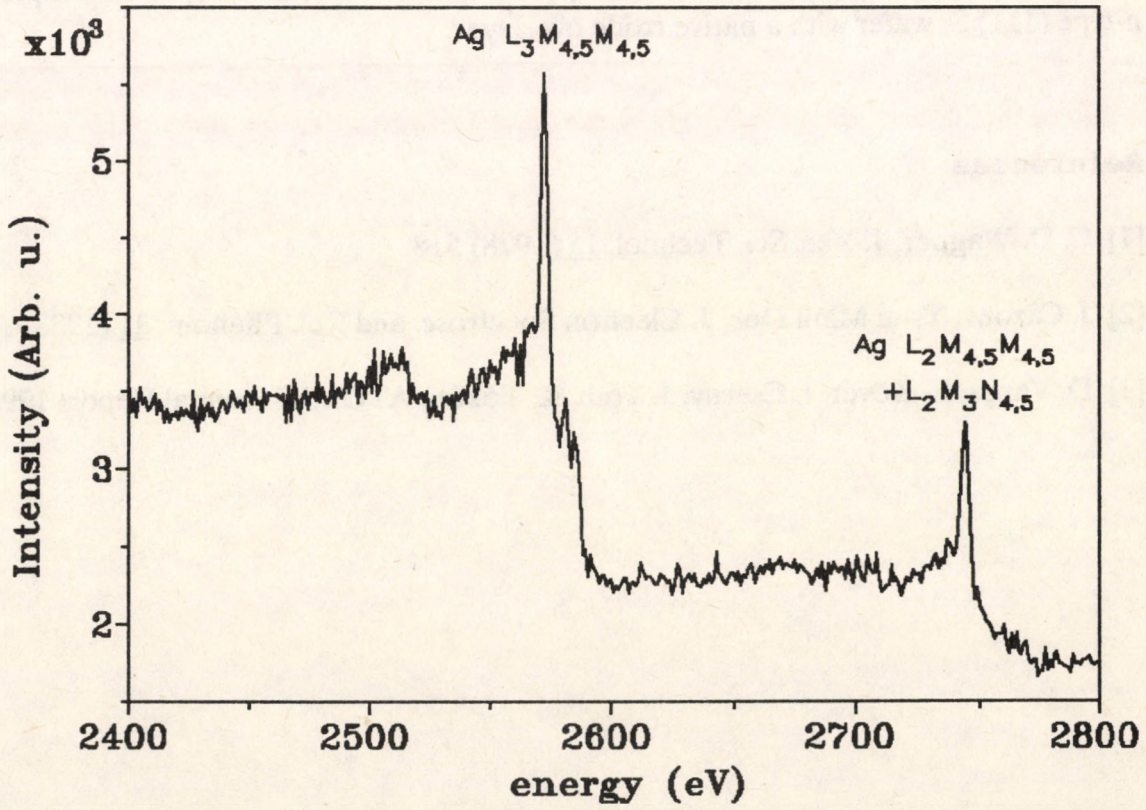

Fig. 1 Ag LMM Auger spectra excited by Mo bremsstrahlung from a polycrystalline silver sample.

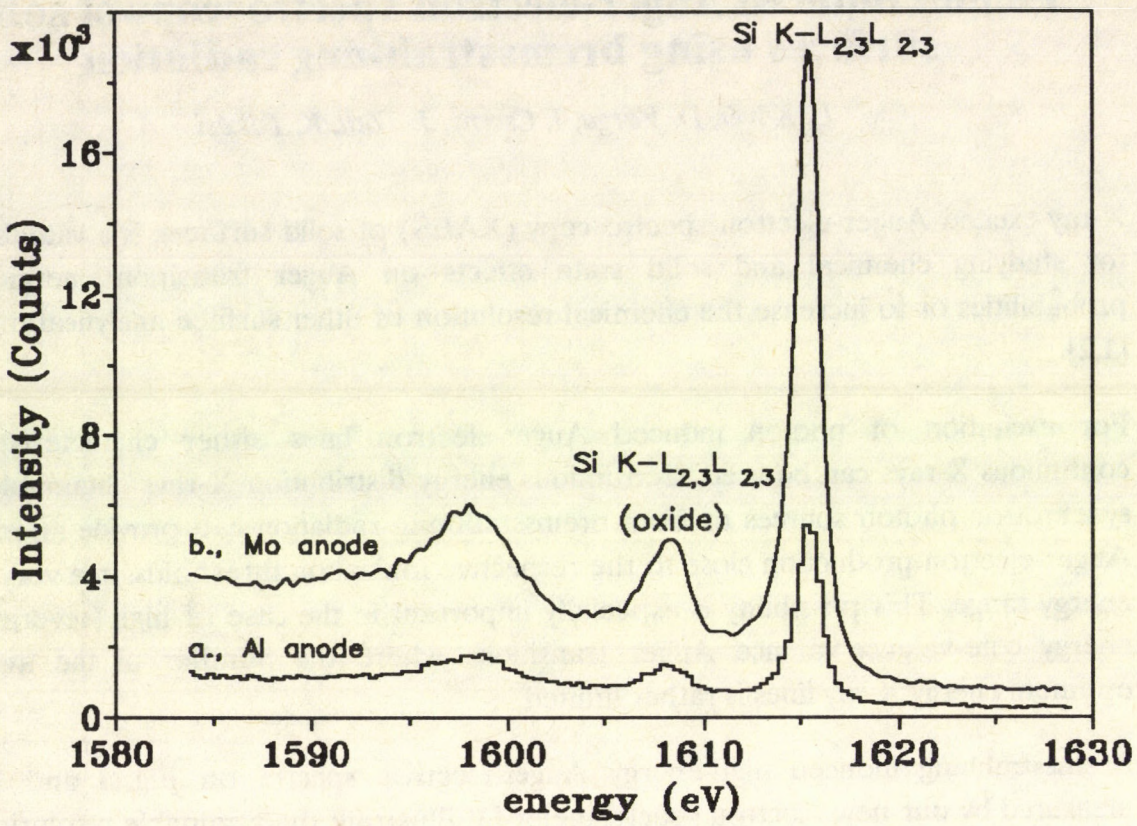

Fig. 2 Si KLL Auger spectra excited by continuous X-rays from Al (Fig. 2a) and Mo (Fig. 2b) anodes using the same source parameters (15 kV, 15 mA). The sample is an n-type (111) Si wafer with a native oxide overlayer.

References

[1] C. D. Wagner, J. Vac. Sci. Technol. 15 (1978) 518

[2] J. Cazoux, Tran Minh Duc, J. Electron Spectrosc. and Rel. Phenom. 31 (1983) 13

[3] D. Varga, L. Kövér, I. Cserny, J. Tóth, K. Tőkési, ATOMKI Annual Report 1990

Macroscopic Quantum Interference in BiSrCaCuO Screen Printed Films

S. Mészáros, K. Vad, G. Halász, N. Hegman and G. Katona *

The screen–printed–film technique is a promising preparation method of studying high T_c superconducting materials. BiSrCaCuO screen–printed films of thickness between 20 and 40 μm were prepared on alumina substrate by the method described in ref. [1] and their current conduction properties were studied experimentally. The films were equipped with Ag-Pt current and voltage contacts prepared by the screen–printing technique with less than one Ohm resistance to the film. The distance between the potential contacts was 6 mm, the width of the film was 1 mm. The film contained low T_c 2212 phase checked by X-ray diffraction. The experimental arrangement and measurement method were the same as the ones published in ref. [2], in the study of similar properties of $YBa_2Cu_3O_{7-x}$ ceramics. The modulation of the voltage by weak external magnetic field was studied at 4.2 K by passing continuous current through the sample and generating weak magnetic field perpendicular to the film by a small coil driven by a triangular wave current. To study the cross section dependence of current–voltage characteristics the width of the film was systematically reduced by scraping a part of the film between potential contacts. The number of intergrain juctions in this region was reduced and their individual characteristics were not averaged out. At quite a small cross section current pulses were able to cause permanent change in the film including total destruction as well. This effect was used to reduce the number of effective junctions by controlled current pulse treatment of the film immersed in liquid He similarly to the method used for YBaCuO thin films in ref. [4].

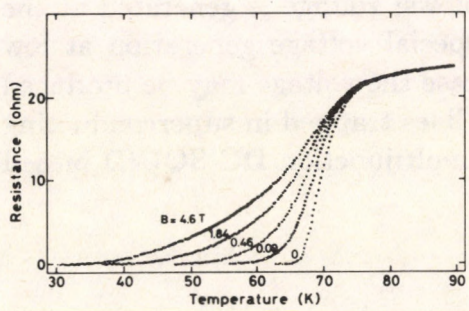

Fig. 1. Resistance-temperature curves of a typical sample in magnetic fields

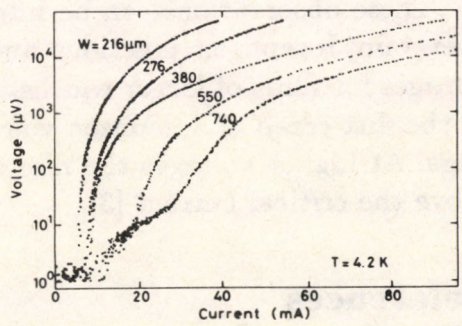

Fig. 2. Current-voltage characteristics for different film widths at 4.2 K

The resistance–temperature curves were measured at current densities 30 mA/cm^2 to 30 A/cm^2. The magnetic field dependence was measured in longitudinal magnetic fields. The apparent feature of the R-T characteristics measured on the films (see fig. 1) was the lack of separation of two regions on the curves as it was observed for YBaCuO ceramics in ref. [2]. The separation of resistance contributions of grains and grain boundaries was not possible in this case. The

$H_{c2}(O)$ value was calculated from the shift of zero resistance temperature due to magnetic field and found to be 12 T. Current–voltage curves showed neither simple power–law nor exponential dependence of voltage on current in contrast with $YBa_2Cu_3O_{7-x}$ bulk materials [2]. The size dependence of current/voltage characteristics is shown in fig.2. At larger widths voltage appears at a current independent of width and all curves follow the same line up to a turning point where a steep increase of voltage takes place. The position of the turning point depends on the width. At smaller widths the steep increase starts right at zero voltage state. Critical currents were measured from the current–voltage characteristics using 3 μV/cm electric field criterion and the position of the turning point. These values are displayed in fig.3. Quantum interference is clearly seen for all widths (see fig. 4) and for voltages above the turning point but invisible below it.

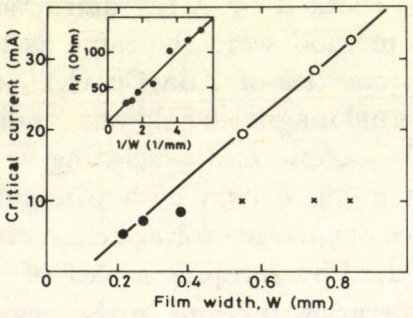

Fig. 3. Film width dependence of critical current calculated from:x, 3 μV/cm criterion; o, turning point position. Inset shows the width dependence of the normal state resistance.

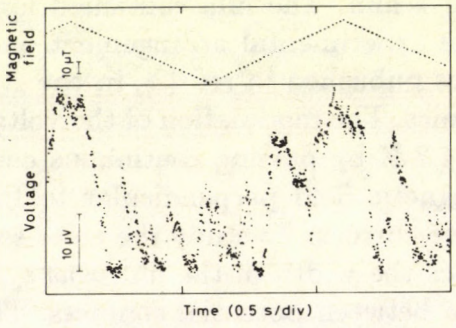

Fig. 4. Quantum interference for a film of 186μm width; upper curve: magnetic field of the coil; lower curve: voltage at fixed current.

These observations can be interpreted as follows: voltage is generated at the intergrain Josephson junctions and there is a special voltage generation at low voltages for films of larger widths. In the latter case the voltage may be produced by the flux creep of Josephson volrtices and flux lines trapped in superconducting rings. At higher voltages the film operates as a multijunction DC SQUID biased above the critical current [3].

References

*Microelectronic Co. 'MEV', H-1325 Budapest, P.O.B. 21., Hungary

1. E. Besenyei, G. Katona, P. Arató and A. Kele, Supercond. Sci. Techn. **2** 220 (1989)
2. S. Mészáros, K. Vad, G. Halász, F.J. Kedves and Sz. Balanyi, Physica **"C" 167** 139 (1990)
3. De Bruyn Oubuter and De Waele, 1970 Progr. in Low Temp. Phys. Vol.6. ed. C.J. Gorter (Amsterdam-London: North Holland) pp 243-288
4. D. Robbes, A.H. Miklich, J.J. Kingston, Ph. Lerch, F.C. Wellstood and J. Clarke, Appl. Phys. Lett. **56** 2240 (1990)

Industrial Applications at the Debrecen Cyclotron Laboratory

I. Mahunka, F. Ditrói, S. Takács and L. Vasváry

The demand for the application of nuclear technique in the industrial research and development is continuously growing. The activation technique is one of the most fre- quently used methods in the field of materials science and in the high technology industry. Using this technique analytical information can be gained, or on the basis of TLA, the mechanical wear, corrosion and erosion can be measured or monitored also even at "on-line" arrangement. The charged particle beams or the secondary fast neutron sources of the cyclotron can be used for the irradiation.

For the activation technique based on charged particle beams of our cyclotron [1] a complex analytical chamber has been developed. With this chamber it is possible to use the prompt (PIXE, PIGE, NRA) and delayed (CPAA) analytical me- thods and to perform irradiations for the wear measurements in the vacuum chamber or outside. The chamber can be sepa- rated from the accelerator vacuum and filled up with any kind of gas even at over pressure, to carry out measurements in different gas atmospheres.

For sample preparation and handling a small laboratory has been established [4] and equipped with vacuum eva- porator, metal microscope, size measuring equipment, poli- shing mashine, lead shielded box for the activated samples, etc.

Topics of the nuclear analytical methods, which have been investigated from the point of view of industrial interest, are the following:

- Investigation of oxygen and other trace elements in high purity Al materials [5,6];
- Microelemental composition of motor oil after different duration of use [7];
- Trace elements in glass samples [8];
- Investigation of bulk oxygen concentration of high purity gallium samples. [9].

The Thin Layer Activation (TLA) method is that part of the nuclear activation technique which is especially used for the investigation of different type of wear.

In our institute we have a project for the TLA mea- surement in cooperation with the Institute for Engine Deve- lopment. In the frame of this cooperation a set of experi- ments on steel–based materials has been carried out. The samples were irradiated with different particles and ener- gies. The measured and calculated activity–depth functions have been compared to build up the proper calibration curves[10].

The other project under development in our institute by using TLA method is the wear measurement of cutting edge of turning tools made from boronitrid (BN) and industrial diamond (ID). At this investigations we have a plan for the "on–line" measurements. The cutting edges are activated in case of BN via the $^{10}B(p, \alpha)^{7}Be$ and in case of ID via the $^{12}C(^{3}He,2\ \alpha)^{7}Be$ reactions. The iron component of the

cutting edges in both cases give possibility for the activation via the $^{56}Fe(p,n)^{56}Co$ reaction too.

References

1. Z. Kormány, A. Valek, ATOMKI közl., **26** 171 (1984)
2. L. Andó, F. Ditrói, A. Fenyvesi, I. Mahunka, T. Molnár, F. Szelecsényi, S. Takács, F. Tárkányi, ATOMKI Ann. Rep. p.45 (1986)
3. F. Szelecsényi, F. Tárkányi, ATOMKI Ann. Rep. p.116 (1988)
4. I. Mahunka, I. Dombi, S. Takács, F. Ditrói, IAEA 1989 INDC(Hun)-027/G p.21
5. S. Takács, F. Ditrói, I. Mahunka, NIM **B10/11** 1051 (1985)
6. S. Takács, F. Ditrói, I. Mahunka, NIM **B43** 90 (1989)
7. F. Ditrói, I. Mahunka, S. Takács, S. Seif El-Nasr, J. Radioanal. Nucl. Chem. **130** 263 (1988)
8. F. Ditrói, S. Takács, I. Mahunka, Z. Gémesi, to be published in NIM B
9. I. Mahunka, F. Ditrói, S. Takács, ATOMKI Ann. Rep. p.60 (1989)
10. S. Takács, F. Ditrói, I. Mahunka, IAEA 1989 INDC (Hun)- 027/G p.18
11. E. Browne, R. B. Firestone, Table of Radioactive Isotopes, (Ed. V. S. Shirley) J. Wiley and Sons, 1986

Vertical Concentration Profiles of Fine and Coarse Aerosol Particles Collected Over an Urban Sampling Site in the Outskirts of Budapest

S. Amemiya †, I. Borbély-Kiss, T. Katoh †, E. Koltay,
E. Mészáros ‡, Á. Molnár ‡, Gy. Szabó, M. Varga ‡

The process of deposition of atmospheric aerosols to the ground is governed by a complexity of factors related to the atmosphere the ground surface and the properties of depositing species. Detailed knowledge on the deposition is of basic importance in pollution transport modeling and in estimating environmental loading. The chemically specific characterisation of aerosol samples collected at different altitudes in surface air and planetary boundary layers correlated with meteorological parameters from simultaneous observations is considered recently as an important tool of studying dry deposition of atmospheric particulate matter [1],[2]. Aircraft measurements and sampling at meteorological towers are known as regular ways for such type of investigations.

In the present experiments aerosol samples have been collected at different heights in the air layers 0–30 m and 0–100 m. Samplers consisting of miniature SIBATA minipumps and two–stage Nuclepore filter stacks [3] were mounted at the meteorology tower of Institute for Atmospheric Physics on the former case, while a 15 m^3 balloon has been used for lifting three samplers in the latter one. Vertical distribution for temperature, humidity and wind velocity have been measured by a radiosonde at the same site. Coarse and fine dust layers deposited onto Nuclepore filters were subjected to PIXE elemental analysis at the Nagoya University.

The sampling site – a dry grassy area – is situated in the outskirts of Budapest, southeast from the city. Atmospheric conditions were moderately unstable (strong insolation, surface wind speed 4 m/s (70°), from ten to hundred m temperature difference amounted to 1.4 C° (with ground temperature 28.0 C°), relative humidity 49 %).

The vertical distribution of absolute concentration data found both in coarse and fine fractions for thirteen selected elements are plotted in Fig.1. Data show much similarity with those in [2]. Coarse-to-fine ratios help one to separate crust derived elements from anthropogenic ones. General decrease of the concentrations with increasing height indicates upward transport under given meteorological conditions, i.e. underlying air surface represents the primary source for the aerosols. Therefore, a direct determination of deposition velocities seems to be impossible under such conditions.

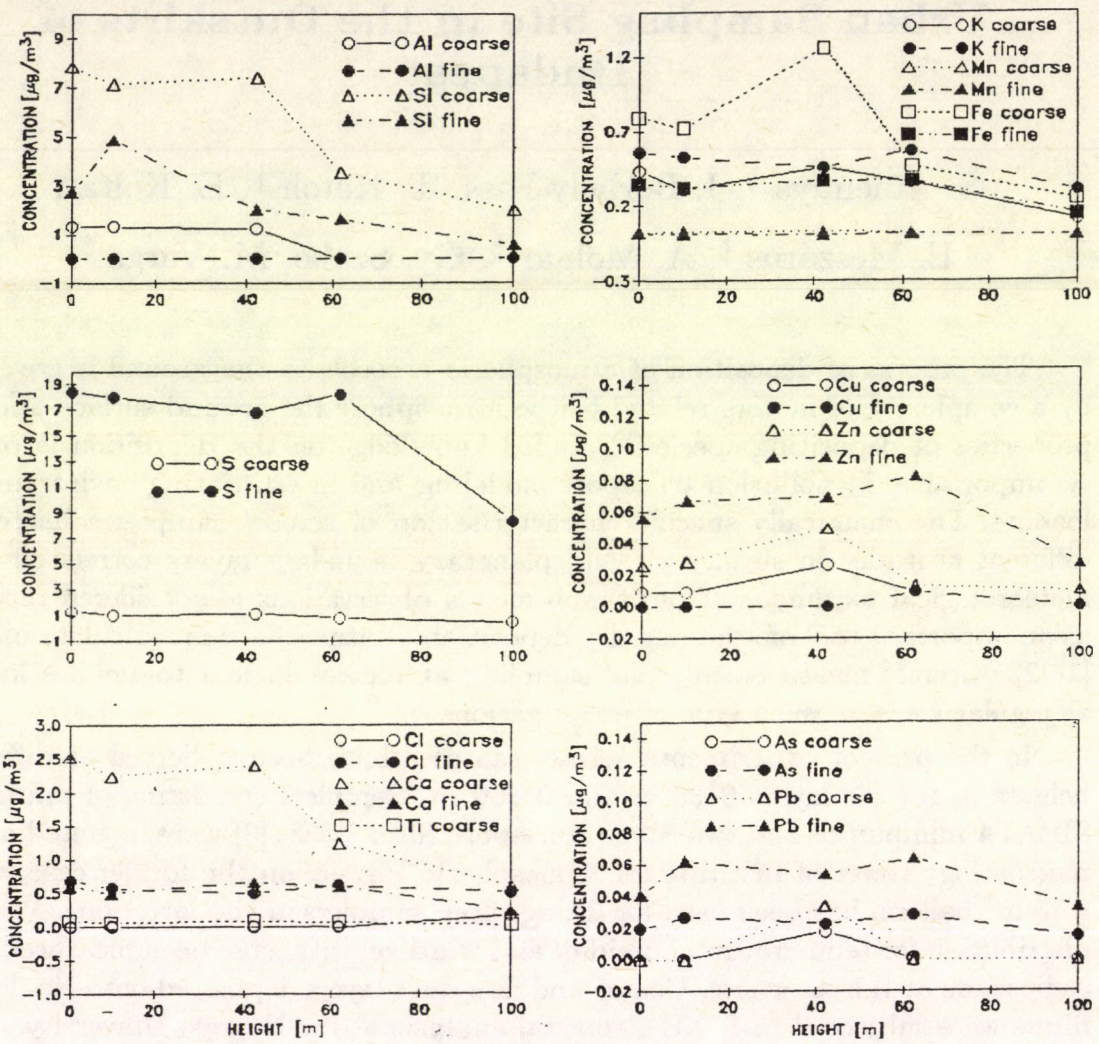

Fig. 1.

† Department of Nuclear Engineering, Faculty of Engineering, Nagoya University, Furo-Cho, Chikusa-Ku, Nagoya, Japan
‡ Institute for Atmospheric Physics, H-1675 Budapest, P.O.Box 39 Hungary

1. P.S. Guest, W.H. Mach, J.W. Winchester, J. Geophys.Res. **89** (1984) 1459
2. C.I. Davidson, Yee–Ling Wu, in Control and Fate of Atmospheric Trace Metals, eds.: J.M. Pacyna and B. Ottar (Kluwer Academic Publishers, Dordrecht 1989) 147-202
3. previous report of the same volume

Short-Range Transport of Aerosols Emitted by the Pálháza Pearlite Plant, Hungary

S. Amemiya †, S.K. Biswas ‡, I. Borbély-Kiss, T. Katoh [1],

E. Koltay, Gy. Szabó

The concentration of particles emitted from an elevated point source may be calculated for the neighbourhood of the source by the Gaussian plume formula. It describes the plume as being spread horizontally and vertically in Gaussian shape with dispersion coefficients increasing with downwind distance from the point source. Washout and fallout coefficients are used as basic parameters, some meteorological data are taken into account through corrections for air stability classes. Stack dimensions, ejection velocity and gas temperature represent the technological data of the emission source [1].

The majority of applications is related to the distribution of total emitted particulate matter. In the present work we deal with the distribution of separate elemental constituents, due to the following motivs:

- the environmental effects of different constituents are strongly different,
- due to different size distribution and deposition velocities of different constituents their transport properties and consequently the ground level concentrations may be strongly different. E.g.,elements of dispersion and accumulation mode size distribution originating from stone milling and oil burning in the emission of the present plant, respectively, will behave differently.

A validity of the simple Gaussian formalism can be expected in the former case, while particle coagulation, condensation and adsorption of gaseous species may cause deviations in the latter one, mainly in the immediate neighbourhood of the emission sources.

Aerosol samples have been collected in the interval 0.2 - 5.5 km downwind distance from the source along the Kemencepatak-valley in which the plant is located. Air of 0.4 m^3 volume was pumped through two-stage aerosol samplers consisting of 8 μm and 0.4 μm Nuclepore filters as first and second stages. In such a way particles were divided into coarse and fine fractions. The samples were subjected to PIXE elemental analysis. The longitudinal distributions for the sum of eight observed elements and for separate fractions of four selected elements are plotted in Fig. 1 .

The qualitative features can be summarized as follows:

- crust related elements (e.g. Si) and total particulate concentrations are predominant in coarse fraction, they show up strong decrease with transport distance,
- oil related elements (e.g. S and Zn) are predominant in fine fraction, their concentrations are relatively stable during short range transport. The build-up of coarse sulphur fraction can be observed with increasing distance,

– in some cases the superposition of point source emission and general background results in distributions different from the above types (e.g. Ca). A quantitative evaluation in the frame of Gaussian model is underway.

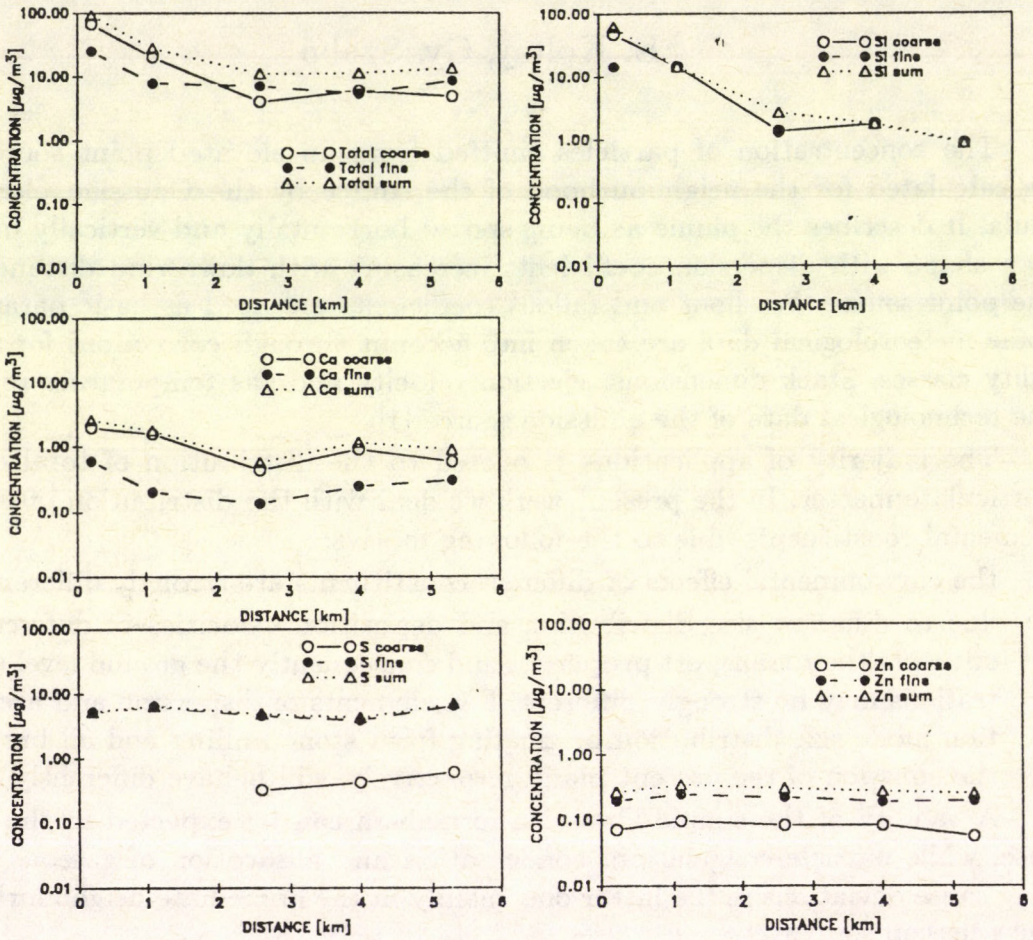

Fig. 1.

† Department of Nuclear Engineering, Faculty of Engineering, Nagoya University, Furo-Cho, Chikusa-Ku, Nagoya, Japan
‡ Atomic Energy Centre, P.O.Box 164, Dhaka 1000, Bangladesh

1. E.Koltay, IJPIXE **1** (1990) 93

Classification of Late Roman Glass Sealings by the PIXE–PIGE Method

I. Borbély–Kiss, Zs. Fülöp, T. Gesztelyi†, Á.Z. Kiss,

E. Koltay and Gy. Szabó

In Hungarian museums a special group of late Roman glass pastes are found. These pastes are flat with irregular border and have two holes lengthwise. According to iconographical and stylistic studies they were made mainly in the 3–4. centuries A. D. It is supposed that they served as official sealings. This special group of glass pastes can be classified according to the figures (one or two portraits, masks or Gorgo heads) seen on the surface.

The knowledge of the chemical composition of glass sealings could give further arguments to the characterisation made on the basis of visible parameters. It is interesting to answer also the question whether the groups created by the classification according to the pattern seen on the glass sealings are reflected by any grouping of the elemental composition of the specimens. Because of the small size and the delicate pattern of the glass sealings only nondestructive elemental analysis can be considered. The PIXE and PIGE methods suit for this argument very well. The set of specimens described above consisting of the 20 glass sealings, 2 ancient glass pastes along with 5 pieces of glass melt originating from ancient glass-works were washed with pure alcohol then irradiated by the proton beam of the 5 MV Van de Graaff accelerator of the institute. Through the detection of the arising gamma and X–rays the concentrations of the following elements were determined: Na, Mg, Al and Si (with PIGE), Si, P, S, Cl, K, Ca, Ti, Cr, Mn, Fe, Co, Ni, Cu, Zn, Sr, Zr, Ba and Pb (with PIXE). Finally on the basis of the elemental concentration values deduced a classification of the samples was performed using cluster analysis.

From the elemental analysis it can be concluded, that the concentrations of the main components of the glass specimens studied correspond the ancient Sodium–Calcium–Silicate–glasses. The classification based on the correspondences of elemental concentrations supported the grouping created through the visible parameters in three out of four cases. Nevertheless, further investigations are needed to determine the surface weathering of glass pastes which seem to have more friable structure than glass melts.

† University of Debrecen, Department of Classical Philology

1. T. Gesztelyi, I. Borbély–Kiss, Zs. Fülöp, Á. Z. Kiss, E. Koltay and Gy. Szabó, to be published in the Proc. of the European Workshop on Technology and Analysis of Ancient Gemstones, Ravello (Italy), 9–12 December, 1990.

Application of PIGE Method for the Determination of Sodium and Boron in Aerosol Samples

S. K. Biswas †, Zs. Fülöp, Á. Z. Kiss, E. Koltay

and E. Somorjai

PIGE method based on the measurement of prompt gamma rays emitted from $^{23}Na(p,p'\gamma)^{23}Na$, $^{10}B(p,\alpha\gamma)^{7}Be$ and $^{10}B(p,p'\gamma)^{10}B$ reactions has been used for the analysis of Na and B content in thin aerosol samples ([1],[2],[3]). Na is important as a sea salt element in atmospheric aerosols, while B is a tracer of coal burning emissions([4]). A resonance free energy region around 2.64 MeV was chosen for all the measurements to obtain a reasonably stable yield. The gamma radiation was detected at 90° with the proton beam direction using a 105 cm^3 Ge(Li) detector. Calibration for concentration determination was made using evaporated targets (viz. Na_2WO_4, $NaCl$ and $NaBO_2$) of different thicknesses ranging from 80 - 300 $\mu g/cm^2$ which corresponds to maximum proton energy loss of 30 keV within the sample. As shown in Figure 1. a linear correlation between the yield and concentration was obtained within the range of thickness with correlation coefficient 0.94.

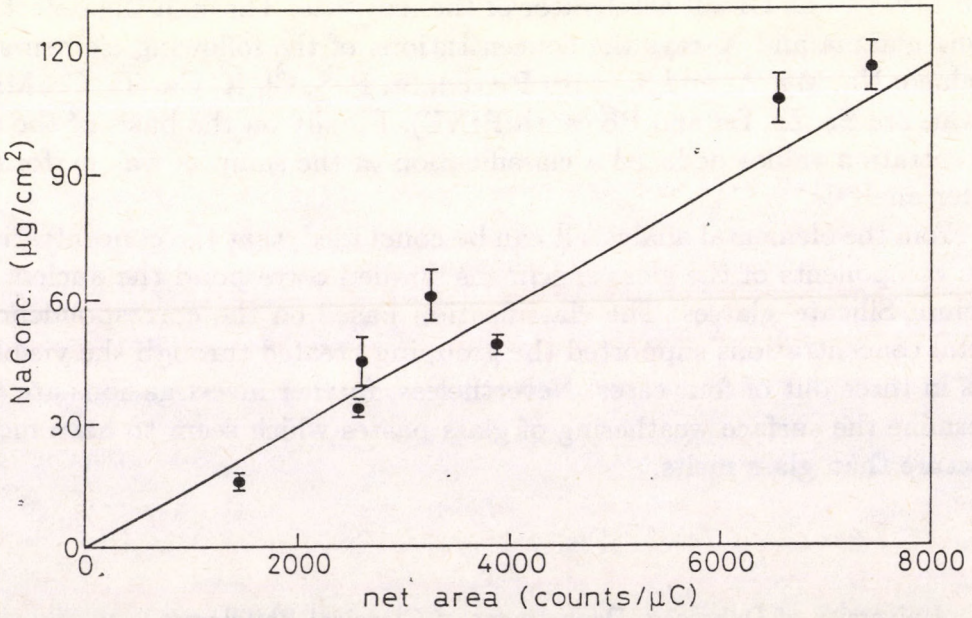

Fig. 1.

The minimum detection limit (MDL) for the method was found to be 148 ng/m^3 for Na at 439 keV γ–line, 460 ng/m^3 and 1712 ng/m^3 for B at 429 keV and 718 keV γ–lines, respectively, for 5 μC of charge and a typical air volume of

4 m^3 collected on 11.6 cm^2 exposed filter area. The detection limit may also be improved using better designed shielding around the detector and such work is in progress in the laboratory.

† Atomic Energy Centre, P. O. Box 164, Dhaka 1000, Bangladesh

1. Á. Z. Kiss et al. , J. Radioanal. Nucl. Chem. Art. **89**(1) (1985) 123
2. C. Boni et al. , Nucl. Instr. and Meth. B**40/41** (1989) 620
3. L. Asking et al. , Nucl. Instr. and Meth. B**22** (1987) 368
4. T. R. Fogg, K. A. Rahn, Geophys. Res. Letters **1** (1984) 854

Investigation of Radon Permeability Coefficients of Different Plastic Foils

J. Hakl, I. Hunyadi and M. Tóth-Szilágyi

Soil, rocks and the majority of common building materials contain small amounts from the radioisotopes of the naturally occurring uranium and thorium decay series. ^{222}Rn (radon) and ^{220}Rn (thoron) the gaseous members of these series are of particular importance either from point of view of health hazards associated with inhalation exposures or as natural trace elements of geoscience.

The separate estimation of radon and thoron concentrations is a common task, which can be satisfactory fulfilled by using of proper membranes.

The most important parameter which determines the suitability of membrane for this task is its permeability.

Using a new mathematical approach based on the description of non equilibrium condition of the radium and radon system it is possible to determine radon permeability coefficient for different synthetic materials with solid state nuclear track detector technique [1]. The developed new theoretical and experimental procedure allowed us to reduce considerably the exposition times down to some hours in contrary to that required to reach steady-state condition.

By the practical application of the method several plastic materials used in our laboratory for radon-thoron separation as filter membrane in radon dosimetry were examined. The obtained radon permeability data are given in table 1.

Table 1. Permeability constants for some plastic materials.

Material	Permeability coeff. $[10^{-8}\mathrm{cm}^2\mathrm{s}^{-1}]$
Folpack	4.7
Dom Pak	12.9
Hostaphan	0.02
Mylar	0.02
Makrofol KG	0.06
Makrofol G	0.01
PE (light)	13.2
PE (heavy)	5.3

As a practical result of the reported investigation the PE(light) and Dom Pak have been chosen as a filter material in a radon dosimeter developed also in our laboratory to separate the radon isotopes.

Reference

1. J. Hakl, I. Hunyadi and M. Tóth-Szilágyi: Radon permeability of foils measured by SSNTD technique (non equilibrium approach) (Accepted for publication in Nucl. Tracks and Rad. Meas.)

Radiocarbon Chronology of Late Neolitic Settlements in the Tisza-Maros Region, Hungary

E. Hertelendi and F. Horváth†

A new research program has been carried out in Szeged during the last fifteen years in order to investigate the chronological questions and the settlement pattern in the Hungarian Tisza region in the time of transition between the Late Neolithic and Early Copper Ages. In the course of this project nearly fifty charcoal and bone samples have been dated from the neolithic stratified tell - settlements of Hódmezővásárhely–Gorzsa, Szeged–Tápé–Lebő, Hódmezővásárhely–Kökénydomb, Szegvár–Tűzköves and from the horizontally spread out settlement of Deszk–Vénó.

The new data outline the time sequence of given settlements inside the Hungarian Late Neolithic Age as follows [1]:

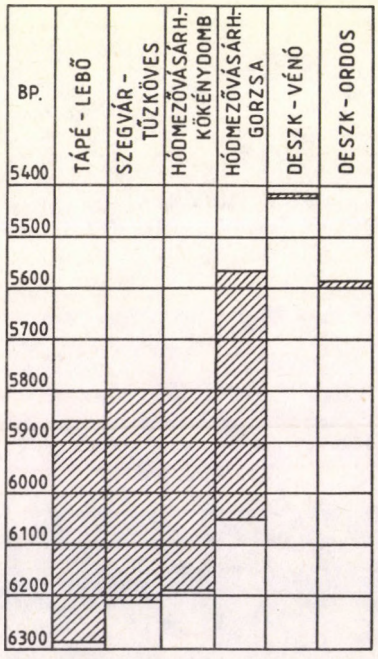

Tápé–Lebő:	$6290 - 5860BP \pm 60$
Szegvár–Tűzk.:	$6210 - 5800BP \pm 60$
Hódmv.–Kökényd.:	$6190 - 5800BP \pm 60$
Hódmv.-Gorzsa:	$6050 - 5570BP \pm 60$
Deszk-Ordos:	$5595BP \pm 65$*
Deszk-Vénó:	$5420BP \pm 60$

* (Bln-1934)

The duration of Tápé–Lebő fills nearly the whole period of the Szakálhát Culture, earlier data are known, however, from the site Battonya–Gödrösök (Bln-1970; $6370 \pm 60BP$) [2]. The second date of Tápé–Lebő signs a late Tisza Culture (Gorzsa D) settlement layer on the top of the tell. This period is paralell with

the Vinca A–B and C period on the base of radiocarbon dates from Serbia [3]. Dates of Szegvár–Tűzköves and Hódmezővásárhely– Kökénydomb belong to the early and classical period of the Tisza Culture and, are paralell with Vinca B and C, while Gorzsa – which means the classical and late periods of the Tisza Culture – is synchronous with Vinca C and D. The radiocarbon data from Gorzsa are in full concordance with the dates known from the East Hungarian Herpály and West Hungarian Lengyel Cultures [4]. The single date from Deszk-Vénó is belonging to the Proto-Tiszapolgárhát period, and parallel with Lengyel III Culture in Transdanubia ($5420 \pm 60 BP$).

References

†Móra Ferenc Museum, Szeged, Hungary

1. E. Hertelendi, F. Horváth: Archeológiai Értesítő (in press)
2. J. Szénászki: Archeológiai Értesítő, **110** 246 (1983)
3. J. Chapman: BAR International Series **117**(I) 1981–Part I, 17–31
4. L. Tálos, P. Raczky (eds), The Late Neolithic of the Tisza Region. Budapest – Szolnok, 1987, 29

The XRF Analysis of Two Prehistoric Bronze Objects

M. Kis-Varga, J. Gömöri *

Two ancient bronze objects found at Haschendorf (Burgenland in Austria) and at Balkakra (Sweden) were compared for their composition by using isotope excitation XRF analysis. The reason of performing the comparison was that the Balkakra drum is the only known duplicate of the 2500 years old Haschendorf drum which is supposed to be a relic of the sun cult. The two objects have the same appearance: their shapes, dimensions and the ornaments resemble very much. The archaeologists have the assumption that the two drums were manufactured in the same workshop in the Carpathian Basin. Fig. 1. shows the Haschendorf finding: the cylindrical side plate ends in ten wheel- like parts, and there are an upper stripe and conical decorations on it. The lid of the drum is removable. The drawing of a section of the Balkakra drum (Fig. 2.) shows similar appearance.

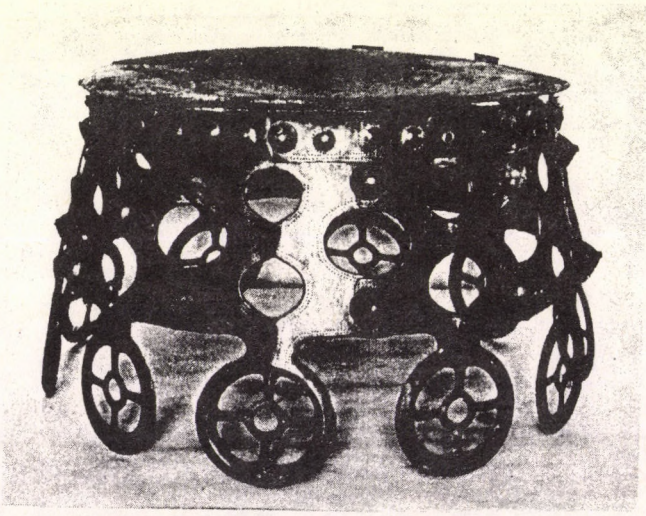

Fig. 1. The Haschendorf drum.

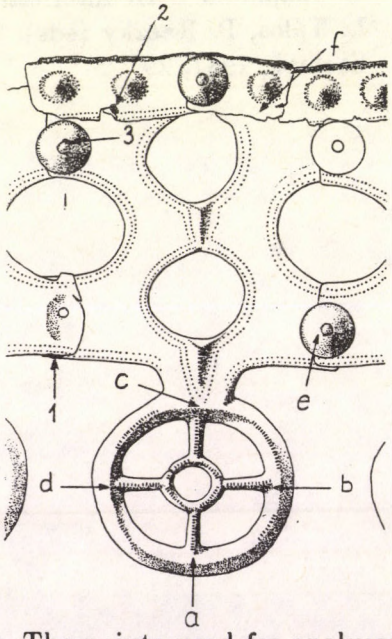

Fig. 2. The points used for analyses:1-3 Balkakra, a-f Haschendorf

The Haschendorf drum was analysed at 42 points (some of them are signed by letters on Fig. 2.): each wheels, the conical decorations, the side plate, the metal stripe and the lid. In the case of Balkakra drum we could measure only three small fragments originated from points signed by 1-3 on Fig. 2. The results in Table 1. show that the same binary Cu-Sn alloy was observed at points 1 and 3, and at points a-d and e as well. There is however significant difference between the upper stripes (see points 2 and f). The lower Cu/Sn ratio in Haschendorf drum allows one to conclude that the stripe was fixed to that drum later or the drum was repaired.

Table 1. The composition of Hashendorf- and Balkakra drums.

Sampling points	Cu(%)	Sn(%)
1.	86.8 ± 1.5	13.2 ± 1.5
a–d.	84.0 ± 1.6	16.0 ± 1.6
2.	85.4 ± 1.5	14.6 ± 1.5
f.	77.4 ± 1.7	22.6 ± 1.6
3.	87.8 ± 1.5	12.2 ± 1.5
e.	85.8 ± 2.6	14.4 ± 2.6
Hashendorf lid	86.8 ± 1.5	13.2 ± 1.5
Contaminants at points a–e: As=0.13% , Ag=0.008% and Pb=0.026%		

Table 1. also includes the small amounts of As, Ag and Pb measured at points a-e on Haschendorf drum.

In addition to the direct comparison of the two drums, attempt has been done to make clear the provenance of the drums. Some similar age bronze objects found at Velemszentvid near Haschendorf were also analysed. The results in Table 2. show that most of these objects differ from Haschendorf drum. Only the plates No. 13, 15 and 27 have similar Cu and Sn concentrations to that of the drum. The level of contaminants however in Velemszentvid objects is considerably higher. It is interesting that the Cu and Sn content of objects No. 33 (a fragment originated from the ancient foundry) is very close to the Hschendorf stripe.

Table 2. The composition of Velemszentvid bronze objects.

Sample No.	Cu	Sn	As (%)	Ag	Pb	Sb	Note
8.	83.6	1.8	-	0.6	7.6	6.3	cast ring
13.	85.0	15.0	-	0.05	-	-	plate
15.	85.9	14.1	-	-	-	-	plate
24.	87.1	11.5	-	0.1	0.81	0.54	plate
26.	80.0	18.9	-	0.08	0.56	-	cast ring
27.	86.3	13.2	0.37	0.07	-	-	plate
33.	74.5	22.6	-	0.22	1.37	-	foundry fragment
36.	81.9	14.3	-	0.17	2.51	1.03	fragment of cast bracelet

As a clonclusion it can be ascertained that the bulk materials of the two drums are the same binary bronze alloy (cca. 86 % Cu and 14 % Sn) having contaminants of As, Ag and Pb. The provenance study has shown that among the control objects tha plate shaped ones have similar compositions to the drums, while the objects manufactured by casting technology are more contaminated.

*Liszt Ferenc Museum, Sopron

EARTH AND COSMIC SCIENCES, ENVIRONMENTAL RESEARCH

Geochronological Studies with the K/Ar Method in 1990

K. Balogh, E. Árva–Sós, Z. Pécskay

In 1990 several publications appeared which were submitted in earlier years.

Dating of the Bao Loc and Dilinh area (South Vietnam) revealed that here the basaltic volcanites were produced during two distinct phases (8-12Ma and 1-2Ma before present) and demonstrated that bauxitization was connected only to the older phase [1] (cooperation: Hung Geol. Inst., Budapest; Geol. Exp. No. 6., Vietnam). The first measurements were performed on the Pliocene-Quaternary basalts in Armenia (coop.: Geochron. Lab. Arm. Acad. Sci., Jerevan), the results may be used as key data for the chronostratigraphy of that area [2]. Dating of Paleogene volcanites from the Smoliansky Region (Central Rhodope, Bulgaria) resulted ages in the 29.9-31.9Ma range (coop.: Geol. Inst. Bolg. Acad. Sci., Sofia) [3].

Dating of $<2\mu$m clay minerals (coop.: Geochem. Res. Lab. Hung. Acad. Sci., Budapest; Hung. Geol. Inst., Budapest) showed that in the Bakony Mts. (W Hungary K/Ar ages were controlled by different phases of of Hercynian orogeny, while in the Bükkium (N Hungary), with the exception of the Uppony Mts., the clay minerals were overprinted in the Lower Cretaceous.

Tholeiitic gabbro from the Adriatic sea (coop.: Dept. Geol., Urbino Univ., Italy) resulted 200.3Ma and 199.5Ma ages with the $^{40}Ar/^{36}Ar$-$^{40}K/^{36}Ar$ and ^{40}Ar(rad)-K isochron methods, respectively.

The suitability of cryptomelane for K/Ar dating has been confirmed by obtaining concordant radiometric and stratigraphic ages on Jurassic samples (coop.: Dept. Miner., Eötvös Univ., Budapest).

The Mesozoic age of a basic magmatite from borehole Nagykökényes (N Hungary) has been proved (coop.: Hung. Geol. Inst., Budapest).

Dikes, representing variable types of a differentiation series from between the Mecsek and Villányi Mts. were dated and showed that volcanic activity is confined to the Lower Cretaceous in this area (coop.: Hung. Geol. Inst., Budapest; Ore Mining Comp. at Mecsek, Pécs).

Mesozoic magmatites from the Danube-Tisza Interfluvial Region either give the real age of their formation (Jurassic, Lower Cretaceous), or show the rejuvenating effect of diffferent phases of Alpine orogeny (coop.: Dept. Miner. Petrogr. Geochem., József Univ., Szeged).

K/Ar ages of magmatites from the Tóalmás - Darnó - Bódva zone are in a 40Ma long period in the Upper Jurassic and Lower Cretaceous. The scatter of ages is attributed to secondary effects. In NE Transdanudia rocks of the lamprophyric - carbonatitic association resulted ages in the 65 - 77Ma interval (coop.: Dept. Petrogr. Geochem., Eötvös Univ., Budapest).

Lower and Middle Miocene age has been established for the tuffs in the northwestern part of the Mecsek Mts. (coop.: Ore Mining Comp. at Mecsek, Pécs).

Ages in the 8.7 - 13.4Ma interval were obtained for volcanic rocks from the Gutîi Mts., Romania (coop.: IPEG Maramures, Baia Mare, Romania).

Uniformly Oligocene ages were measured on latites from the Fruska Gora Mts., Yugoslavia, so the assumption of older ages is unsupported. Middle Oligocene age has been measured on the dacite and trachybasalt from the Rogozna Mts., Yugoslavia, but the assumed 2 volcanic phases could not be differentiated (coop.: Univ. of Belgrade, Yugoslavia).

References

1. E. Árva-Sós, K. Balogh, Nguyen van Quy, Cs. L. Ravasz, L. Ravasz-Baranyai, D. ch. v. ng. L. K. **1** 21 (1989)
2. K. Balogh, G. P. Bagdasarian, K. I. Karapetian, Z. Pécskay, E. Árva-Sós, R. Kh. Gukasian, Izv. AN ArmSSR, **43** 25 (1990)
3. A. Harkovska, Z. Pécskay, K. Balogh, Geol. Balc. CA, **20** 66 (1990)

Isotope Hydrological Evidence of Geomorphological Changes in North–Eastern Hungary

E. Hertelendi, L. Marton† and L. Mikó†

Stable isotope and radiocarbon data of groundwaters stored in Quaternary aquifers in North-Eastern Hungary can not be explained by climatic changes alone. More than two hundred δD, $\delta^{18}O$ values and radiocarbon ages of waters from 79 wells show that the recharge areas changed during the time of upper pleniglacial and late glacial. According to Borsy [1] during the Würm glaciation and even in the Holocene Epoch the northern margin of the Nyírség sunk about 20-25 m and the central part rised about 30 m. This geodynamical event resulted in a drastic change of the recharge areas and modified the direction of groundwater flow. Prior to the tectonic movements in the Quaternary the study area (Figure 1.) was watered mostly by precipitation having its catchment area in the surrounding mountains.

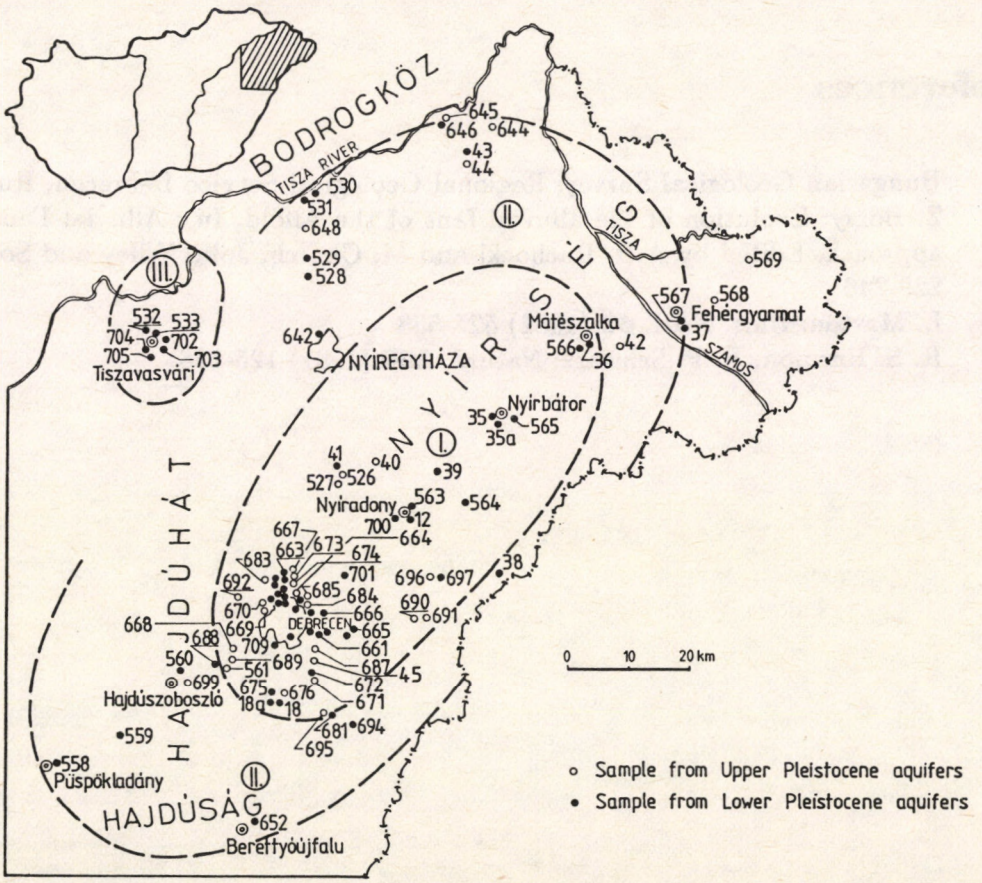

Fig. 1. Sampling sites of ground water stored in Pleistocene aquifers in North Eastern Hungary. Groups I., II,. and III. are shown in Figure 2.

Groundwaters of the studied area can be distributed into three groups (Figure 2.).

(I) Groundwaters recharged by precipitation in the very site after the topographical changes, progressively expelling the preexistent groundwater masses from these layers. The ages of these waters are between 2400-14700 years. A recharge rate of $20 \pm 2mm\ y^{-1}$ to the major aquifers in the central part of the area and an average recharge rate of $7 \pm 11mm\ y^{-1}$ in the whole area was determined by environmental isotope methods [2].

(II) Groundwaters recharged by meteoric waters precipitated at higher elevations prior to the topographical changes (altitude effect) with 13000-35000 years of radiocarbon ages and stored in Lower Pleistocene sequences.

(III) Special group of groundwaters with a catchment area of higher altitudes having larger delta deviations than samples of the same radiocarbon ages in the group I.

Our data are consistent with the geomorphological results giving isotope hydrological evidence of a geodynamical event during the late pleniglacial and late glacial periods.

References

† Hungarian Geological Survey, Regional Geological Service Debrecen, Hungary

1. Z. Borsy: Evolution of the alluvial fans of the Alföld. In : Alluvial Fans– A field approach. Edited by A.H. Rachocki and M. Church, John Wiley and Sons, 1990 , 229-246
2. L. Marton: Hidr. Közl. **62** (1982) 525-533
3. R. S. Harmon, H. P. Schwarz: Nature, **290** (1981) 125-128

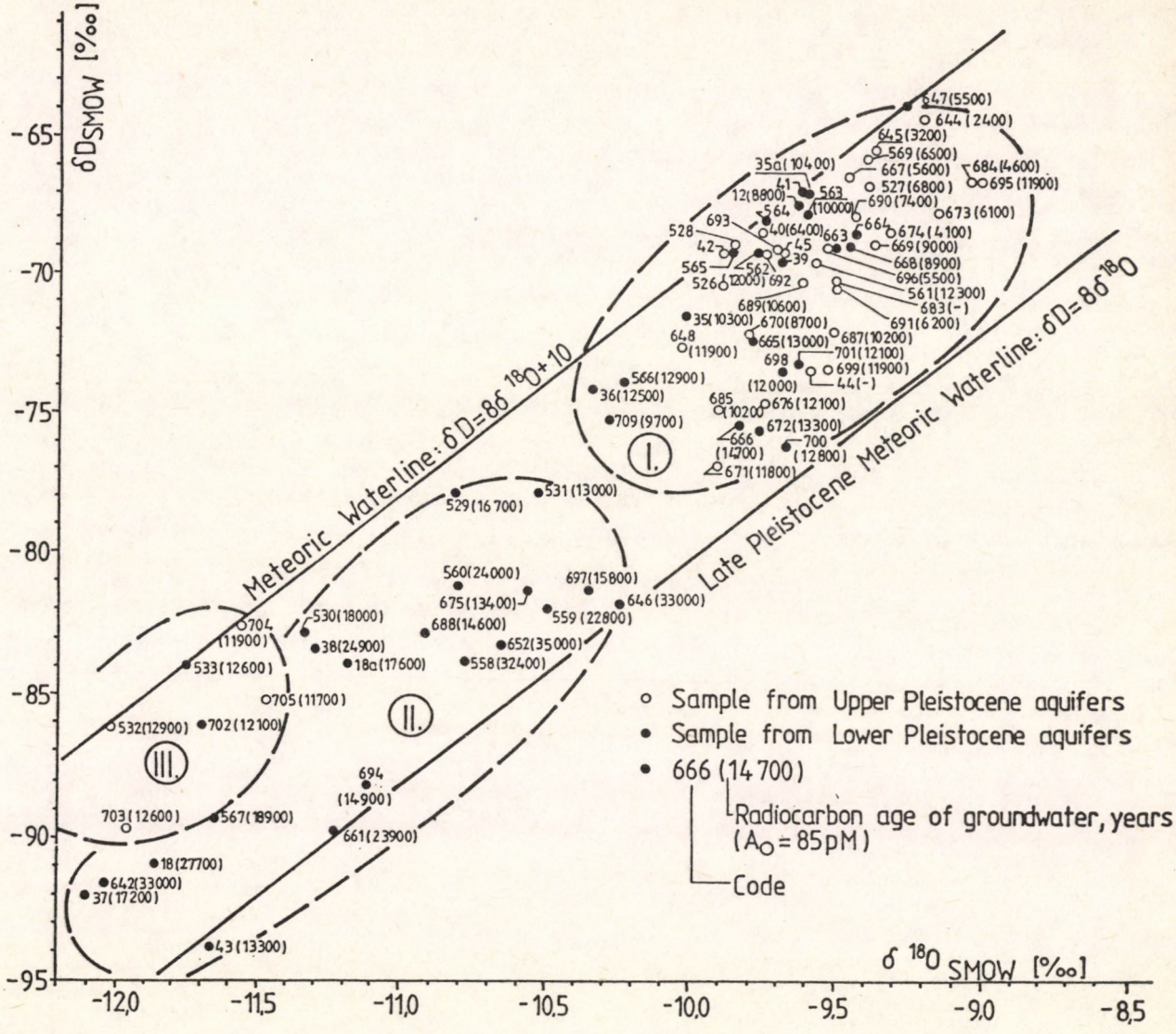

Fig. 2. Relationship between δD and $\delta^{18}O$ of known age groundwaters in Pleistocene aquifers. All our data fall between the Meteoric Water Line and Late Pleistocene Water line [3].

BIOLOGICAL

AND

MEDICAL RESEARCH

Study of Micro Elements in Monkeys Exposed to Hypokinesia

J. Bacsó, I. Uzonyi, A. V. Bakulin *, A. S. Rachmanov * and V. S. Oganov *

In our earlier investigations, the concentrations of Ca and other micro elements in rat hair was found to be in correlation with concentrations measured in bone (tibia). It was interesting to investigate whether the same or similar correlations can be found in other animals (e.g. monkeys) and the concentration of micro elements measured in hair furnishes correct data on concentration and variation of micro elements in tissues. "NON INVASIVE TEST"

In hair and different bone samples (corpus vertebrae Th6=V; os parietal (fragment:fr)=P; epiphysis proximalis ulnae (fr)=Ue; diaphysis ulnae (fr)=Ud; diaphysis tibiae (fr)=T of 9 monkeys (some of them) exposed to flight and hypokinesia, the concentration [mg/kg] of elements P,S,Cl,K,Ca,Mn,Fe,Ni,Cu,Zn, As,Se,Br,Rb,Sr,Zr,Mo,Cd,Hg and Pb were measured. As it is not known (to us (Bacsó, Uzonyi) till now) which animals were exposed to flight and to hypokinesia and which animals served as controls, the effect of hypokinesia (the difference in measured concentrations compared to that of in controls) was not investigated. A common statistical evaluation of data (correlation test) was carried out revealing relationships between the variation of elemental concentrations in tissues. Correlations were investigated between the elements in tissues and between tissues for the same element.

EXPERIMENTAL The sampling of bones and "Hair B" was carried out after decapitation of animals at the end of experiment. "Hair A" samples were collected at the beginning of experiment. The hair samples were cut using scissors and pressed into pellets (ø10mm, m=~100mg) for XRFA measurement without any pretreatment. Bones were defattened in 4:1 ration mixture of petroleum ether and chloroform for 8 hours and desiccated at room temperature in exiccator, and after grinding they were pressed into pellets of 10-20mg weight and ø8mm. Altogether 17 hair and 41 bone samples were prepared. The concentration of elements were determined by energy dispersive X-ray fluorescence analysis (ED XRFA). Elements were excited selectively by Fe-55 (P,S,Cl,K,Ca,I) and I-125 (Mn,Fe,Ni,Cu,Zn,As,Se,Br,Rb,Sr,Zr,Mo,Cd,Hg and Pb) ring shaped radioisotope sources. PC computer programs (AXIL/IAEA, XRF-BIO/ATOMKI) were used for spectrum evaluation and concentration calculations.

DISCUSSION Numerous inter–element and inter–tissue correlations (relations) have been observed. It was found that

1. The variations of micro elements in hair make it possible to follow the variation of the metabolism of micro elements in bones (in internal tissues).

2. The variation of mineral content in different bones exceeds the level of biological variability, what should be taken into account in studies of hypokinesia and effect of micro gravity to mineral metabolic rate.

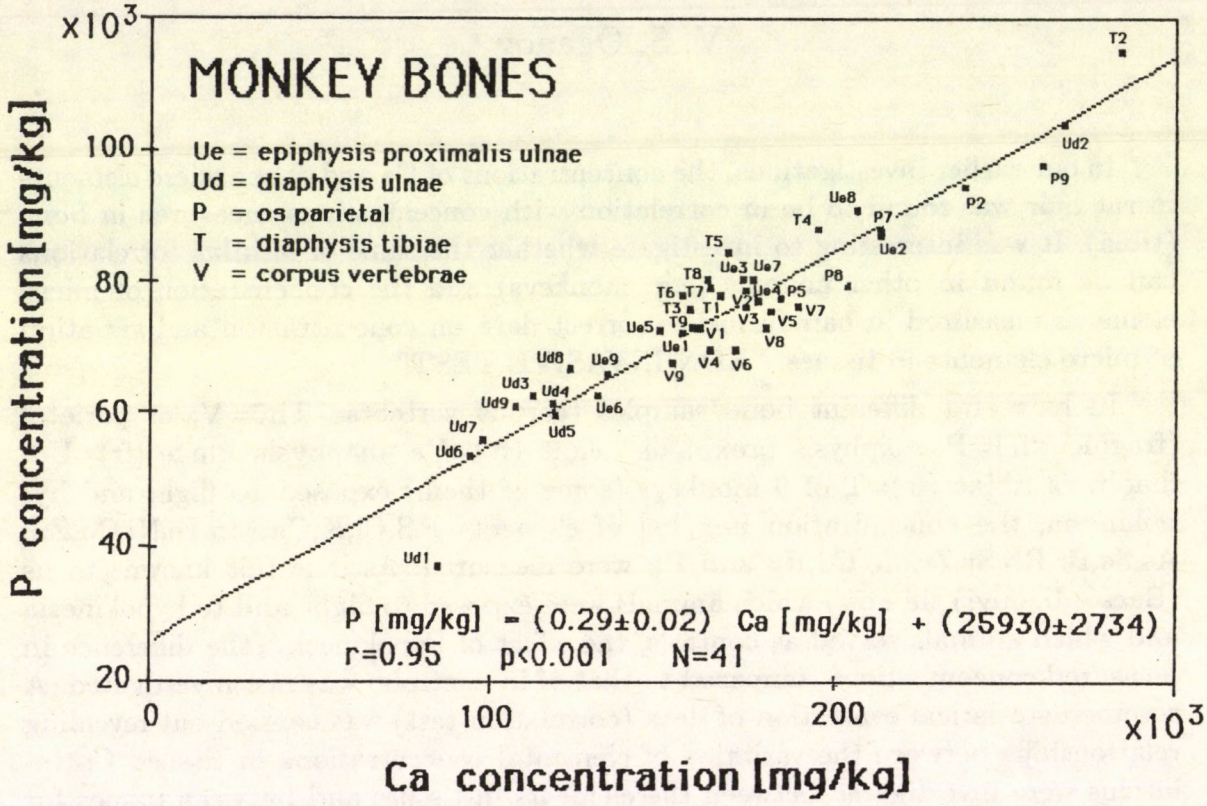

Fig. 1. P concentration vs. Ca concentration in different bones of monkeys (Macaca rhesus); experimental animals (exposed to micro gravity, hypokinesia) as well control ones.

*Institute of Biomedical Problems (IBMP), Moscow, USSR

Microprocessor-controlled gas analyser system for multi-channel mass spectrometric measurement of plant gases

G.Langer, S.Bohátka, Cs.Trajber, S.Fekete, I.Gál,

J.Gál, K.Sepsy, J.Szádai, I.Szabó, L.Kiss

Determination of gas exchange of plants is carried out under artificial conditions or discontinuously and includes only a very limited number of components in most cases. Thus, some kind of experiments cannot be achieved with the conventional techniques or the obtained results cannot be interpreted easily at the in vivo level.

In order to overcome these difficulties an analyser system was contsructed consisting of quadrupole mass spectrometer equipped with membrane probes [1,2], full - automatic vacuum system and growth chamber.

The mass spectrometer is controlled by a personal computer. Data acquisition is accomplished by the computer, the calculated values are displayed an stored. Mass range is 1 - 300 atomic mass unit. 64 components can be programmed simultaneously according to the user's selection.

Ten membrane probes are attached to the quadrupole with the help of electropneumatic valves /fig.1./. At a given time only one probe is connected to the mass spectrometer, the others are pumped by separate high vacuum system. 300 liter/sec oil diffusion pumps produce the vacuum for the quadrupole mass spectrometer and the sampling probes. The ultimate pressure is $5 * 10^{-8}$ mbar. To ensure automatic day-and-night operation, a microprocessor control unit is used for "guarding" the apparatus. In case of any malfunction - interraption in water or compressed air supply - appropriate safety operations are done automatically. After ceasing the failure the microprocessor control unit is able to restart the vacuum systems. This is highly important in the measuring of gas exchange of plants where polonged processes are monitored [3].

References

1. G.Langer, S.Bohátka, I.Berecz, B.Schlenk, P.Bornemisza-Pauspertl, K.Kiss, I.Buzás, G.Pártay, L.Mózsik, F.Sági: Vacuum,Vol**34**(1984)757-758;
2. G.Langer, S.Bohátka, I.Berecz, P.Bornemisza-Pauspertl, M.Csatlós, L.Mózsik, F.Sági: International Agrophysics 3(4)(1987)361-364;
3. F.Sági, G.Langer, L.Mózsik, M.Csatlós: Proc. of 4th International Conference Physical Properties of Agricultural Materials and their Influence on Technological Processes, Rostock Sept. 4-8, 1989.719-723;

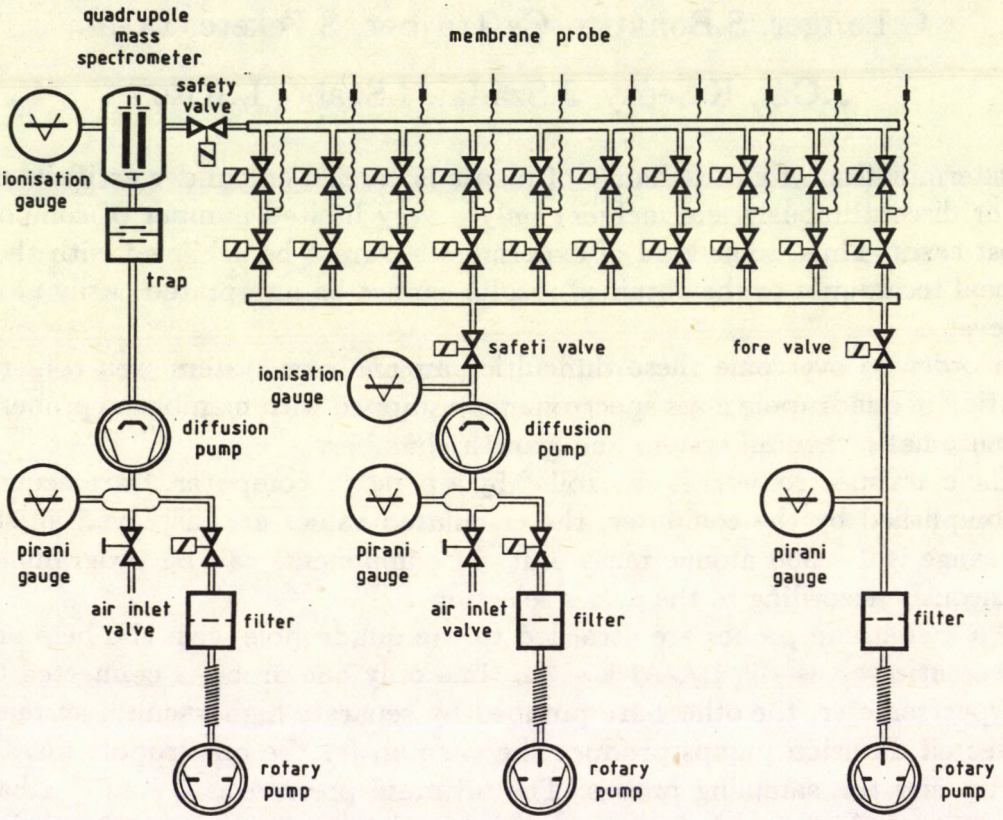

Fig. 1. Set-up of the mass spectrometer analyser system

Status Report on the Fast Neutron Irradation Facility for Radiobiological Purposes at the MGC-20E Cyclotron

A. Fenyvesi, I. Mahunka, T. Molnár *

The importance of fast neutrons in human cancer therapy is unquestionable because of their high LET (Linear Energy Transfer) values. The developements of the eighties in the fields of the accelerator technique and the targetry have resulted a spread of medical purpose advanced fast neutron irradiation facilities producing neutrons with mean energy of 14 MeV or above. These neutrons are applicable for treatment of deeply seated tumors, too. In some therapeautical cases fast neutron dose fractions are combined with other treatment modalities.

Although there are huge number of possibilities to combine modalities however most of them have not been tested by complex radiobiological studies. There are also some problems in the treatment planning and the related physical dosimetry mainly because of the shortage of some neutron cross section data and uncertainties of existing ones.

Presently these are the main application fields and reasons for the importance of the fast neutron irradiation facilities used for radiobilogical and biomedical purposes.

In 1990 the main application fields of the p(18 MeV)+Be, d(10 MeV)+Be and d(10 MeV)+D_2 neutron sources [1] based on the MGC-20E cyclotron were:

- RBE and OER measurements using different mammalian and human cell cultures as well as healthy and tumor tissue and cell cultures [2]
- cell kinetic investigations [3]
- study of effects of radiosensitizers and radioprotectors [4]
- biological dosimetry investigations for human applications

Studies are in progress within the framework of cooperations with the following institutions:

- "Frederic Joliot–Curie" National Institute of Radiobiology and Radiohygenie, Budapest
- Clinics of Radiology, Debrecen University Medical School
- Central Research Laboratory, Debrecen University Medical School
- Biomedical Cyclotron Laboratory, Debrecen University Medical School

*Biomedical Cyclotron Laboratory, Debrecen Medical University School, Nagyerdei krt. 98., H-4010 Debrecen, Hungary

1. I. Mahunka, *et al.*, Proc. of the 4th Symp. on Med. Appl. of Cyclotrons, 28-31 May 1986, Turku, Finnland, in Ann. Univ. Turkuensis, D:27, 1988
2. A. Csejtei, *et al.*, Magyar Radiológia, **63** 152 (1989)
3. A. Csejtei, *et al.*, ATOMKI Annual Report 1989
4. A.M. Dám, *et al.*, Measurement of OER and RBE for p(18 MeV)+Be fast neutrons, in Proc. of the Seventh Tihany Symp. on Radiation Chemistry, September 9-14 1990, Balatonszéplak, Hungary, Akadémiai Kiadó, Budapest (in press)

Iodine–123 Production at the Debrecen Cyclotron

L. Andó, P. Mikecz, I. Mahunka, A. N. Tcheltsov *, I. A. Suvorov *

Iodine–labelled radiopharmaceuticals are very frequently used in the nuclear medicine. Considering the importance of the ^{123}I a number of nuclear reactions have been investigated for its production [1]. On the basis of these investigations it can be concluded that if highly enriched ^{123}Te (>90%) is used, the ^{123}Te(p,n)^{123}I reaction has a great potential for production of ^{123}I by using small compact cyclotron. The main problem of this production could be the high impurity level of ^{124}I and ^{130}I which derives from the isotopic composition of commercially available enriched tellurium material.

For improvement of radionuclidic purity of the product we use a higher enrichment of ^{123}Te in the target material. The production of highly enriched (95.6%) [^{123}Te] tellurium material was carried out at the I. V. Kurchatov Institute of Atomic Energy. From this tellurium two targets were prepared and irradiated at our MGC-20E cyclotron for measurement of the ^{123}I yields and the relative impurities of ^{121}I, ^{124}I and ^{130}I at different energies [2].

The ^{124}I impurity level was considerably decreased in consequence of the higher enrichment of ^{123}Te thus the produced ^{123}I is suitable for medical applications for longer time after irradiation. The amounts of ^{125}I, ^{126}I, ^{130}I and ^{131}I were not detectable because of the very low concentrations of the tellurium isotopes having mass number of 125 or higher in the new target material.These new clear–iodine based radiopharmaceuticals were used routinely in Hungarian medical institutions during this year.

From yield data we have calculated the cross sections of the ^{123}Te(p,n)^{123}I reaction. We have to note that there are significant discrepancies between the current results and the earlier published data [3]. Therefore the excitation function for this reaction should be remeasured in the energy range of less then 18 MeV, interesting at practical production. The data evaluated from our measurement will be published in the near future.

References

*I. V. Kurchatov Institute of Atomic Energy, Moscow, USSR

1. Proc. Panel Discussion on Iodine–123 in Western Europe, (Edited by S. M. Qaim *et al.*) KFA Report Jül–Conf–20, 1976
2. B. Scholten, *et al.*, Appl. Radiation Isotopes, **40** 127 (1989)
3. L. Andó, *et al.*, J. Radioanal. Nucl. Chem., Letters **146** (3) 169 (1990)

Production Possibility of Astatine Isotopes with the Debrecen Cyclotron

Z. Szűcs and F. Szelecsényi

Recently, astatine has attracted renewed attention from the standpoint of radiobiological and therapeutical application, particularly with respect to the use of astatine–labelled monoclonal antibodies. The antibody is an appropriate vehicle for specific transport of At to centers of diseases in the body providing a useful tool for "killing" of tumors. On the other hand, both the organic and inorganic aspects of the chemistry of astatine have stimulated continuing interest, especially in connection with the formation of complexes and the stability of ionic compounds [1].

The aim of this study was to investigate the production possibilities of different astatine radioisotopes with the Debrecen MGC-20E multiparticle cyclotron. Taking into account of the parameters of the accelerator and the published thick target yields of different charged particle induced nuclear reactions leading to different astatine isotopes, the method of choice for production of At isotopes is the Bi(^{3}He,xn) process.

Natural, metallic Bi targets melted on Cu backing were used for thick target yield measurements. The samples were irradiated in the external ^{3}He beam of the cyclotron with maximum energy of 28 MeV. The activity of the irradiated targets was determined by Ge(Li) gamma-ray spectroscopy. Our preliminary results are summarized in table 1.

Table 1. Measured thick target yields of astatine isotopes produced via Bi+ ^{3}He reaction

Radioisotope	^{208}At	^{209}At	^{210}At	^{211}At
Yield (MBq/μAh)	2.1 ± 0.3	22.6 ± 3.1	1.4 ± 0.2	$<0.3 \pm 0.1$

For separation of astatine from natural Bi target drydistillation method was used with 85±5% overall yield.

On the basis of our yield data, the only economical production way for producing astatine isotope is the ^{209}Bi (3He,3n) ^{209}At reaction at a small compact cyclotron.

1. K. Rössler, Radiochimica Acta **47** 1 (1989)

Synthesis of C-11 Labelled Palmitic Acid

P. Mikecz, Z. Kovács, F. Szelecsényi

The radiolabelled fatty acids have an important role in the nuclear medicine. They can be used to quantitate myocardial free fatty acid metabolism and detect areas of ischemia and infarction. The ^{123}I labelled heptadecanoic acid already is in use in Hungarian hospitals with normal gamma cameras [1]. Since it is planned to obtain a positron emission tomograph in Debrecen some labelling procedures with positron emitting isotopes have been developed. One of these is the ^{11}C labelled palmitic acid, ($[^{11}C]PA$) which was synthesized by the slightly modified method of Padgett et al [2].

$[^{11}C]$ carbon dioxide, produced via the $^{14}N(p.\alpha)^{11}C$ nuclear reaction by the bombardment of nitrogen gas containing 1% oxygen with 18 MeV protons, was frozen into the reaction vessel by liquid nitrogen. Immediately after the freezing a solution of n-penta-decylmagnesium bromide in anhydrous diethyl ether was introduced into the vessel. When the temperature of the Grignard reaction mixture reached 20 °C it was quenched by 6 M sulfuric acid. The separated organic phase was then mixed with saturated aqueous $NaCl$ solution for removing the inorganic by-product $Mg(OH)Br$. The purification from the organic impurities such as n-penta-decane, 1-pentadecanol, ^{11}C labelled dipentadecyl ketone etc. took place on the neutral aluminium oxide column which was previously washed with 0.2% glacial acetic acid in diethyl ether. The unwanted compounds left the column when it was washed with diethyl ether, while only the $[^{11}C]PA$ remained on the column. The $[^{11}C]PA$ was eluted with 1% glacial acetic acid in diethyl ether. The synthesis required about 30 minutes, and the non–time–corrected yield was 25%. The identification of $[^{1}1C]PA$ was done by TLC analysis. A portion of the product was spotted on a silica plate, and developed with hexane-diethyl ether-acetic acid (95:5:1). The inactive impurities were detected by sulfuric acid, while the $[^{11}C]PA$ by scanning of the positron activity along the silica plate with plastic scintillator. The Rf value of the $[^{11}C]PA$ was found to be 0.44. This work was supported by the National Scientific Research Found (OTKA).

References

1. M. Horváth, et al. Izotóptechnika **31** 61 (1988)
2. H. C. Padgett et al. Int. J. Appl. Radiat. Isot. **33** 1471 (1982)

DEVELOPMENT OF METHODS AND INSTRUMENTS

IBM PC–XT/AT Based Multichannel Analyser for Nuclear Spectroscopy

J. Molnár, A. Paál, B. Sulik

At the beginning of 80s two multichannel analysers (MCA) were designed for nuclear spectroscopy measurements. One of the MCAs emulated by CAMAC modules has been used at the ATOMKI Cyclotron Laboratory [1]. The second one is a bench-top 1024 channel instrument equipped with 4 channel routing unit [2]. Both analysers are controlled by 8 bit single board computers. Their common block diagram is shown in Figure 1.

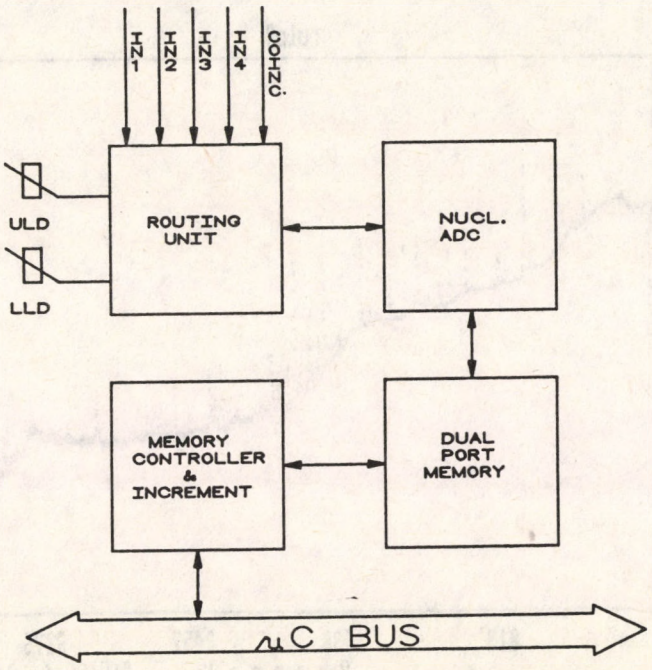

Fig. 1. Block diagram of the MCAs

The advent of the high power and relatively cheap IBM PCs made it possible to implement a bench-top Personal Computer Analyser using an add-on card in the computer. This way the need for external buffer and the expensive NIM or CAMAC system have been eliminated.

At the Laboratory of Computing Technics and Application of JINR (Dubna) a 4096 channel analog to digital converter (ADC) was developed. The ADC together with a flexible MCA emulation software for PC can satisfy wide range of user's requirements in the field of nuclear and atomic physics measurements.

As the conversion time of the Wilkinson ADCs depends on the clock frequency and on the input pulse amplitude to be converted we designed an ADC based on

the successive–approximation principle. We could realise a fix 10μs conversion time and less than 1% differential nonlinearity using a modified sliding scale method [3] without any reduction in the measurement range.

The dual port memory and the control logic were mounted on a single slot card together with the analog circuitries on a separate piggy–back one.

The programs written in TURBO PASCAL can perform gamma analysis of gamma ray spectra from Ge(Li) or HPGe detectors. Special routines are provided for MCA control and data acquisition, system calibration, peak search and multiplex resolution, and both qualitative and quantitative analysis. A spectrum collected by the 4K Analyser is shown in Figure 2.

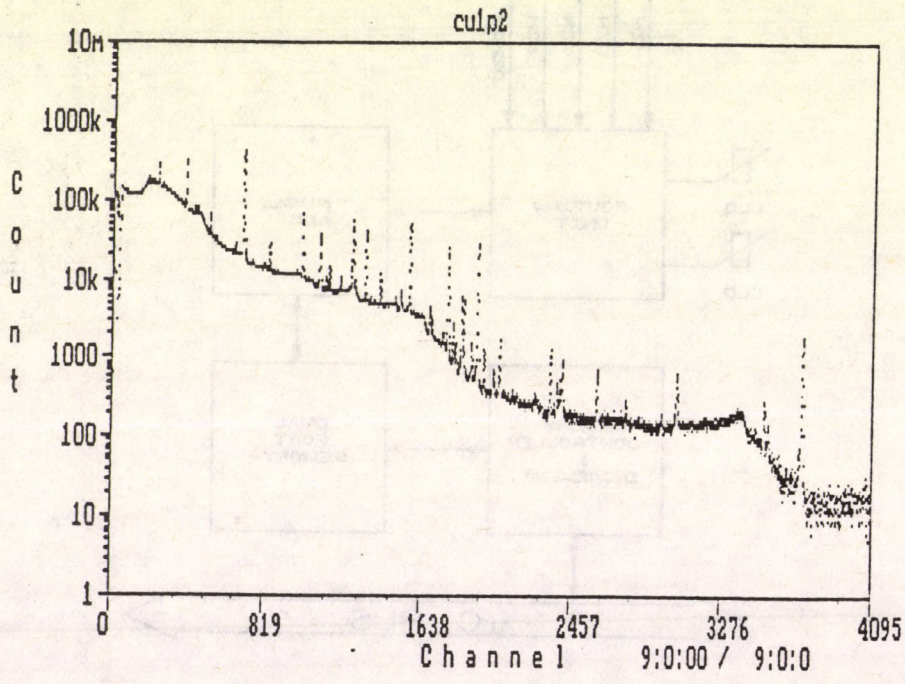

Fig. 2. Gamma spectrum of Cu target excited by 8.09GeV proton bombardment

References

1. A. Paál, K. Sepsy, A. Vass, International Symp. on Nuclear Electronics XIIIth July 2-6 1985. Dubna D13-85-793 336 (1985)
2. A. Paál, K. Sepsy, B. Sulik, Scientific Instrumentation **3** 95 (1988)
3. J. Molnár, A. Paál, B. Sulik, Patent applied for. Registration: 2251-866/90, 1990

Computer Modelling of Digital Noise Filtering for Nuclear Spectrometry

T.Lakatos

A real-time fully digital signal processing system was developed earlier in our Institute. The noise filtering for every input pulse is provided by weighted averaging of the series of the digitized momentary values of the preamplifier output voltage [1]. A special fast high resolution analog to digital converter (ADC) developed for this aplication was applied to the digitizing.

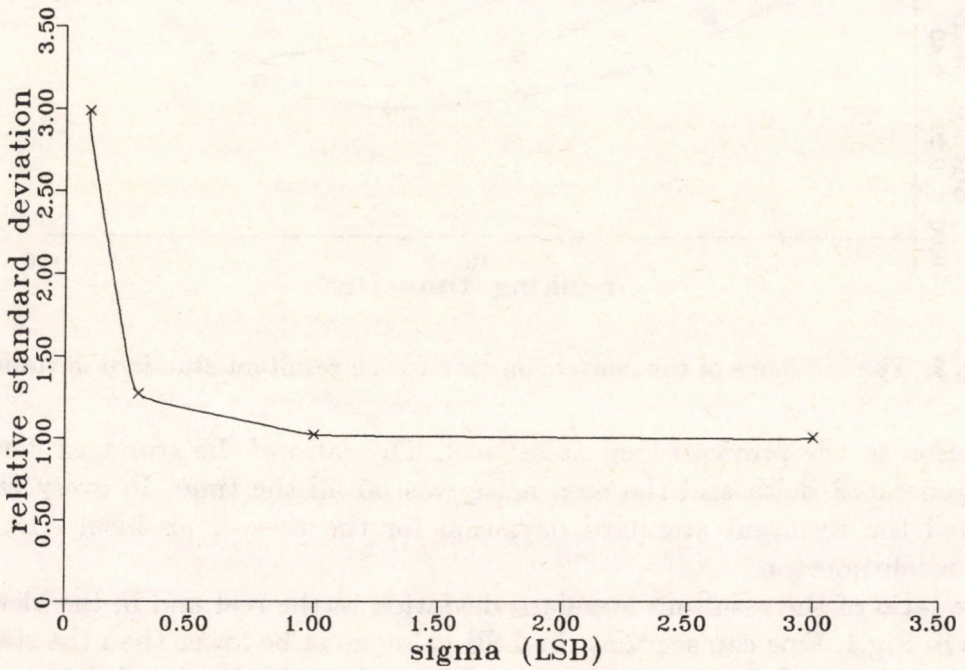

Fig. 1. The relative standard deviation as a function of the standard deviation of the input delta noise

This ADC must have no influence on the signal to noise ratio (energy resolution) of the system. If the conversion rate and/or the resolution of the converter are not high enough, than the resultant signal to noise ratio will be low, causing significant degradation of the energy resolution.

Therefore, it is very important to determine the influence of the above two parameters. The experimental tests are complicated and costly and it is difficult to separate the effects caused by the speed, the resolution and the nonlinearity of the ADC, but with computer modelling one can study those simply and independently.

The influence of the resolution of the ADC was tested first.

The values of the delta (serial) noise for each momentary value were made by generating independent random numbers with normal distribution and the step (parallel) noise values by adding independent random numbers with normal

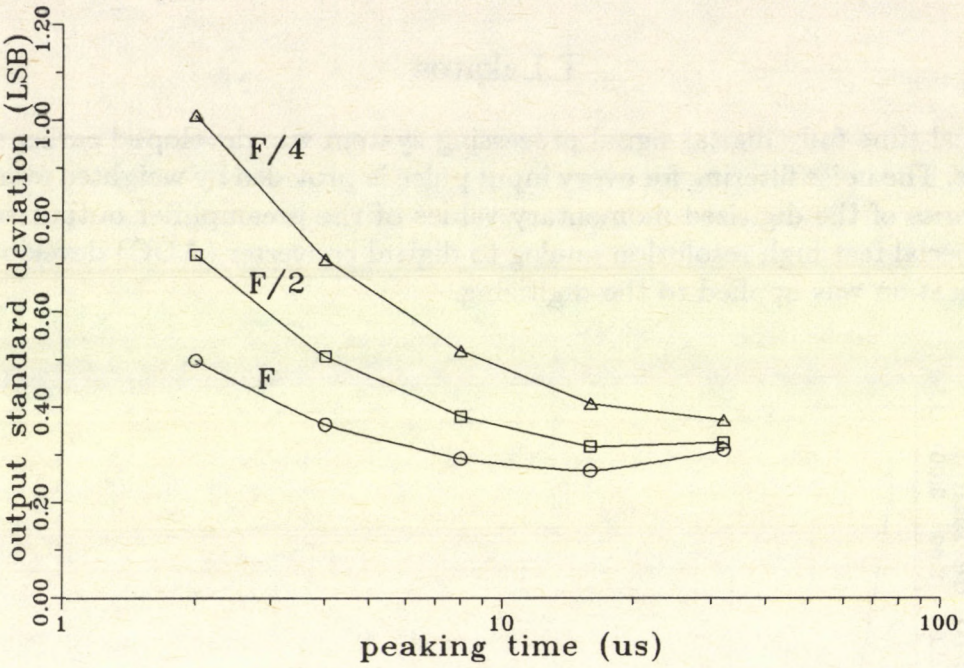

Fig. 2. The influence of the conversion rate to the resultant standard deviation

distribution to the previous step noise level. The ratio of the standard deviation of the generated delta and the step noise was 30 all the time. In every case we calculated the resultant standard deviation for the case of an ideal ADC with infinite resolution too.

The ratio of the resultant standard deviation in the real and in the ideal case is given in Fig.1. One can see that the LSB value must be lower than the standard deviation (sigma) of the input delta noise to not degrade the signal to noise ratio.

It is expected that the conversion rate of the ADC must be as high as the Shannon s sampling law demands it. The question is how much will be the deterioration of the signal to noise ratio if the conversion rate is lower then the above. The results of the computer modelling are shown on the Fig.2. The curve taken with conversion rate according to the Shannon's law is marked with F, the F/2 and F/4 curves are the results of modelling at one half and at a quarter of the above rate. A nonlinearity-free infinite resolution ADC is assumed here.

Reference

1. T. Lakatos, Nucl. Instr. Meth. B47 (1990) 307

Beam Diagnostic System for the MSI CRYRING

Th. Lindbad *, U. Rosengärd *, A. Paál, G. Székely

Cryring is a heavy ion synchrotron-storage ring under construction with internal and extracted beams [1]. Highly charged ions from an electron beam ion source [2] will be accelerated by a radiofrequency quadrupole accelerator, RFQ [3] to 300 keV/u.

Cryring will be equipped with different diagnostic elements to measure the low energy ion beam profile, to monitor the beam position in the ring and to control the voltage of the accelerator structure [4] keeping the beam centered in the beam tube. Block diagram of the monitoring system is given in Figure 1.

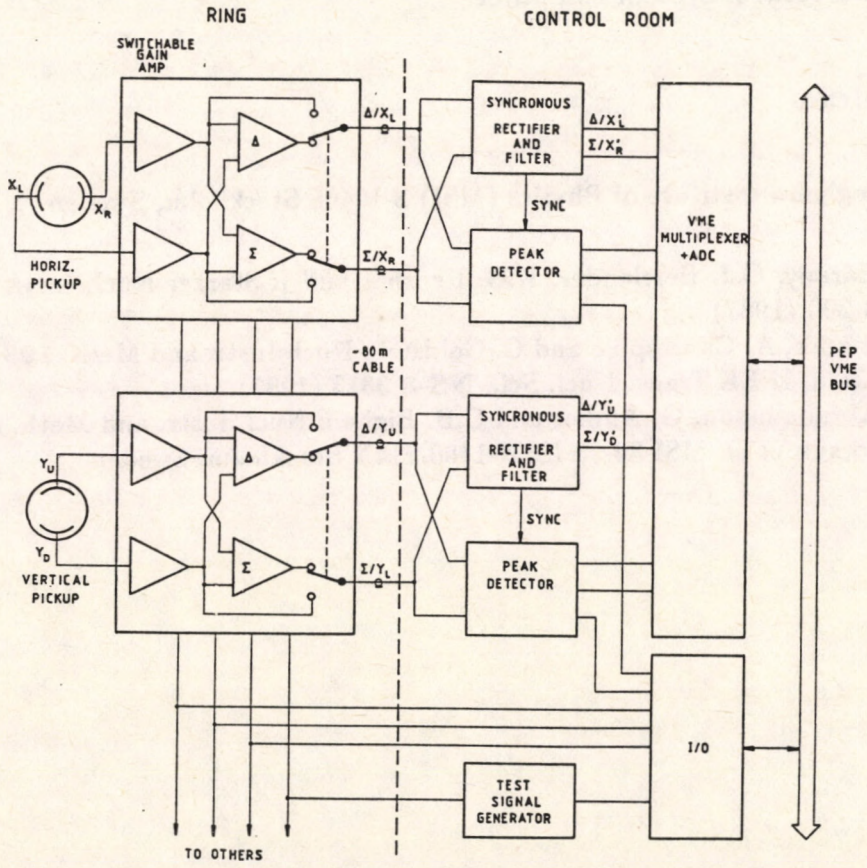

Fig. 1.. Block diagram of the beam monitoring system

The system is designed to provide position information for both single turn orbit and multiturn measurements with beam intensities in the range 10^7 to 10^{11}.

For signal processing in single turn/turn–by–turn measurements a wide bandwidth modul, in multiple turn (closed orbit) measurements a narrow bandwidth one are used which rely on signals generated by beam pick–ups. To minimalize the noise and input capacitance of the preamplifiers are connected directly to the vacuum feedthroughs on the pick–ups.

The function of the modules placed in the control room is to convert the difference and sum signals to DC levels appropriate for digitalization. One of the modules is a peak detector used for single turn measurements [5]. For turn–by–turn measurements a fast peak detector card will be used at a fixed detector pair. 256 subsequent position and intensity signals are converted and the results of the conversions are written into a memory. For the closed orbit measurements a syncronous rectifier is used to handle the incoming beam signals.

The DC signals derived from the two modules are digitized and read out under the control of a VME–based PEP microprocessor system, which will be connected to the main control system computer.

References

*Manne Siegbahn Institute of Physics (MSI) S-10405 Stockholm, Sweden

1. A. Bárány, C.J. Herrlander, K.G. Rensfelt and I. Starker Nucl. Instr. and Meth. **B23** 200 (1987)
2. I. Arianer, A. Cabrespine and C. Goldstein Nucl. Instr. and Meth. **193** 401 (1982)
3. H. Klein, IEEE Trans. Nucl. Sci., **NS-3** 3313 (1983)
4. K. Abrahamsson, G. Andler and C.B. Bigham Nucl. Instr. and Meth. (1988)
5. S. Borsuk *et al.* MSI 89-20 ISSN-1100-214X Stockholm, Sweden

Comparison of Different Methods Used for Fast Neutron Beam Mapping

L. Medveczky, J. Hakl, A. Fenyvesi and T. Molnár *

At the MGC type cyclotron in Debrecen intense (p,n) and (d,n) fast neutron beams were established mainly for medical purposes. The flux density distribution of the fast neutron beam was mapped in a water phantom with ionization chambers and also with solid state nuclear track detectors.

The obtained neutron dose rate distribution profiles had an asymmetry which could be attributed to the non sufficient alignment of the neutron collimator setup. All the measured profiles were correlated within the limit of experimental error.

Mapping fast neutron beams with SSNTDs does not required longer irradiation time than 10-20 min (as it is usual in oncological therapy) thereby the activation of the irradiation facility was minimized. The shorter irradiation time also reduced the effects of uncertainties caused by instabilities in the charged particle beam.

References

*Biomedical Cyclotron Laboratory, Medical University School of Debrecen, 4012 Hungary

1. L. Medveczky, J. Hakl, A. Fenyvesi and T. Molnár: Fast neutron radiation field measurements in a water phantom (Accepted for publication in Nucl. Tracks and Rad. Meas.)

On the Applicability of PIXE Microanalysis at 10^5 eV Bombarding Energies

S. K. Biswas †, I. Borbély–Kiss, U. M. El–Ghawi ‡,E. Koltay and Gy. Szabó

Optimum detection parameters of PIXE can be achieved around 2 MeV bombarding energy due to the fact that Coulomb interaction between accelerated protons and atomic electrons of the inner shells gives maximum ionisation cross sections for most elements in the proton energy range 2–10 MeV [1]. Therefore, the routine application of PIXE is limited to laboratories with Van de Graaff or small cyclotron accelerators in the MeV range.

In earlier papers some attempts have been made to use PIXE on low energy accelerators – routinely used as neutron generators – with low beam energy of several hundred kilovolts ([2],[3],[4]). Such machines are widely available, simple to service, less expensive and would offer an extension of research activity in a neutron physics laboratory toward microanalytical topics.

In order to make a critical evaluation of the applicability of low beam energies the PIXE set–up [4] and evaluation routine [5] regularly used in the present institute was used in the determination of minimum detection limit (MDL) in the energy range 2.5–0.25 MeV. Data were obtained on thick carbon and stainless steel targets by measuring the background of the matrix and calculating X–ray production cross sections of the trace elements to deduce MDL–s.

The results are illustrated in Fig.1 presenting MDL–s for thick carbon matrix under the following experimental conditions: total collected charge: $1\mu C$, solid angle $1.12 \times 10^{-4} sr$, detector resolution 210 eV for MnK_α. The question of applicability in terms of competition with alternative microanalytical methods is a subject of further investigation.

† Atomic Energy Centre, P. O. Box 164, Dhaka–1000, Bangladesh
‡ Tajura Nuclear Research Centre, P. O. Box 84462, Tripoli, Libya

1. R. Boro and S. Cipolla, Nucl. Instr. and Meth. **131** (1975) 343
2. D. I. Bales et al. , Advan. X–ray Anal. **18** (1975) 299
3. R. G. Musket and W. Bauer, J. Appl. Phys. Vol. **43**, No.11, (1972) 4786
4. I. Borbély–Kiss et al. , Nucl. Instr. and Meth. B**12** (1985) 496
5. L. Zolnai and Gy. Szabó, Nucl. Instr. and Meth. B**34** (1988) 118, B**36** (1989) 88

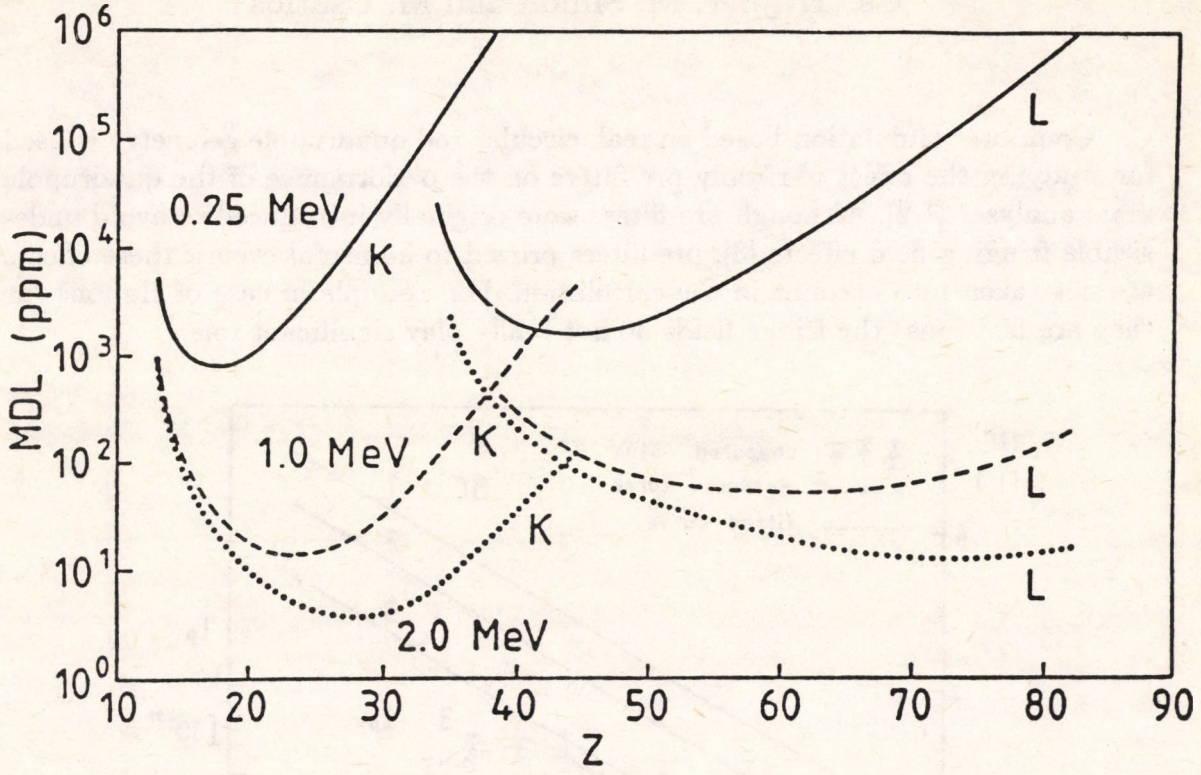
MDL (ppm)
Z
0.25 MeV
1.0 MeV
2.0 MeV
K
L
K
K
L
L
10^6
10^5
10^4
10^3
10^2
10^1
10^0
10
20
30
40
50
60
70
80
90

Fig. 1.

Pre-filters in Quadrupole Mass Spectrometers

Cs. Trajber, M. Simon and M. Csatlós

Computer simulation based on real, circular rod quadrupole geometry is used for studying the effect of rf-only pre-filters on the performance of the quadrupole mass analyser [1,2]. Although pre-filters were originally introduced to avoid undesirable fringing field effects [3], pre-filters proved to be useful even if these effects are not taken into account in the calculation. For example in case of He ions (as they are fast ions) the fringe fields do not really play significant role.

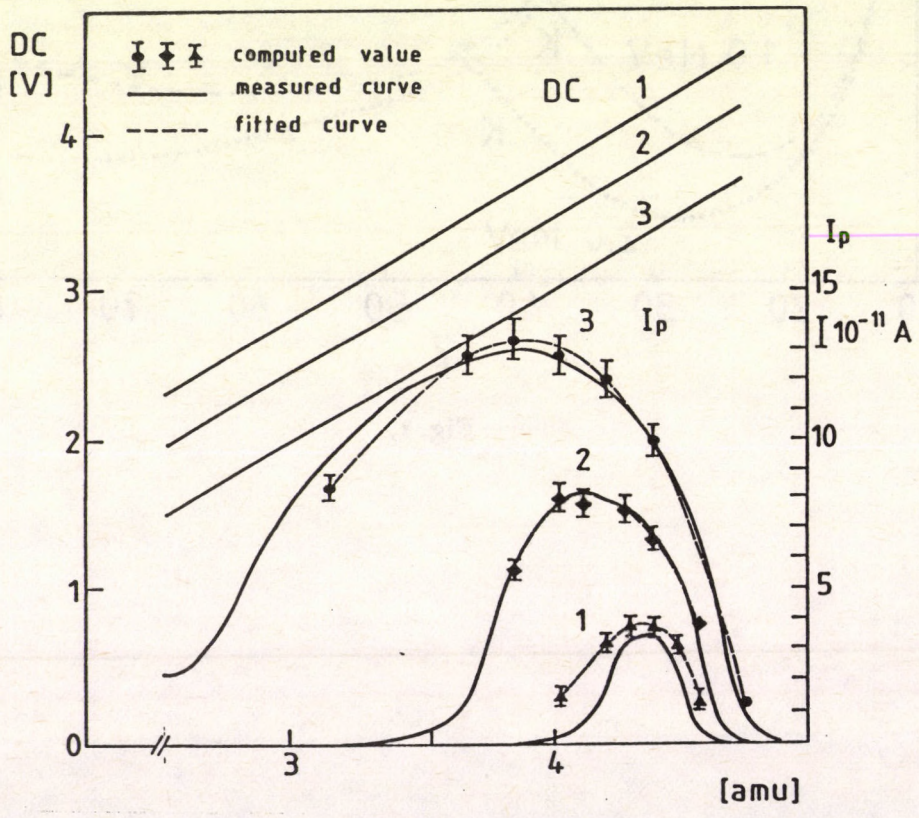

Fig. 1. Experimental and calculated He peaks belonging to the three scan lines (DC 1,2,3). Quadrupole analyser without pre-filter.

In fig. 1 one can compare the peaks obtained by scanning on three different scan lines in the He stability region with the main analyser both experimentally and by the simulation. In case of normal filter operation, the computer simulation values are in good agreement with the measured peaks. Since the ions enter the "perfect", abruptly beginning quadrupole field in the model, the acceptable

agreement suggests that the fringe fields do not perturb significantly the motion of light ions.

The effect of the pre-filters was studied by computer simulation and experimentally. The experimental and the calculated results are in good agreement. The results are shown in fig.2. The intensity as a function of the pre-filter length has a definite maximum. The length of the main analyser was 100 mm. The optimum pre-filter length found by the simulation is 12 mm. At this pre-filter length the increment of the transmission was about 80% in case of the simulation and about 50% experimentally.

Consequently, mass spectrometers supplied with pre-filters produce better performance than the analyser itself not only for higher masses, where the fringing field effects are considerable, but also for lower ones where they can be neglected. Presumably the pre-filters of optimum size remarkably enlarge the effective inlet aperture of the main filter.

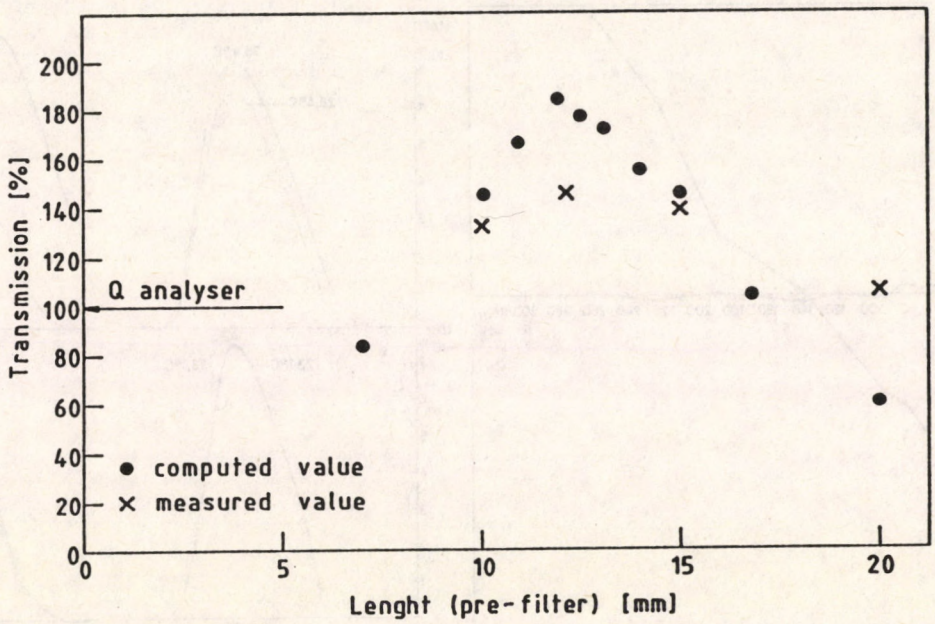

Fig. 2. Calculated and several measured relative peak-intensities plotted against the pre-filter length. The transmission of the main analyser is taken 100%.

References

1. Chisholm T, Stark A M 1970 J. Phys. D**3** 1717
2. Birtles A B 1972 J. Phys. D**5** 1396
3. Brubaker W M 1968 Advances in Mass Spectrometry Vol**4** (Amsterdam: Elsevier)

Data Acquisition and Control System for Quadrupole Mass Spectrometer Using an Add-on Card to an IBM PC

A. Paál, J. Szádai, G. Székely

The application of microcomputers to collect and analyze data has been in the Institute for several years [1-3]. Much more, than simple data logging is now required if the full benefit of computer software is to be used in the improvement of quadrupole performance. According to this concept were designed the RF/DC unit, the dedicated interface card and the PCQMS software package for the Q300PC quadrupole mass spectrometer series to replace the earlier designed one (Q300C).

RF/DC unit

The stability of peak location and the actual resolution first of all are determinated by the RF generation, namely by the AC amplitude stabilizing loop.

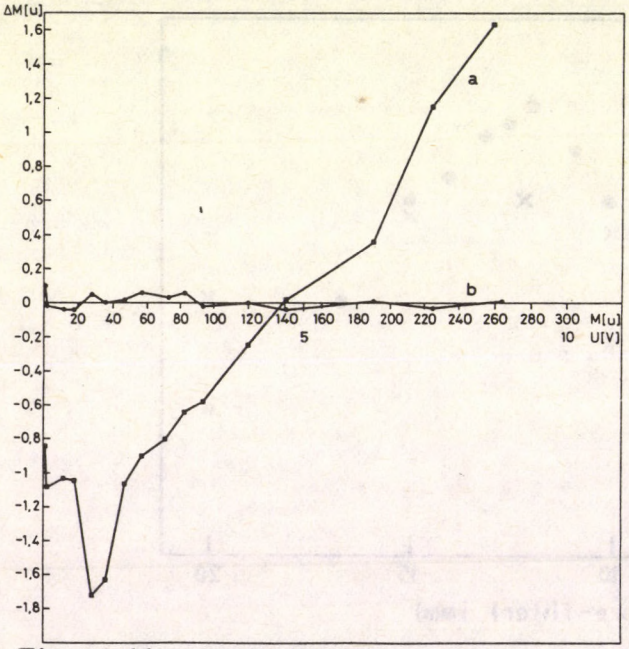

Fig. 1. Mass scale linearity vs. control voltage. a., Q300C model b., redesigned Q300PC series

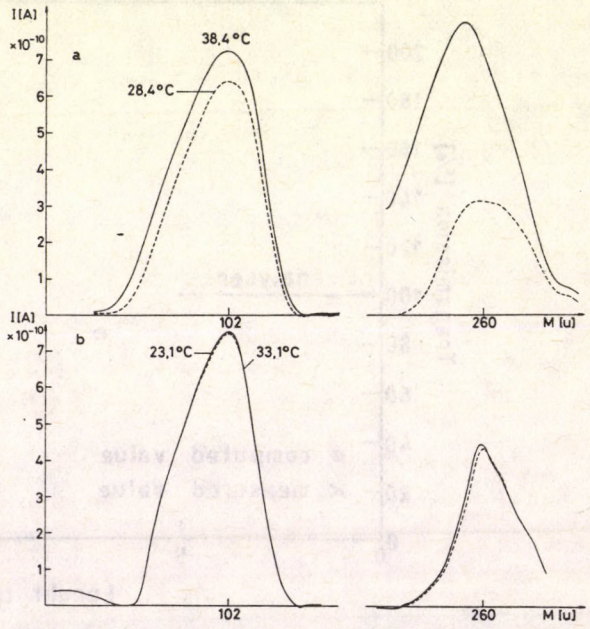

Fig. 2. Temperature stability of the RF/DC unit at two different atomic mass unit. a., Q300C model b., redesigned Q300PC series

To maintain the resolution at a constant value and to correct the peak location throughout the operatinal mass range the control loop was modified (patent applied for). Results obtained with the benefit of the second loop and the modified rectifier circuit, are tipically 20 times better than that obtained with the previous model. The measured mass scale linearity and the temperature stability of the RF/DC unit are shown in Figure 1 and 2.

Interface card

At the design of the dedicated interface card the main goal was not to sacrify overall system performance and data throughput inherent with the quadrupole mass filters. The add-on card to the IBM PC can perform the following tasks:

1. set and measure the parameters of the ion source, electrometer amplifier,
2. select the mass range to be measured,
3. change the resolution of the spectrometer,
4. digitize the output signal of the electrometer amplifier and store the measured data using the DMA capabilities of the IBM PC.

The block diagram of the card is shown in Figure 3.

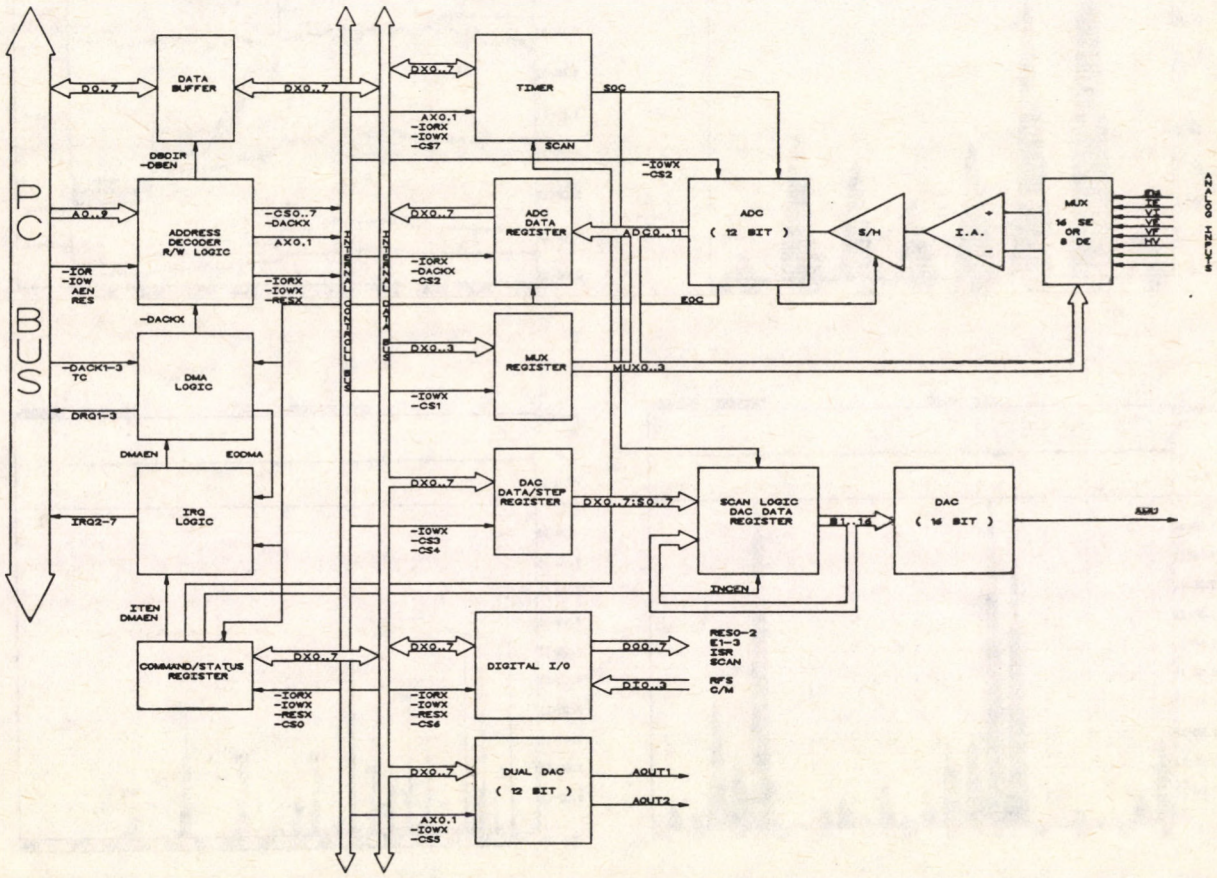

Fig. 3. Block diagram of the interface card

Software features

Two main measuring modes are: ion monitoring (up to 8 ions) and continuous scan of a selected mass range. The main functions of the program are: **Main menu – Edit General Parameters – Edit Channel Parameters – Set Display Mode – Start/Stop Ion Source – Start/Stop Measurement – Save/Restore Data File – Temporary Quit to DOS – Exit from This Program**

Display modes, all in high resolution graphics, are provided to include Ion Monitoring Table, Ion Monitoring Analog, Intensity vs. Time or Temperature, Scan Bargraph, and Scan Analog. Figure 4.

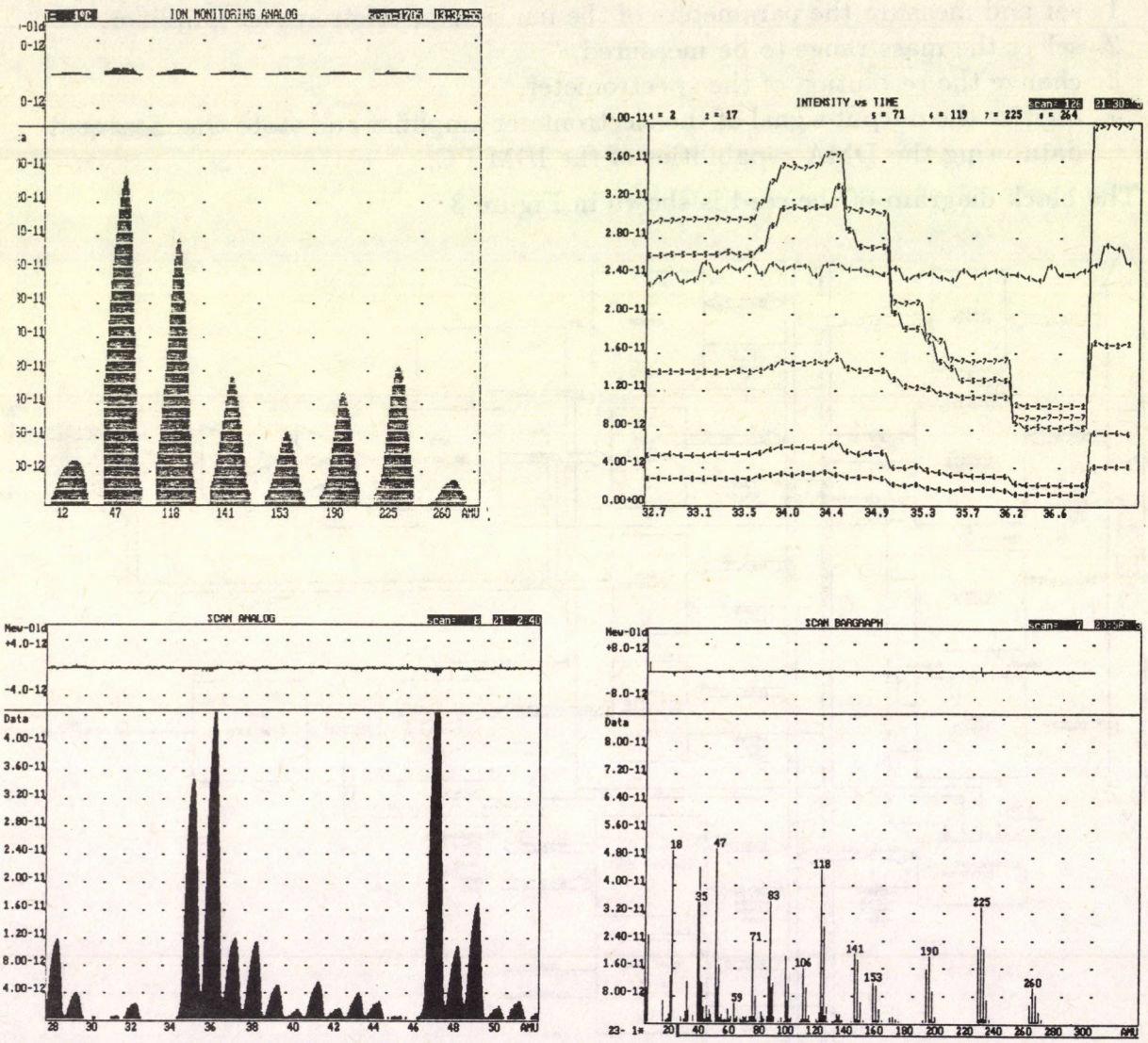

Fig. 4. Display modes of the PCQMS

References

1. J. Molnár, A. Paál, Mérés és Automatika, **28** p.469 (1980)
2. Z. Diós, K. Sepsy, I. Szabó, G. Székely, Computer Physics Communications **41** p.423 (1986)
3. A. Paál, K. Sepsy, B. Sulik, Scientific Instrumentation **3** p.95 (1988)

A High-Energy Electron Spectrometer for Multimethod Surface Analysis

D. Varga, L. Kövér, I. Cserny, J. Tóth, K. Tőkési

A complex electron spectrometer (Fig. 1) has been built for multitechnique studies of solid surfaces.

The electron analyzing part is based on a 180^{o} hemispherical electrostatic analyzer with a working radius of 250 mm, and with the option of electron energy multidetection, focussing in the 20-500 eV pass energy range and floatable up to 10 keV. The construction of the analyzer provides the possibility to place a smaller hemispherical analyzer inside the inner electrode. This second analyzer can be applied for electron energy loss and ion scattering spectroscopy.

Electrons from the sample are transported to the analyzer inlet slit by the help of a multielement input lens system with zoom focussing (for an object of fixed position and energy, the energy of the image can be varied whilst its position remains constant) consisting of a combination of cylindrical and Bessel-box type lens elements. The parameters of the lens system are: magnification = -1; object-image distance= 596.6 mm; maximum input energy = 10 keV; retardation ratio = variable between 0.2-40. Both fixed retarding ratio and fixed analyzer transmission operating modes can be used.

Two twin-anode 30 kV X-ray sources are providing a selection of characteristic X-ray lines for exciting photoelectron and Auger-electron spectra. Auger transitions can be induced by continuum X-rays as well by using respective high atomic number (Mo, W) anodes.

Application possibilities of ion and electron beams for modification and characterization of sample surfaces are ensured by the construction of the sample chamber. A precision UHV sample manipulator makes possible three dimensional motion of the samples. Tilting and azimuthal rotation can be utilized for angular resolved studies of depth profiles or diffraction effects.

For various sample preparations another UHV system is joined to the sample chamber; separably by a gate valve. This preparation chamber is equipped with a sample introduction gate and it includes a sample conveyor mechanism.

The vacuum pumping of the spectrometer system is provided by different (triode ion-getter, closed-loop refrigerator cryo, turbomolecular, diffusion, Ti sublimation) UHV pumps, the pressure in the sample chamber is ca $7x10^{-7}$ Pa without baking.

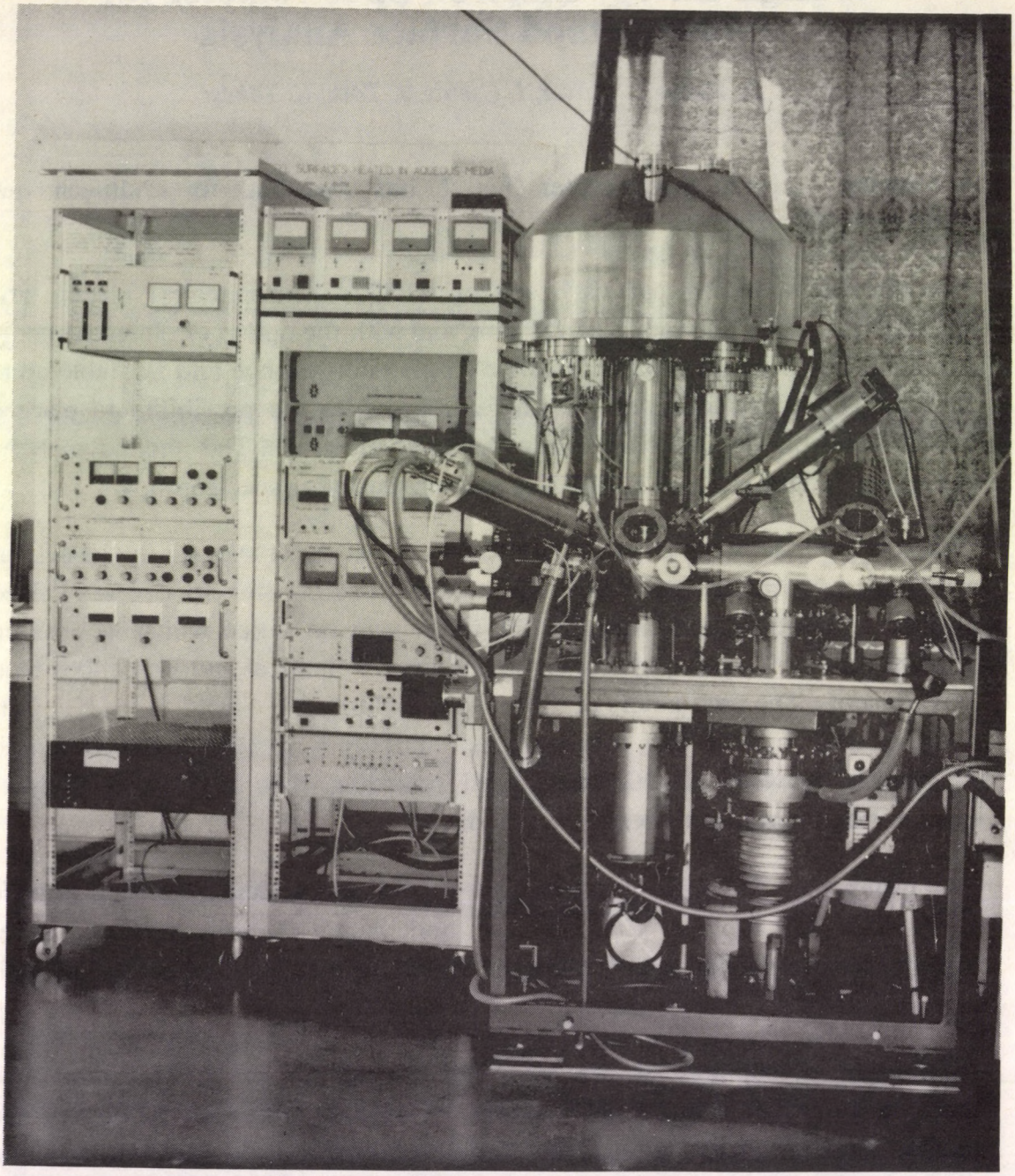

Fig. 1 The view of the new high-energy electron spectrometer (ESA-31)

Microminiature Refrigerator

G. Máthé

In order to improve the sensitivity or signal–to–noise ratio of low noise amplifiers, infrared detectors, and many other devices, it is usually necessary to cool down to cryogenic temperatures. This has been done in the past with liquid cryogens and more recently with miniature cryocoolers. However, the miniature cryocoolers which operate to 80 K or thereabouts, typically have a refrigeration capacity of the order of 1-10 W, while the devices themselves dissipate a few milliwatts at most. This very large mismatch between the cooling capacity and the required refrigeration suggested to develop a microminiature refrigerator which would match more closely the refrigeration needs.

We realised the suggestion of W.A. Little [1,2] who etched a pattern of fine grooves in the surface of a thin plate of glass to define the heat exchanger system of a Joule–Thomson device. The pattern is fabricated on the basis of photolithographic process. Finally the glass plates are fixed together.

Performance characteristics

The microminiature refrigerator operates with high purity gases,nitrogen or argon are preferred. To reach the required minimum contamination level, zeolite 4 A was used as a molecular sieve. The gas pressure has to be above 10 MPa to initiate an effective cool down. The refrigeration capacity of the device depends very strongly on the gas pressure, while the minimum temperature is independent of it. The dimensions of our refrigerators are 75xl2x3 mm and can be seen in Fig.1. Standard cylinder of dry gas operates the cooler for about 50 hours.

The typical characteristics can be seen in Fig.2.

References

1. W.A. Little, Rev.Sci.Instrum. **55** (5), 661 May 1984
2. S. Garvey, S. Logan, R. Rowe, W.A. Little, Appl. Phys. Lett. **42** (12), 1048 June 1983

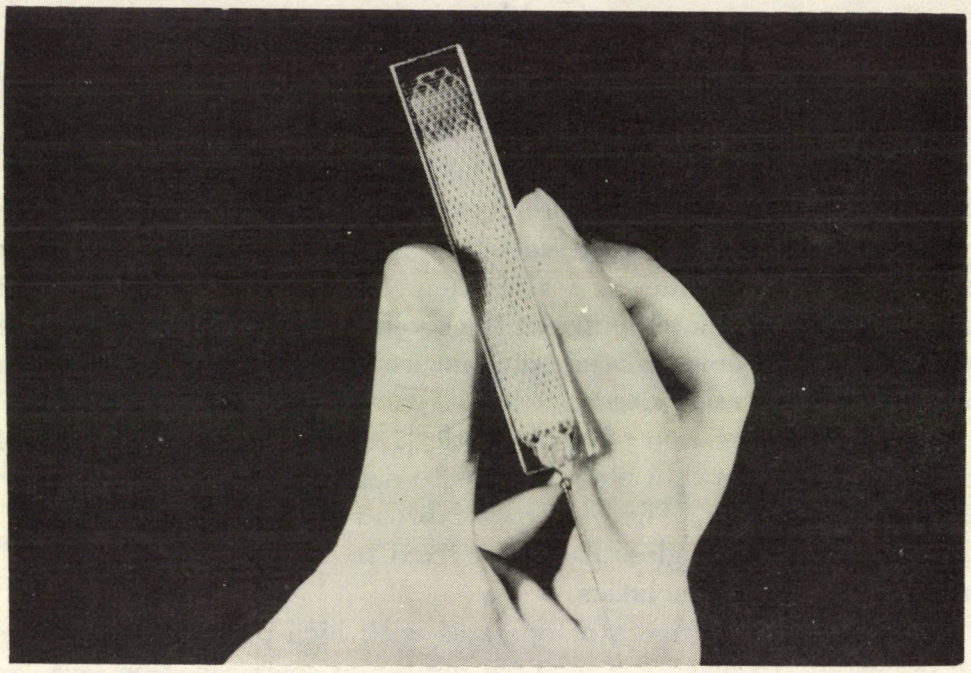

Fig. 1.

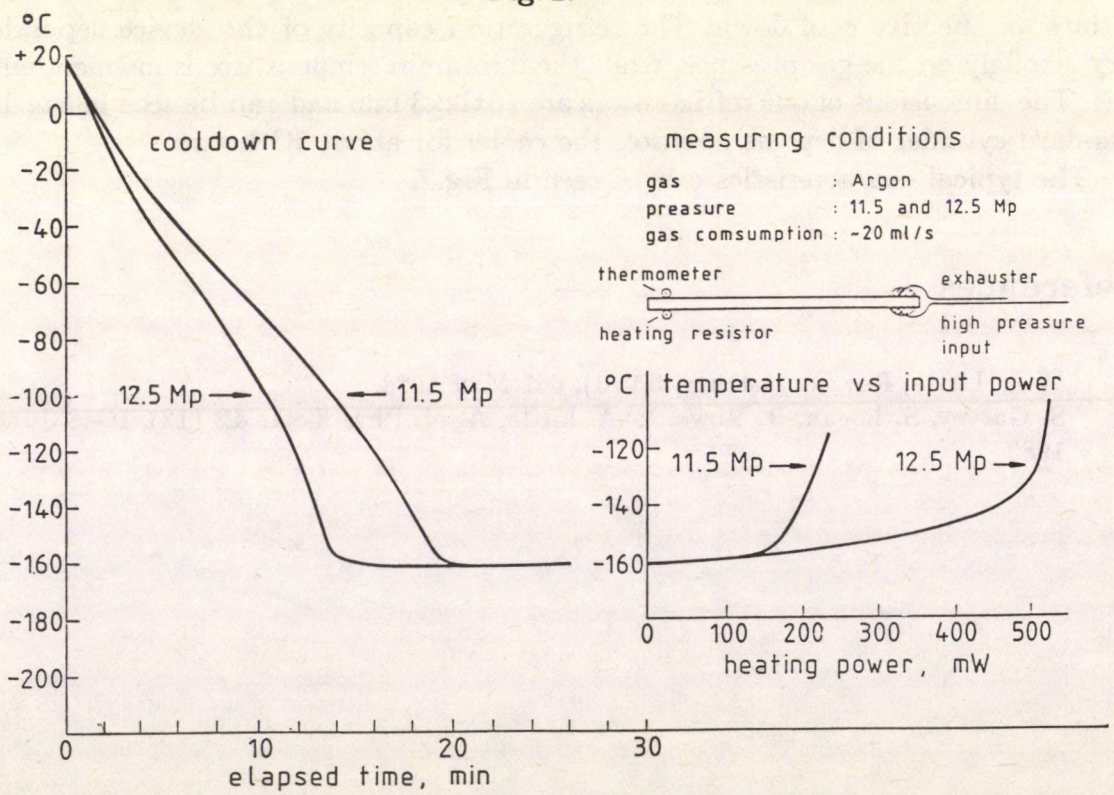
°C
+20
0
-20
-40
-60
-80
-100
-120
-140
-160
-180
-200
cooldown curve
12.5 Mp
11.5 Mp
0
10
20
30
elapsed time, min
measuring conditions
gas : Argon
preasure : 11.5 and 12.5 Mp
gas comsumption : ~20 ml/s
thermometer
exhauster
heating resistor
high preasure input
°C
temperature vs input power
-120
-140
-160
11.5 Mp
12.5 Mp
0
100
200
300
400
500
heating power, mW

Fig. 2.

Long Term Aging Effect on the Sensitivity of Hungarian Made CR-39 Solid State Nuclear Track Detector: (MA-ND/α)

I. Csige and I. Hunyadi

The sudden drop of the sensitivity of CR-39 in a few weeks after manufacturing is well known [2]. Now we have studied long term aging effects for a three years period. MA-ND/α manufactured at 21st January, 1987 in Hungarian Optical Work (Mátészalka) was chosen for this study and the alpha response was measured after different storage time at room temperature.

In the experiments we have used a ^{252}Cf source as an alpha and fission fragment source. The irradiated detectors were etched in NaOH solution of 6.25 M and 70 °C. The etching was interrupted usually in every our for observations and measurements, and continued until track diameters of etched tracks exceeded about 6 micron. Measurements were carried out under an optical microscope with a magnification of 1250.

In the course of the study finally two important parameters were determined, which characterize the sensitivity of the CR-39 type detectors: the etch induction time and the ratio of the track and bulk etch rate.

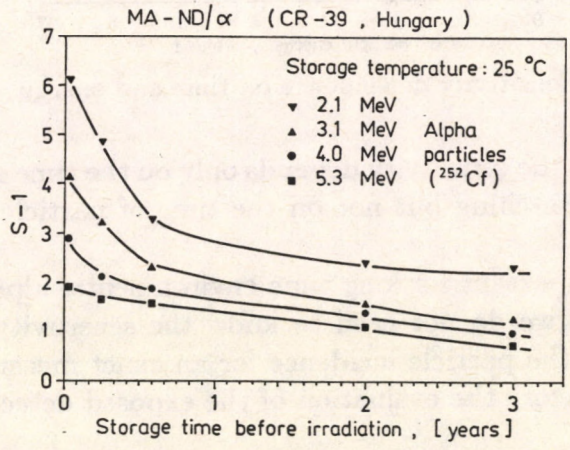

Fig. 1.. The sensitivity decreases even years after manufacturing the detector. The etch induction time does not changes significantly for the same time period.

In tendency a slow decrease of the sensitivity has been observed at each energies even after two years storage time (see Fig. 1.).

In an other experiment the effect of the storage temperature was studied. A three months old MA-ND/α sheet was cut into four pieces, two of them were exposed to ^{252}Cf and one of these was etched and evaluated subsequently the other three were sealed in polyethylene bags. One of them, which was not irradiated was stored in a refrigerator at 4 °C the others at room temperature. 33 months later the

sample from the refrigerator was retrieved and was exposed to ^{252}Cf together with the other unexposed one. These three detectors were then etched and evaluated together. We have found four important results:

1. The bulk etch rate was significantly higher (by 8%) for the samples which had been stored at room temperature. This is just the opposite what Portwood and co-workers found [2].
2. The 3 years old detector showed the same response as the 3 months old if it had been stored at 4 °C, however its sensitivity reduced by a factor of 2 if it had been stored at room temperature.
3. The ratio of the reduced sensitivity at room temperature to that stored at 4°C does not depend too much on the alpha particle energy.

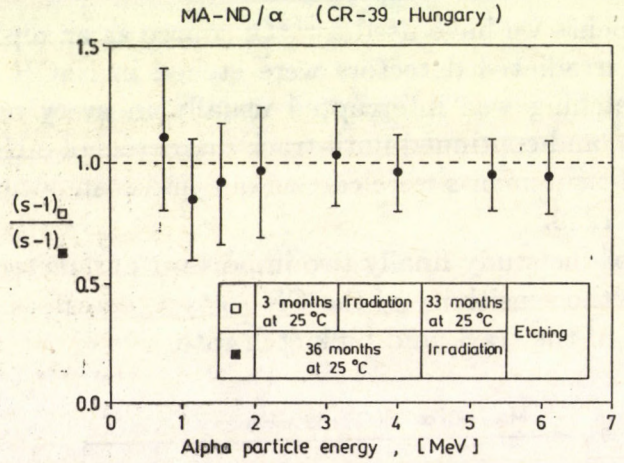

Fig. 2.. Sensitivity dependence on time and energy

4. At room temperature the sensitivity depends only on the time elapsed between the manufacture and etching but not on the time of particle incidence (see. Fig.2.).

This result is very important for long time environmental alpha exposure experiments. It means that we do not need to know the sensitivity history of the detector and the time of the particle incidence for an exact measurement, only a calibration is necessary before the evaluation of the exposed detectors.

References

1. I. Csige, I. Hunyadi and J. Charvat: Environmental effects on induction time and sensitivity of different type of CR-39 (Accepted for publication in Nucl. Tracks and Rad. Meas.)
2. T. Portwood, D. L. Henshaw and J. Stejny Nucl. Tracks, Vol.**12**, Nos 1-6, pp. 109-112 (1986)

Real Time Loss Free Counter Module

J. Gál and G. Bibók

In an earlier work[1] it was shown that a simple way of correction for both the dead time and pile-up losses can be realised using periodic or quasi–periodic pulse train. This technique is based on the recognition which can be formulated as follows: that pulse is lost the pile up time of which overlaps the busy time of another pulse. On the basis of this principle a simple circuit can be constructed. The main characteristic of which is that it causes the same fractional loss from the input periodic pulse train as the pulse processing system from its input pulses. Such a block is shown in fig.1.

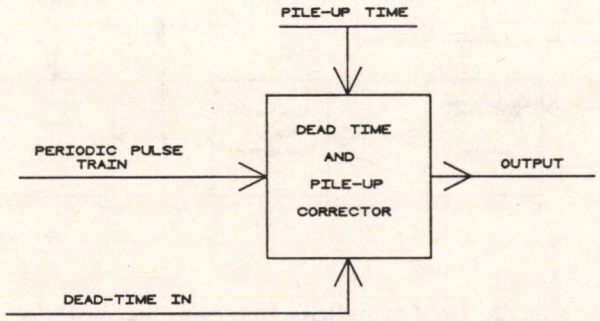

Fig. 1. Dead time and pile–up corrector block

The block has two inputs: one for the system busy time and one for the periodic pulse train with a frequency of F. The block has a possibility to adjust its *pile-up time* equal to that of the pulse processing system. The output of the block is also a pulse train with a frequency of f.

Denoting the input rate of the pulse processing system by R and the output rate by r the following simple formula holds:

$$R/r=F/f.$$

Using this block a real time correction module was constructed. The simplified block diagram of the module is shown in fig. 2. The input signals of the module are the dead time pulses of the pulse processing system. The average rate of these pulses is equal to the output rate of the system and the width of a single pulse corresponds to the total dead time initiated by an input pulse of the pulse processing system. The differential ratemeter and control amplifier controls the voltage to frequency converter output frequency in such a way that the average of the rate–frequency difference at the inputs of the differential ratemeter becomes zero. Since the dead time and pile–up corrector block causes the same fractional loss as the pulse processing system the output frequency of the voltage frequency converter gives the "loss free" rate of the system. If the averaging time constant of

the differential ratemeter is low enough the output frequency of the voltage to frequency converter can follow the variation of the "loss free" rate. In this case the correction can be considered as a real time correction i.e. it gives an accurate result both in varying and constant counting rates.

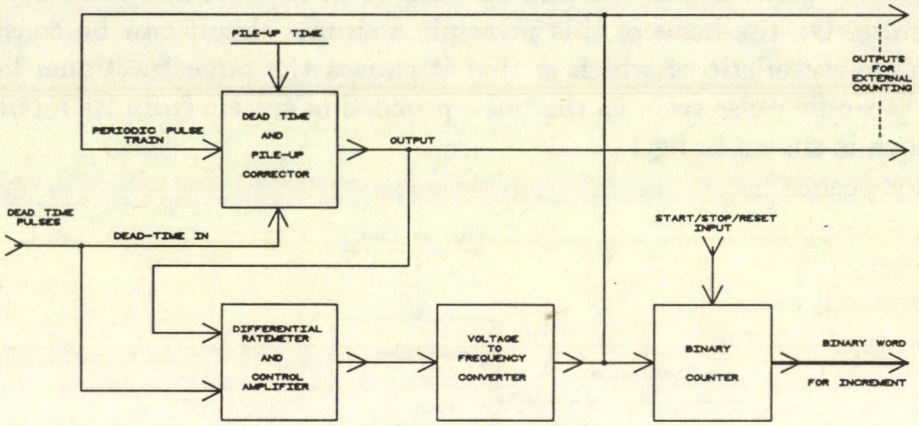

Fig. 2. Real time loss free counter module

The binary counter counts the voltage to frequency converter output pulses during the time interval between two storing processes in the multichannel analyser. The content of the counter gives a number by which the content of the corresponding channel of the multichannel analyser – as it was suggested by Harms [2] – has to be incremented.

It is obvious that there is an other possibility for correction: the ratio of the number of the input and the output pulses of the dead time and pile up corrector block counted during the measuring interval gives a correction factor by which the content of each channel of the multichannel analyser has to be multiplied.

The loss free counter which has been built in a single NIM module has the possibility to choose between these two methods of correction.

Testing the module – in different experimental situation – is in progress.

References

1. J. Gál and G. Bibók, Nucl. Instr. and Meth. **206** 465 (1983).
2. J. Harms, Nucl. Instr. and Meth. **53** 192 (1967)

A new Hardware and Software Developed for Copper Alloy Analyser type XRFA-5

T.Lakatos, P.Kovács, J.Szádai, G.Székely

In the production of copper alloys a large amount of waste matter of unknown origin and composition is melted and a rapid and accurate analysis of the melt taken from the furnace is therefore very important.

More than 10 years ago a copper alloy analyser based on energy dispersive X-ray fluorescence method was developed in our Institute for a Hungarian copper smelting works [1]. Due to the new developments in pulse processing electronics and the every day use of IBM PC/AT computers it was reasonable to accomplish an improvement of the old equipment.

1. The Digital Signal Processor and Analyser

The NZ-881 Digital Signal Processor and Analyser is a fully digital equipment for processing and analysing the signals of semiconductor X-ray detectors [2]. It is working together with IBM or compatible personal computers using an interface card and the supplied software. A high speed, opto-coupled communication line is applied between the main part of the spectrometer and the PC interface. The nonvolatile analyzer memory, and the measuring time clock is built in the former.

The NZ-881 provides the following functions : High resolution high speed digital noise filtering, very high throughput rate adaptive filtering, pile-up detection and elimination, live-time correction, multichannel amplitude analyzing, measuring time preset, powering the detector, preamplifier and getter ion pump.

The NZ-881 has several unique features such as : Provides the theoretically possible maximum throughput rate at a given shaping time. In adaptive mode of signal filtering the maximum undistorted output pulse rate is 20 times higher then in the chase of semi-Gaussian shaping. Traditional analog to digital converter (ADC) is not used in the system, and therefore the ADC dead time is excluded. The NZ-881 gives high signal to noise ratio due to the finite semi-cusp-like weighting function of the digital filter. In the normal (non adaptive) mode of operation the resolution is theoretically independent of the input count rate. Parameter settings are simple through software.

2. The Software

The analytical problem to be solved is the determination of eight elements (Mn, Fe, Ni, Cu, Zn, Pb, Sn and Sb) in copper alloys. The X-ray spectra are excited by an Am-241 isotope and are measured by a Si(Li) X-ray spectrometer. The correction for interelement effects is performed with an empirical correction method according to the Lachance-Traill algorithm [3].The computer program has been written in Pascal language and it consists of two main parts.

2.1. DISIP

It is a general use, standalone analyser program having the main functions as follows: Setting the parameters of the signal processor (peaking time, adaptivity, gain, noise discrimination level), setting the measuring time, starting and stopping the measurement, the display functions (movement of the spectra or/and the channel cursor), setting the ROIs, simple peak evaluation, hardcopy. All these functions are arranged into eight main menus and settled in logical order. The refreshment of the screen is continuous even during the accumulation of the spectra.

2.2. XRFA-5.01

This part of the software which is in close connection with the program DISIP executes the calculations of concentrations. It is a menu-organized program too. The screen is divided into four parts (windows) displaying the main menu, two sub-menus and the analytical results as well. The selection of the required menu function can be performed by moving a brightened window cursor.

In the main menu one can select four type of copper alloy (brass, tin-bronze, aluminium-bronze and red brass) to be measured.

The Data In/Out sub-menu contains the result and the spectrum loading and saving functions and the directory function respectively.

In the Setting sub-menu user can set the measuring time, the automatic saving and printing modes, the evaluation of former spectra saved on floppy disk.

The complete equipment was installed in June of 1990. Since that time it has been continually working and proved to be stable and accurate enough to fulfil the user's requirements.

References

1 P.Kovacs and M.Kis-Varga, X-Ray Spectrometry,Vol.15, 221-225 (1986)
2 T.Lakatos, Nucl. Instr. Meth. B47 (1990) 307
3 G.R. Lachance and R.J. Traill, Can. Spectrosc. 11, 43, (1966)

Status Report on the Cyclotron

A. Valek

The operation of the cyclotron and its measuring centre met the requirements of the users. The overall working time of the cyclotron was 3961. The utilization was concentrated to 9 months and January, July and August were reserved for maintenance and developments, similarly to the previous years. The cyclotron was available for users 2709 hours, the effectively used beam time is summarized in Table 1.

Table 1. Effectively used beam time

Projects	Beam time (hours)	%
Nuclear spectroscopy	593	28
Nuclear reactions	617	29
Isotope production	388	18
Neutron source	294	14
Materials sciences	115	6
Charged particle irradiation	97	5
Total	2104	100

In the maintenance period, beside the regular repairs and tests, in January the newly installed septum was thoroughly tested in cooperation with the expert of the manufacturer and in summer the cooling towers were renewed.

As developments, the working characteristics of the ion source was examined; the gas handling system of the ion source was modified to improve its reliability; the installation of an industrial process controller system, designed by the TU Budapest, to easy the operation of the cyclotron began. The later program is financed by the National Scientific Foundation for Technical Developments.

Activities at the Van de Graaff Accelerator Laboratory

L. Bartha, Á. Z. Kiss, E. Koltay, A. Nagy, E. Somorjai and Gy. Szabó

During 1990 the beam time of the VDG–1 machine amounted to 436 hours. The accelerator delivered beams according to the needs of electron spectrometry group working in atomic physics, the only user this time. Aiming at an improvement in deflecting beams of higher magnetic rigidity a new analyzing magnet has been set up in the beam transport system. After alignment and calibration it is being used with earlier power supply, the use of the full capacity of the deflection system will be permitted by a replacement of the power supply, as well. The development of a new power supply with increased power is underway. The 5 MV machine was operating for 1814 hours during this period (Table 1.). In this year all the measurements were performed with proton beams.

Field	Hours	%
Atomic physics:	716	39
Nuclear physics:	633	35
Analytical studies:	406	23
Machine tests:	59	3
Total:	1814	100

Table 1. Time distribution among different research activities

Motivated by an increasing demand for high intensity beams on the one hand and stable beam intensities down to the nA level on the other, new electrode plates have been designed for the acceleration tube , which combine straight field of axial gradient modulation [1] with an efficient screening of the insulator walls of the tube. The new electrodes have been manufactured at the workshop of the Institute and will be inserted in the tube in the next year. After a careful check of the original documentation of the 5 MV Van de Graaff accelerator and evaluation of the experience gathered during its 35,000 hours of operation detailed technical information has been transferred to the Institute of Nuclear Research of the Czechoslovakian Academy of Sciences, Rez, Praha.

1. Á. Z. Kiss, E. Koltay, I. Papp, Gy. Szabó, I. Félszerfalvi, I. Nyilas, Nucl. Instr. Meth. A**268** (1988) 382

PUBLICATIONS

AND

SEMINARS

PAPERS PUBLISHED IN 1990:

Nuclear Physics

1. J. Gulyás, Zs. Dombrádi, T. Fényes, J. Timár, A. Passoja, J. Kumpulainen, R. Julin: **Nuclear Structure of ^{106}In**, Nuclear Physics **A 506** 196 (1990)
2. A. Gizon, V. Barci, H. El-Samman, J. Gizon, B. Nyakó, B. Weiss, L. Zolnai: **Rotational Bands in Doubly-Odd ^{124}Cs and Residual Proton-Neutron Interaction**, Zeitschrift für Physik **A 335** 115 (1990)
3. F. Tárkányi, S.M. Qaim, G. Stöcklin: **Excitation Functions of High-Energy ^{3}He- and Alpha-Particle Induced Nuclear Reactions on Natural Krypton with Special Reference to the Production of ^{82}Sr**, International Journal of Radiation Applications and Instrumentation Part **A**: Applied Radiation and Isotopes **41** 91 (1990)
4. G.D. Dracoulis, T. Kibédi, A.P. Byrne, B. Fabricius, A.E. Stuchbery: **Conversion Coefficients and Yrast State Spins in ^{180}Os**, Nuclear Physics **A 509** 605 (1990)
5. G.D. Dracoulis, B. Fabricius, R.A. Bark, A.E. Stuchbery, D.G. Popescu, T. Kibédi: **Intrinsic States and Rotational Bands in ^{177}Pt**, Nuclear Physics **A 510** 533 (1990)
6. Z. Árvay, T. Csörgő, J. Zimányi: **Rehadronization of Quark–Gluon Plasma by Sequential Fissioning**, Proceedings of the International Workshop on Gross Properties of Nuclei and Excitations XVIII. Hirschegg, Kleinwalsertal, Austria, Jan.15-20, 1990. ed.:F. Beck, H. Feldmeier, W. Nörenberg. Darmstadt, GSI 252 (1990)
7. A. Csótó, B. Gyarmati, A.T. Kruppa, K.F. Pál, N. Moiseyev: **The Back-Rotation of the Wave Function in the Complex Scaling Method**, Physical Review **A 41** 3469 (1990)
8. I. Hunyadi: **Low Energy Charged Particle Nuclear Reaction Studies with SSNTD-S**, International Journal of Radiation Applications and Instrumentation Part **D** Nuclear Tracks and Radiation Measurements **17** 31 (1990)
9. Ch. Iliadis, Th. Schange, C. Rolfs, U. Schröder, E. Somorjai, H.P. Trautvetter, K. Wolke, P.M. Endt, S.W. Kikstra, A.E. Champagne, M. Arnould, G. Paulus: **Low-Energy Resonances in ^{25}Mg(p,γ)^{26}Al, ^{26}Mg(p,γ)^{27}Al and ^{27}Al(p,γ)^{28}Si**, Nuclear Physics **A 512** 509 (1990)
10. F. Tárkányi, F. Szelecsényi, Z. Kovács, S. Sudár: **Excitation Functions of Proton Induced Nuclear Reactions on Enriched ^{66}Zn, ^{67}Zn and ^{68}Zn. Production of ^{67}Ga and ^{66}Ga**, Radiochimica Acta **50** 19 (1990)
11. A.P. Byrne, G.D. Dracoulis, K.J. Schiffer, P.M. Davidson, T. Kibédi, B. Fabricius, A.M. Baxter, A.E. Stuchbery: **34 μs Isomer at High Spin in ^{212}Fr: Evidence for a Many-Particle Octupole Coupled State**, (Rapid Communications), Physical Review C Nuclear Physics **42** 6 (1990)
12. S. Seuthe, C. Rolfs, U. Schröder, W.H. Schulte, E. Somorjai, H.P. Trautvetter, F.B. Waanders, R.W. Kavanagh, H. Ravn, M. Arnould, G. Paulus: **Resonances in the ^{22}Na(p,γ)^{23}Mg Reaction**, Nuclear Physics **A 514** 471 (1990)
13. G. Kalinka: **Új foton- és részecskedetektálási elvek és módszerek (kriogenikus detektorok)**, Izotóptechnika, Diagnosztika **33** 77 (1990)

14. R.G. Lovas, A.T. Kruppa, J.B.J.M. Lanen: **Cluster-Model Interpretation of the ^{6}Li(e,e'p) Reaction**, Nuclear Physics **A 516** 325 (1990)
15. B.M. Nyakó, J. Gizon, V. Barci, A. Gizon, S. André, D. Barnéoud, D. Curien, J. Genevey, J.C. Merdinger: **Evidence for $h_{11/2}$ Proton Alignment in ^{127}Ce**, Proc. Int. Conf. on Spectroscopy of Heavy Nuclei, Crete, Greece, 1989. IOP Publ. LTD. Inst. Phys. Conf. Ser. **105** 89 (1990)
16. P. Tikkanen, J. Keinonen, A. Kuronen, Á.Z. Kiss, E. Koltay, É. Pintye, B.H. Wildenthal: **Short Lifetimes in ^{29}Si-^{29}P for the Test of Small-Model Wave Functions**, Nuclear Physics **A 517** 176 (1990)
17. O. Dragun, V. Brabec, A. Kovalik, M. Fiser, J. Novák, M. Rysavy, V.M. Gorozhankin, Ts. Vylov, V.G. Chumin, K.Ja. Gromov, L. Kövér, I. Cserny, V.V. Zashkvara, B.U. Ashimbaeva: **High-Resolution Spectroscopy of Low-Energy Electrons Emitted in Nuclear Transformations**, Hyperfine Interactions **61** 1309 (1990)
18. T. Fényes, Zs. Dombrádi, A. Krasznahorkay, J. Gulyás, J. Timár, T. Kibédi, V. Paar: **Structure of Odd-Odd in Nuclei**, Fizika **22** 273 (1990)
19. B. Fabricius, G.D. Dracoulis, R.A. Bark, A.E. Stuchbery, T. Kibédi, A.M. Baxter: **High-Spin States and Intrinsic Structure in ^{174}Os and ^{175}Os: Alignments and Strong Interaction**, Nuclear Physics **A 511** 345 (1990)
20. G.D. Dracoulis, P.M. Davidson, A.P. Byrne, B. Fabricius, T. Kibédi, A.M. Baxter, A.E. Stuchbery, A.R. Poletti, K.J. Schiffer: **High-Spin Yrast Isomers in ^{211}Rn and ^{212}Rn with Enhanced E3 Decays**, Physics Letters **B 246** 31 (1990)
21. G.D. Dracoulis, P.M. Davidson, A.P. Byrne, B. Fabricius, T. Kibédi, A.M. Baxter, A.E. Stuchbery, A.R. Poletti, K.J. Schiffer: **High-Spin Yrast Isomers in ^{211}Rn and ^{212}Rn with Enhanced E3 Decays**, Nuclear Physics **A 520** 353 (1990)
22. L. Andó, P. Mikecz, A.N. Tcheltsov, I.A. Suvorov, I. Mahunka: **Pure Iodine-123 Production by Small Cyclotron for Medical Use**, Journal of Radioanalytical and Nuclear Chemistry Letters **146** 169 (1990)
23. T. Vertse, P. Curutchet, R.J. Liotta: **Approximate Treatment of the Continuum**, Physical Review **C** Nuclear Physics **42** 2605 (1990)
24. B.M. Nyakó, J. Gizon, V. Barci, A. Gizon, S. André, D. Barnéoud, D. Curien, J. Genevey, J.C. Merdinger: **First Identification of Collective Excitations in ^{127}Ce**, Zeitschrift für Physik **A 334** 513 (1989)
25. E. Vatai: **Ball-Lightning as Observational Evidence of the Existence of Lepto-Nucleons and Their Clusters**, Il Nuovo Cimento **A 101** 905 (1989)

Atomic Physics

1. I. Kádár, S. Ricz, J. Végh, B. Sulik, D. Varga, D. Berényi: **High-Resolution Ne K Auger Spectra from Collisions Between Ne and H^+, Ne^{3+}, Ne^{10+}, Ar^{6+}, and Ar^{16+} (5.5 MeV/U)**, Physical Review **A 41** 3518 (1990)
2. J. Pálinkás, R. Schuch, H. Cederquist, O. Gustafsson: **Evidence for Electron–Electron Scattering in Simultaneous Capture and Ionization by 1 MeV Protons in He**, Physica Scripta **42** 175 (1990)
3. L. Végh, J. Burgdörfer: **Shakeoff Induced by Fast Charged Projectiles**, Physical Review **A 42** 655 (1990)
4. L. Kövér, I. Cserny, V. Brabec, M. Fiser, O. Dragun, J. Novák: **3p and 3d Core-Level widths in Metallic Technetium: A Study by Internal-Conversion Electron Spectroscopy**, Physical Review **B 42** 643 (1990)
5. L. Sarkadi, T. Vajnai, J. Pálinkás, Á. Kövér, J. Végh, T. Mukoyama: **L3-Subshell Alignment of Argon Following Charge-Changing Collisions with Protons Journal of Physics, B 23** 3643 (1990)
6. L. Sarkadi, T. Mukoyama: **L-Shell Ionization by Antiprotons**, Physical Review **A 42** 3878 (1990)
7. T. Papp, J. Pálinkás, L. Sarkadi: **Magnetic-Quadrupole - Electric-Dipole Mixing in L3 X-Ray Transitions of Heavy Elements**, Physical Review **A 42** 5452 (1990)
8. L. Sarkadi, T. Mukoyama: **Dynamical Subshell Coupling Effects in L-Shell Ionization of Thorium by Heavy Ions**, Journal of Physics **B 23** 3849 (1990)
9. O. Dragun, V. Brabec, A. Kovalik, M. Fiser, J. Novák, M. Rysavy, V.M. Gorozhankin, TS. Vylov, V.G. Chumin, K. JA. Gromov, L. Kövér, I. Cserny, V.V. Zashkvara, B.U. Ashimbaeva: **High-Resolution Spectroscopy of Low--Energy Electrons Emitted in Nuclear Transformations**, Hyperfine Interactions **61** 1309 (1990)

Materials Science and Analysis

1. S. Mészáros, K. Vad, G. Halász, F.J. Kedves, Sz. Balanyi: **Investigation of the Coupling Mechanism Between Superconducting Grains in High-Tc Superconductors**, Physica **C 167** 139 (1990)
2. N.G. Zaitseva, O. Gnotek, A. Kowalew, P. Mikecz, E. Rurarzh, V.A. Khalkin, V.A. Ageev, A.A. Klyuchnikov, L.A. Kuzina, A.F. Linev: **Excitation Functions and Yields for ^{111}In Production Using ^{113,114,nat}Cd(p,xn)^{111}In Reactions with 65 MeV Protons**, International Journal of Radiation Applications and Instrumentation Part **A**: Applied Radiation and Isotopes **41** 177 (1990)
3. K. Vad, S. Mészáros, G. Halász, Sz. Balanyi: **Temperature and Magnetic Field Dependence of Transport Critical Current Density in $YBa_2Cu_3O_{7-x}$ Ceramics**, Cryogenics **30** 660 (1990)
4. S.A. Szabó, I. Borbély-Kiss, J. Kispéter, E. Koltay: **Aktivációs analízis az élelmiszer-analitikában. VIII. Részecske (proton) indukált röntgen - emissziós analízis (PIXE)**, Élelmiszervizsgálati közlemények **36** 39 (1990)
5. F. Ditrói, S. Takács, I. Mahunka, Z. Gémesi: **Trace-Element Study of Glass Samples by Using Activation Methods**, Nuclear Instruments and Methods in Physics Research **B 50** 62 (1990)
6. S. Takács, F. Ditrói, M. Pankotai, P. Fodor: **Microelemental Measurement of Tomato Plants by Using PIXE and ICP Methods**, Nuclear Instruments and Methods in Physics Research **B 49** 195 (1990)
7. M. Kis-Varga: **Röntgencsöves gerjesztés ED röntgenspektrométerekben - eredmények és lehetőségek**, Izotóptechnika, Diagnosztika **33** 95 (1990)
8. L. Kövér, I. Cserny, M. Fiser, V. Brabec, O. Dragun, J. Novák: **Combined Application of ICES and XPS Methods for Quantitative Electron Spectroscopy of Tc Compounds**, SIA /Surface and Interface Analysis/ **16** 215 (1990)
9. I. Borbély-Kiss, E. Koltay, Gy. Szabó, L. Bozó, E. Mészáros, Á. Molnár: **An Evaluation of Elemental Concentrations in Atmospheric Aerosols Over Hungary: Regional Signatures and Long-Range Transport Modelling**, Nuclear Instruments and Methods in Physics Research **B 49** 388 (1990)
10. L. Költő, M. Kis-Varga: **Analyse Römischer Ringfibeln**, Savaria (a vasmegyei múzeumok értesítője), **19** 103 (1990)
11. E. Koltay: **Elemental Analysis of Atmospheric Aerosols: Results and Perspectives of the PIXE Technique**, International Journal of PIXE **1** 93 (1990)
12. I. Török: **High Resolution PIXE with a Crystal Spectrometer**, Radioisotopy, (*czechosl.*) **31** 98 (1990)
13. I. Török: **Nagy felbontású PIXE kristályspektrométerrel**, Izotóptechnika, Diagnosztika **33** 161 (1990)
14. L. Vásáros, P. Mikecz, K. Berei: **Recoil Labelling of Halobenzoic Acids**, Radiochimica Acta, **50** 87 (1990).
15. E. Hertelendi, G. Uchrin, P. Ormai: **^{14}C Release in Various Chemical Forms with Gaseous Effluents from Paks Nuclear Power Plant**, Radiocarbon, **31** 754 (1989)
16. Z. Borsy, E. Félegyházi, É. Csongor: **A bodrogköz kialakulása és vízhálózatának változásai**, Alföldi tanulmányok **13** 65 (1989)

Earth and Cosmic Sciences, Enviromental Research

1. Gy. Somogyi: **Methods for Measuring Radium Isotopes: Track Detection the Environmental Behaviour of Radium**, Technical Reports Series No. 310. Vienna, IAEA **1** 229 (1990)
2. I. Csige, J. Hakl, G. Géczy, L. Lénárt: **Study of Underground Radon Transport**, Proceedings of the International Workshop on Radon Monitoring in Radioprotection, Environmental Radioactivity and Earth Science. Trieste, 1989. ed. L. Tommasino, *et al.* Singapore, World Scientific 435 (1990)
3. K. Balogh, G.P. Bagdasaryan, K.I. Karapetyan, Z. Pécskay, E. Árva-Sós, R.Kh. Gukasyan: **Pervye K/Ar izotopnye datirovki verkhnepliotsen - - chetvertichnykh vulkanicheskikh porod armyanskoj SSR**, Izvestiya Akademii Nauk ARM. SSR, Nauki o Zemle **43** (1990) 25
4. A. Harkovska, Z. Pécskay, K. Balogh: **Pervye dannye ob absolyutnom vozraste paleogenovyh vulkanitov smolyanskogo rajona (Central'nye Rodopy)** Geologica Balcanica **20** 66 (1990)
5. E. Hertelendi: **Sources of Random Error in the Debrecen Radiocarbon Laboratory** Radiocarbon **32** 283 (1990)
6. E. Hertelendi, I. Vető: **Isotopically Light Aquatic Kerogen in the Hungarian Oligocene**, 5th Working Meeting an Isotopes in Nature. Leipzig, Sept.,1989. Proceedings ed.: U. Wanda, G. Strauch, Academy of Sciences of the GDR, Central Institute of Isotope and Radiation Research, Leipzig. 311 (1990)
7. E. Árva-Sós, K. Balogh, Nguyen van Quy, CS. Ravasz, L. Ravasz-Baranyai: **Nhung quan he macma kien tao va viec dinh tuoi cac da bazan kainozoi vung bao loc va di linh nam viet nam bang K/Ar**, Dia Chat Va Nguyen Lien Khoang **21** (1989)

Biological and Medical Research

1. F. Tárkányi, F. Szelecsényi, Z. Kovács, S. Sudár: **Excitation Functions of Proton Induced Nuclear Reactions on Enriched ^{66}Zn, ^{67}Zn and ^{68}Zn. Production of ^{67}Ga and ^{66}Ga**, Radiochimica Acta **50** 19 (1990)
2. I. Borbély-Kiss, E. Koltay, Gy. Szabó, É. Pintye, E. Groska, Á. Kiss: **The Effect of Radiotherapeutic Irradiation on the Elemental Concentration of Iron in Human Erythrocytes and Blood Plasma**, Nuclear Instruments and Methods in Physics Research **B 49** 254 (1990)
3. J. Steinbach, K. Günther, E. Lösel, G. Grunwald, P. Mikecz, L. Andó, F. Szelecsényi, G.J. Beyer: **Temperature Course in Small Volume (^{18}O) Water Targets for (^{18}F) F- Production**, International Journal of Radiation Applications and Instrumentation Part **A**: Applied Radiation and Isotopes **41** 753 (1990)
4. L. Andó, P. Mikecz, A.N. Tcheltsov, I.A. Suvorov, I. Mahunka: **Pure Iodine-123 Production by Small Cyclotron for Medical Use**, Journal of Radioanalytical and Nuclear Chemistry Letters **146** 169 (1990)
5. I. Dobránszky, J. Bacsó, P. Nyirkos, I. Uzonyi, M. Debreceni, Cs. Mészáros: **Aranykezelés mellékhatásai bőrön két eset kapcsán**, Bőrgyógyászati és Venerológiai Szemle **66** 173 (1990)
6. Gy. Somogyi, I. Nikl, I. Csige, I. Hunyadi: **Radon aktivitás koncentrációjának mérése és a belégzésből eredő sugárterhelés meghatározása hazai lakások légterében**, Izotóptechnika, Diagnosztika **32** 177 (1989)
7. Cs. Béres, A. Fenyvesi, T. Molnár, I. Mahunka, P. Jakucs, Z. Kovács, P. Mikecz: **Tölgyfák vízszállításának vizsgálata ^{24}Na izotópnyomjelzéses módszerrel**, Izotóptechnika, Diagnosztika **32** 184 (1989)

Development of Instruments and Methods

1. L. Bartha, Á.Z. Kiss, E. Koltay, Gy. Szabó: **Light Heavy-Ion and Molecular Beams from a Radio-Frequency Ion Source**, Nuclear Instruments and Methods in Physics Research **A 287** 156 (1990)
2. L. Záborszky: **Visszacsatolt műveleti erősítők jellemzőinek további javítása a hibafeszültség visszacsatolásával**, Mérés és automatika **38** 58 (1990)
3. L. Medveczky: **Calibration of and Measurements with a Neutron Dosimeter Consisting of Fission Foils and an SSNTD**, International Journal of Radiation Applications and Instrumentation Part **D** Nuclear Tracks and Radiation Measurements **17** 51 (1990)
4. T. Lakatos: **Adaptive Digital Signal Processing for X-Ray Spectrometry**, Nuclear Instruments and Methods in Physics Research **B 47** 307 (1990)
5. I. Török, **Line Identification and other Simple Wavelength-Dispersive X-Ray Spectrometric Calculations Using a Pocket Calculator**, X-Ray Spectrometry **19** (1990) 159
6. G. Székely, Th. Lindblad, L. Hildingsson, W. Klamra: **On the Reduction of Data Storage from High-Dispersion Experiments**, Nuclear Instruments and Methods in Physics Research A **292** 431 (1990)
7. J. Bacsó: **A totál reflexió alkalmazása a röntgenemissziós analízisben**, Izotóptechnika, Diagnosztika **33** 67 (1990)
8. G. Kalinka: **Új foton- és részecskedetektálási elvek és módszerek (kriogenikus detektorok)**, Izotóptechnika, Diagnosztika **33** 77 (1990)
9. Gy. Máthé: **Si(Li) Detektorok hűtési lehetősége Joule-Thomson-Effektus felhasználásával**, Izotóptechnika, Diagnosztika **33** 104 (1990)
10. G. Kalinka: **Izotópgerjesztésű, szekunder targetes forrás tervezése félvezető detektoros röntgenspektrométerekhez**, Izotóptechnika, Diagnosztika **33** 107 (1990)
11. I. Uzonyi: **Energiadiszperziv röntgenemissziós analitika alkalmazása biológiai és geológiai minták elemösszetételének a meghatározására**, Izotóptechnika, Diagnosztika **33** 120 (1990)
12. G. Henrion, R. Henrion, J. Bacsó, I. Uzonyi: **Ausgewahlte Methoden der Korrelationsanalyse am Beispiel der Spurenelementrelationen im Menschlichen Körper**, Zeitschrift für Chemie **30** 204 (1990)
13. T. Kibédi, G.D. Dracoulis, A.P. Byrne: **Lens-Mode Operation of a Superconducting Electron Spectrometer in (Hi,Xn) Reactions**, Nuclear Instruments and Methods in Physics Research **A 294** 523 (1990)
14. D. Bhattacharyya, B. Basu, P. Pal, S.C. Mukherjee, A.K. Ganguly, I. Hunyadi: **Charge Resolution of a Hungarian Brand Cr-39(MA-ND) Detector Exposed to a ^{84}Kr Beam of Energy 0.45A GeV**, Nuclear Instruments and Methods in Physics Research **B 47** 466 (1990)
15. F. Lauritsen, S. Bohátka, H. Deng: **A Membrane-Inlet Tandem Mass Spectrometer for Continuous Monitoring of Volatile Organic Compounds**, Rapid Communications in Mass Spectrometry **4** 401 (1990)

16. G. Dajkó: **Fast Neutron Spectrometry Using Cr-39 Track Detectors**, Radiation Protection Dosimetry **33** 9 (1990)
17. I. Berecz, K. Balogh, S. Bohátka, E. Hertelendi, L. Kövér, G. Langer: **Developments in Mass and Electron Spectrometry**, Acta Chimica Hungarica **127** 525 (1990)
18. S. Biri, S.L. Bogomolov: **Matematicheskoe modelirovanie aksial'no--simmetrichnoj ionno-opticheskoj sistemy**, Zhurnal Tehnicheskoj Fiziki **60** 17 (1990)
19. S. Biri, A.A. Efremov, J. Molnár: **Interfejs dlya upravleniya i avtomaticheskogo izmereniya na osnove personal'nykh komp'yuterov tipa IBM PC-XT/AT**, Mikropotsessornye Sredstva i Sistemy 343 (1990)
20. S. Biri, S.L. Bogomolov, I. Koós, A. Sándor: **Raschet ionno-opticheskoj sistemy inzhektora mnogozaryadnykh ionov**, Soobshcheniya Oiyai, **R9-90-187** 1 (1990)
21. G. Dajkó, K. Turek: **Electrochemical Etching of Cr-39 Detectors Irradiated with Alpha Particles**, International Journal of Radiation Applications and Instrumentation Part **D** Nuclear Tracks and Radiation Measurements **16** 241 (1989)
22. I. Harangozó, L. Debreceni, S. Kiss, J. Szádai: **Multichannel Programmable Internal Friction Measuring System**, Acta Universitatis Debreceniensis de L. Kossuth Nominatae, Ser. Phys. Et. Chim. **26** 81 (1989)
23. E. Hertelendi, É. Csongor, L. Záborszky, J. Molnár, J. Gál, M. Győrffi, S. Nagy: **A Counter System for High-Precision ^{14}C Dating**, Radiocarbon **31** 399 (1989)

CONFERENCE CONTRIBUTIONS AND TALKS:

Nuclear Physics

1. I. Hunyadi, B. Cujec, I.M. Szöghy: **Low Energy Charged Particle Nuclear Reactions by SSNTD-S, the $^{12}C(^{12}C,^{8}Be)^{16}O$ at Subcoulomb Energies**, Rabotsego soveshchaniya "Tverdotel'nye trekovye detektory yader i ikh primeneniya", Dubna, USSR, 6-8 Februar, 1990.
2. J. Cseh, G. Lévai: **Cluster States of Light Nuclei in Terms of the Vibron Model**, Symposium in Honor of Akito Arima: Nuclear Physics in the 1990's. Santa FE, USA, 1-5 May, 1990 .
3. G. Lévai, J. Cseh: **Algebraic Approach to Cluster States of Odd-Mass Nuclei**, ibid.
4. G. Lévai, J. Cseh: **An Algebraic Model of Cluster States in Odd-Mass Nuclei**, XVIII-th International Colloquium on Group Theoretical Methods in Physics, Moscow, USSR, 3-9 June, 1990.
5. S.M. Qaim, F. Tárkányi, G. Stocklin, M. Sajjad, R.M. Lambrecht, H. Schweickert: **Excitation Functions of (p,2n) and (p,pn) Reactions on Highly Enriched ^{124}Xe with Special Reference to the Production of ^{123}I.**,(abstr.: Princeton University, Princeton, New Jersey, p. 100), Eighth International Symposium on Radiopharmaceutical Chemistry, Princeton, USA, 24-29 June, 1990.
6. F. Szelecsényi, Z. Kovács, F. Tárkányi, Gy. Tóth: **Production of ^{110}In for Pet Investigation Via $Cd(^{3}He,Xn)^{110}Sn$-^{110}In Reaction with Low Energy Cyclotron**, (abstr.: Princeton University, Princeton, New Jersey, pp. 95-96),
7. S. Engstler, C. Angulo, U. Greife, K. Neldner, G. Raimann, C. Rolfs, U. Schröder, E. Somorjai: **New results in Electron Screening Investigation**, Nuclei in the Cosmos. International Symposium on Nuclear Astrophysics, Baden/Vienna, Austria. 18-22 June, 1990.
8. H.P. Trautvetter, S. Seuthe, C. Rolfs, U. Schröder, W.H. Schulte, E. Somorjai, F.B. Waanders, R.W. Kavanagh, H. Ravn, M. Arnould: **Search for Resonances in the $^{22}Na(p,\gamma)^{23}Mg$ Reaction**, ibid.
9. Zs. Fülöp, A.Z. Kiss, E. Koltay, E. Somorjai, J. Keinonen, P. Tikkanen: **Átmeneti erősségek meghatározása a ^{25}Mg-^{25}Al tükörmagokban**, (abstr. p. 8), X. Magyar Magfizikus Találkozó, Sárospatak, 1990. aug. 21-24.
10. S. Engstler, U. Greife, G. Raimann, U. Schröder, C. Rolfs, E. Somorjai: **Elektron–árnyékolás hatása az alacsony–energiás fúziós hatáskeresztmetszetekre**, (abstr.: p. 13), ibid.
11. J. Gulyás, Zs. Dombrádi, T. Fényes, A. Krasznahorkay, J. Timár: **A páratlan–páratlan indium atommagok szerkezete**, (abstr.: p. 14), ibid.
12. Z. Gácsi, J. Gulyás, T. Fényes, Zs. Dombrádi: **A $^{114,116,118}Sb$ atommagok szerkezete**, (abstr.: p. 15), ibid.
13. M. Józsa, Z. Máté, L. Zolnai: **Az optikai potenciál alacsonyenergiájú viselkedésének vizsgálata p + Sn rugalmas szórásban**, (abstr.: p. 16), ibid.
14. B.M. Nyakó, L. Zolnai, M. Józsa: **Nagyspinű magállapotok vizsgálata**, (abstr.: p. 17), ibid.
15. T. Fényes: **Magfizika nehéz ionokkal**, (abstr.: p. 18), ibid.

16. G. Lévai, J. Cseh: **Páratlan tömegszámú atommagok klaszter szerkezetének algebrai modellje**, (abstr.: p. 23), ibid.
17. R.G. Lovas: **Az alfától az alfa-bomlásig**, (abstr.: p. 24), ibid.
18. K.F. Pál: **A forgás hatása magállapotok belsö szerkezetére**, (abstr.: p. 25), ibid.
19. Z. Árvay, T. Csörgő, J. Zimányi: **Phaser: Hasadási lánc mechanizmus, ritkaanyag és antianyag termelés a Kvark-Gluon plazma hadronizációjában**, (abstr.: p. 29), ibid.
20. J. Pálinkás: **Egzotikus elektronbefogási folyamatok**, (abstr.: p. 32), ibid.
21. I. Csige, G. Géczy, J. Hakl, I. Hunyadi, L. Lénárt, I. Nikl: **Radon a környezetben, lehetőségek és veszélyek**, (abstr.: p. 37), ibid.
22. F. Szelecsényi, Z. Kovács, F. Tárkányi, Gy. Tóth: **A ^{110}Sn-^{110}In előállítása MGC ciklotronnal**, (abstr.: p. 37), ibid.
23. T. Fényes, Zs. Dombrádi, Z. Gácsi: **Structure of Odd-Odd Sb and In Nuclei**, International Summer School on Nuclear Physics, Mikołajki, Poland, Aug. 26–Sept. 5, 1990.
24. Zs. Dombrádi, T. Fényes, V. Paar: **Proton-Neutron Multiplet States in Odd-Odd Indium Nuclei**, 7th International Symposium on Capture Gamma-Ray Spectroscopy and Related Topics, Asilomar, California, 14-19 Oct., 1990.
25. T. Vertse: **Approximate Treatment of the Continuum**, Workshop on the Structure and Decay of Resonant States in Nuclei, Stockholm-Uppsala, Sveden, 1-3 Oct., 1990.
26. B.M. Nyakó, G. Cata-Danil, J. Gizon, S. André, V. Barci, A. Bucurescu, D. Curien, C. Foin, J. Genevey, A. Gizon, L. Hildingsson, W. Klamra, J.C. Merdinger, L. Zolnai: **Collective Bands in ^{128}Ce**, Int. Conf. on High Spin Physics and Gamma-Soft Nuclei, Pittsburg, USA, Sept., 1990.
27. J.L. Weil, J.D. Boone, R. Go, Z. Gácsi: **Level Lifetimes in ^{116}Sn**, Urbana-Champaign Meeting of the Nuclear Physics Div., APS. Urbana-Champaign, USA. 28. Sept., 1990.
28. Zs. Dombrádi: **Deduction of Proton-Neutron Interaction from Empirical Matrix Elements**, ibid.
29. Zs. Dombrádi: **Evidence for Core Polarization Interaction in the Single Closed Shell Region**, ibid.
30. K. Jansson, P. Carlson, K. John-And, A. Kerek, S. Szilágyi: **Status of the Cplear Experiment**, 12th Nordic Meeting on Particle Phyics, Spatind, Norwey, 6-10 jan. 1990.
31. S. Engstler, U. Greife, A. Krauss, K. Neldner, G. Raimann, C. Rolfs, U. Schröder, E. Somorjai, G. Blőge, K. Langanke, H. G. Reusch: **Progress on Electron Screening Investigations Proc. Fifth Workshop on Nuclear Astrophysics**, ed.: W. Hillebrand, E. Müller, Ringberg Castle, Tegernsee, **36** 1989.

Atomic Physics

1. L. Sarkadi, T. Vajnai, J. Pálinkás, Á. Kövér, J. Végh: **Energy Dependence of the L3-Subshell Alignment of Argon Induced by Ionization and Electron Capture in H^+Ar Collisions**, (Contribution, ed.: T.D. Mark, F. Howorka, pp. 259-262), Symposium Atomic and Surface Physics (SASP90), Obertraun, Austria, 18-24 March, 1990.
2. I. Török, B. Sulik, L. Sarkadi, J. Végh: **Investigation of the Satellite Sstructure of M Alpha and M Beta X-Ray Lines**, 1st Debrecen-Miskolc-Uzhgorod Triangle Seminar on Atomic Collision Processes, Debrecen, Hungary, 12 March, 1990.
3. E. Takács, S. Ricz, J. Végh, B. Sulik, D. Varga, D. Berényi: **Anomalies in Auger Line Shapes and Angular Distributions Observed in Ion-Atom Collision Experiments**, ibid.
4. T. Vajnai, L. Sarkadi, J. Pálinkás, Á. Kövér, J. Végh: **Energy Dependence of the L3-Subshell Alignment of Argon Induced by Ionization and Electron Capture in H^+-Ar Collisions**, ibid.
5. K. Tőkési, G. Hock: **Case Studies in 3-Body Coulomb CTMC Calculations**, ibid.
6. J. Pálinkás, T. Papp, L. Sarkadi, C. Neelmeijer, K. Brankoff, D. Grambole, D. Heissler, F. Herrmann, W. Rudolph: **Influence of Multiple Ionization on the L3 Subshell Alignment**, Physics of Highly Charged Ions, Abisko, Sweden, 28 May, 1990.
7. L. Gulyás, Á. Kövér, L. Sarkadi, Gy. Szabó, J. Pálinkás, T. Vajnai, D. Berényi: **Cusp Inversion in the Collision System He^+-He**, 1st Debrecen-Miskolc-Uzhgorod Triangle Seminar on Atomic Collision Processes, Debrecen, Hungary, 12 March, 1990.
8. J. Pálinkás, T. Papp, L. Sarkadi: **M2-E1 Mixing in Ion-Induced L X-Ray Transitions**, (Book of Abstracts p. S35), 15th International Conference on X-Ray and Inner-Shell Processes, Knoxville, Tennessee, USA, 9-13 July, 1990.
9. T. Papp, J. Pálinkás, L. Sarkadi, J. Végh, C. Neelmeijer, K. Brankoff, D. Grambole, C. Heiser, V. Herrmann, W. Rudolph: **Experimental Study of the L3 Subshell Alignment of Multiply Ionized Atoms**, (Book of Abstracts p. F05), ibid.
10. I. Török, B. Sulik, L. Sarkadi, J. Végh: **On the Ssatelite Structure of Ta M Alpha and M Beta X-Ray Lines**, (Book of Abstracts p. G10), ibid.
11. L. Gulyás, Á. Kövér, Gy. Szabó, T. Vajnai, D. Berényi: **Testing the Series Expansion Method Used for Studying the "Cusp" Spectra**, (ATOMKI Rep. 1990/1 p. 3) 4th Workshop on High-Energy Ion-Atom Collision Processes, Debrecen, 17-19 Sept. 1990.
12. H. Fukuda, L. Végh, I. Shimamura, T. Watanabe: **Singly Ionizing Proton-He Collisions at Very Small Scattering Angles**, (ATOMKI Rep. 1990/1 p. 4), ibid.
13. L. Gulyás, L. Sarkadi, T. Vajnai, Gy. Szabó, Á. Kövér, J. Pálinkás, D. Berényi: **Cusp Inversion in He^+-He,Ar Collision Systems**, (ATOMKI Rep. 1990/1 p. 5), ibid.

14. K. Tőkési, G. Hock: **Classical Trajectories During Atomic Collisions**, (ATOMKI Rep. 1990/1 p. 7), ibid.
15. S. Ricz, J. Végh, B. Sulik, D. Varga, E. Takács, I. Kádár, D. Berényi: **Anomaly in Auger Spectra of Fast Heavy Ion Impact on Ne in Forward and Backward Direction**, (ATOMKI Rep. 1990/1 p. 11), ibid.
16. T. Vajnai, L. Sarkadi, Á. Kövér, J. Végh: **Study of the Line Shape of Auger Electrons Excited by Direct Ionization and Electron Capture**, (ATOMKI Rep. 1990/1 p. 12), ibid.
17. K. Tőkési, S. Ricz, E. Takács, B. Sulik: **e^- Impact Energy Dependence of the L3 Subshell Alignment of Ar**, (ATOMKI Rep. 199/1 p. 12), ibid.
18. K. Tőkési, G. Hock: **Particle and Antiparticle-H Collisions**, (ATOMKI Rep. 1990/1 p. 15), ibid.
19. B. Sulik, V. Montemayor, N. Stolterfoht, I. Kádár: **Dynamic Screening in Ion-Atom Collisions**, (ATOMKI Rep. 1990/1 p. 20), ibid.
20. E. Takács, S. Ricz, J. Végh, B. Sulik, T. Papp, B. Tóth, D. Berényi: **Systematic Study of the Anisotropy of the Ne K-Auger Satellites in Ion-Atom Collisions**, (ATOMKI Rep. 1990/1 p. 23), ibid.
21. T. Papp, I. Török: **Angular Distribution Measurements of Th M X-Ray Lines**, (ATOMKI Rep. 1990/1 p. 23), ibid.
22. K. Tőkési, G. Hock: **Case Studies in 3 Body CTMC Calculations. (Particle and Antiparticle -H^0 collisions)**, ibid.
23. O. Dragun, V. Brabec, A. Kovalik, M. Fiser, J. Novák, M. Rysavy, V.M. Gorozhankin, TS. Vylov, V.G. Chumin, K.YA. Gromov, L. Kövér, I. Cserny, V.V. Zashkvara, B.U. Ashimbaeva: **High-Resolution Spectroscopy of Low-Energy Electrons Emitted in Nuclear Transformation**, 8th International Conference of Hyperfine Interactions, Prague, Czechoslovakia, 14-19 Aug. 1989.
24. S. Ricz, J. Végh, I. Kádár, B. Sulik, D. Varga, D. Berényi: **Fast Multicharged Ion Induced Satellite Auger Electron Angular Distribution**, 11th International Conference on the Application of Accelerators in Research and Industry, Denton, Texas, USA, 5-8 Nov. 1990.
25. B. Sulik, I. Török, A. Ágoston, I. Kádár: **The Intensity Distribution of Ion-Induced K-Alpha Ln X-Ray Satellites and the Geometrical Model of Ionization**, (abstr.: Bull. Amer. Phys. Soc., 35 (1990). No. 8, p. 1712 Pa. 12), ibid.
26. T. Vajnai, L. Sarkadi, Á. Kövér, J. Végh: **Study of Line Shape of Auger Electrons Excited by Direct Ionization and Electron Capture**, ibid.
27. L. Végh, R.L. Becker: **Angular Correlation of an Auger Electron with a Photoelectron in the Direction of Linear Polarization**, (Book of Abstracts, D23) 15th International Conference on X-Ray and Inner-Shell Processes, Knoxville, Tennessee, USA, 9-13 July, 1990.
28. R.L. Becker, L. Végh, J.H. Macek: **Reflection Symmetry and Angular Correlations of Autoioniztion Electrons**, (Book of Abstracts, D12), ibid.
29. L. Végh, R.L. Becker, J.H. Macek: **Exchange Effect on the Angular Correlation Between Directly Ionized and Autoionized Electrons of the Same Energy**, (Book of Abstracts, D11), ibid.
30. T. Papp: **Multipólus keveredés atomi röntgenátmenetekben**, Fizikus Vándorgyűlés, Veszprém, 1989. aug. 25-27.

Materials Science and Analysis

1. L. Költő, M. Kis-Varga: **X-Ray Fluorescence Analysis of Bronze Objects from the Avar Age**, (abstr.: p. 144) International Symposium on Archaeometry. Heidelberg, 1-6 April 1990.
2. P. Mikecz, Gy. Tóth, F. Szelecsényi: **Comparison of Ion Exchange and Liquid Extraction Methods for Separation of Indium-111 Isotopes from Cadmium Target**, (abstr.: p. 67), 12th Radiochemical Conference, Mariánské Lázné, Czechoslovakia, 7-11 May, 1990.
3. I. Csige, J. Hakl, I. Hunyadi, M. Tóth-Szilágyi, L. Nádor: **The Effect of Track Registration Properties of Cr-39 on Quantitative Element Analysis in Autoradiography**, (abstr.: a/3) XVII International Symposium on Autoradiography - ISA'90, Karpacz, Poland, 23-28 April, 1990.
4. S.K. Biswas, Zs. Fülöp, A.Z. Kiss, E. Koltay, E. Somorjai: **Application of PIGE Method for the Determination of Sodium and Boron in Aerosol Samples**, International Conference on Application of Nuclear Techniques, Crete, Greece, 24-30 June, 1990.
5. S. Mészáros, K. Vad, G. Halász, N. Hegman, G. Katona: **Current Conduction and Macroscopic Quantum Interference in Bi-Sr-Ca-Cu-O Screen Printed Films**, LT19 Satellite Conference on High Temperature Superconductivity, Cambridge, Anglia, 13-15 Aug. 1990.
6. S. Bohátka, H. Deng: **The Influence of Water Activity on Enzyme Reactions in Organic Media**, (abstr.: p. 242), 5th European Congress on Biotechnology, Copenhagen, Denmark, 8-13 July, 1990.
7. O. Dragun, V. Brabec, A. Kovalik, M. Fiser, J. Novák, M. Rysavy, V.M. Gorozhankin, TS. Vylov, V.G. Chumin, K.YA. Gromov, L. Kövér, I. Cserny, V.V. Zashkvara, B.U. Ashimbaeva: **High-Resolution Spectroscopy of Low-Energy Electrons Emitted in Nuclear Transformation**, 8th International Conference of Hyperfine Interactions, Prague, Czechoslovakia, 14-19 Aug. 1989.
8. F. Tárkányi, L. Andó, F. Szelecsényi, F. Ditrói, S. Takács, A. Fenyvesi, T. Molnár, I. Mahunka: **The Use of the Debrecen Cyclotron for Applied Research and Practice**, Conference on Methods of Production of Cyclotron Radioisotopes for Medical Purposes, Debrecen, Hungary, 8-12 Oct. 1990.
9. L. Kövér: **Novel Methods for Calibration of Electron Spectrometers**, Quantitative Surface Analysis. Sixth International Conference. London, 13-16 Nov. 1990.
10. T. Gesztelyi, I. Borbély-Kiss, Fülöp, A.Z. Kiss, E. Koltay, Gy. Szabó: **Late Roman Glass Sealings and Their Measurement by X- and Gamma-Rays**, European Workshop, "Technology and Analysis of Ancient Gemstones". Ravello, Italy. 9-12 Dec. 1990.
11. S.K. Biswas, I. Borbély-Kiss, U.M. El-Ghawi, E. Koltay, Gy. Szabó: **On the Applicability of PIXE Microanalysis at 10 MeV Bombarding Energies**, International Conference on Application of Nuclear Techniques, Crete, Greece, 24-30 June, 1990.
12. Á. Kovách: **Fizikai módszerek a régészetben**, XXXIII. Országos fizikatanári ankét, Eger, 1990. ápr. 6.

Earth and Cosmic Sciences, Environmental Research

1. J. Hakl, I. Hunyadi, L. Lénárt, G. Géczy, I. Csige: **Ten Years Systematic Radon Observations by SSNTD in Hungary**, Rabotsego soveshchaniya "tverdotel'nye trekovye detektory yader i ikh primeneniya", Dubna, USSR, 6-8 Febr., 1990.
2. Á. Kovách, É. Svingor: **Alacsony fokú metamorf folyamatok Rb-Sr kormeghatározása**, Izotópgeokémiai szeminárium (MFT-DAB), Debrecen, 1990. április 2.
3. T. Hámor, E. Hertelendi: **A pannóniai dolomitok béta ^{18}O és béta ^{13}C valamint a magyarországi üledékes piritek béta ^{34}S méréseinek előzetes eredményei**, ibid.
4. L. Mikó, L. Marton, E. Hertelendi: **Szennyeződés leszivárgási lehetőségek vizsgálata izotóphidrogeológiai módszerekkel a debreceni vízművek hatásterületén**, ibid.
5. I. Vető, E. Hertelendi: **A tardi agyag kerogen- és karbonát-tartalmának szén- és oxigénizotóparányai, és környezeti következtetések**, ibid.
6. E. Hertelendi: **Műszerek és módszerek könnyűelemek stabilizotóp eltolódás mérésére valamint radiokarbon kormeghatározására**, ibid.
7. P. Sümegi, Gy. Szöőr, E. Hertelendi: **Alföldi quarter üledékek kronosztatigráfiai és paleoklimatográfiai rekonstrukciója**, ibid.
8. Z. Pécskay, M. Kozák, V. Székyné-Fux, J. Andó: **K/Ar koradatok és földtani értelmezésük ÉK-Kuba területéről származó kőzetmintákon**, ibid.
9. K. Balogh, P. Árkai: **Kőzetek hőtörténetének vizsgálata K-Ar módszerrel: Elméleti alapok és kísérleti eredmények medencebelseji képződményekben**, ibid.
10. K. Balogh: **A nemesgázizotópanalitika lehetőségei a szénhidrogén és vízkutatásban**, ibid.
11. G.P. Guertzen, A.M. Marennyj, R.A. Nymmik, I. Hunyadi, I. Csige, F. Spurny, J. Charvat, L. Just, D. Hasegan: **Predvaritel'nye rezul'taty izmerenij plotnosti potoka tyazhelykh ionov kosmicheskikh luchej na biosputnike "Kosmos-2044"**, (abstr.: p. 48), XXIII Soveshchanie postoyanno dejstvuyushchej rabochej gruppy po kosmicheskoj biologii i meditsine programmy interkosmos, Kosice, Czechoslovakia, 20-26 05. 1990.
12. A.M. Marennyj, G.P. Guertzen, I. Hunyadi, I. Csige, J. Charvat, B. Kopecka: **Predvaritel'nye rezultaty izmerenij flyuensov protonov i tyazhelykh yader ki na sputnike "Kosmos-2044"**, (abstr.: pp. 114-115), ibid.
13. I. Hunyadi, I. Csige, J. Charvat, F. Spurny, G.P. Guertzen, A.M. Marennyj: **Programma rondo - issledovanie vremennogo raspredeleniya zaryazhennykh chastits kosmicheskogo izlucheniya pri pomoshchi passivnykh detektorov.**, (abstr.: p. 195), ibid.
14. I. Csige, I. Hunyadi, G.P. Guertzen, A.M. Marenny: **A Bioszputnyik–9-en nyomdetektorokkal végzett kozmikus ionsugárzás mérésének eredményei**, (A MÉT LV. Vándorgyűlésének előadásai és poszter kivonatai p. 31), A Magyar Élettani Társaság LV. Vándorgyűlése, Budapest, 1990. július 4-6.

15. T. Hámor, Ralish-Felgenhauer, E. Hertelendi: **Early Diagenitic Ferrodolomites in the Upper Miocene of the Pannonian Basin**, 13th International Seclimentological Congress, Nottingham, England, 26-31 Aug. 1990.
16. I. Csige, G.P. Guertzen, J. Charvat, I. Hunyadi, A.M. Marenny, R.A. Nymmik, F. Spurny: **Spectra of Cosmic Ray Heavy Ions Board Cosmos-2044 Satellite**, 15th International Conference on Particle Tracks in Solids, Marburg, FRG, 3-7 Sept. 1990.
17. I. Csige, I. Hunyadi, J. Charvat: **Environmental Effects on Induction Time and Sensitivity of Different Types of Cr-39**, ibid.
18. J. Hakl, I. Hunyadi, M. Tóth-Szilágyi: **Radon Permeability of Foils Measured by SSNTD Technique (non equilibrium approach)**, ibid.
19. L. Medveczky, J. Hakl, A. Fenyvesi, T. Molnár: **Fast Neutron Radiation Field Measurements in a Water Phantom**, ibid.
20. I. Hunyadi, J. Hakl, L. Lénárt, G. Géczy, I. Csige: **Regular Subsurface Radon Measurements in Hungarian Karstic Regions**, ibid.
21. V. Knezevic, Székyné-Fux, R. Steiger, Z. Pécskay, S. Karamata: **Petrology of Fruska Gora Latites-Volcanic Precursors at the Southern Margin of the Pannonian Basin**, Geodynamic Evolution of the Pannonian Basin, Beograd, Yugoslavia, 19. Oct. 1990.
22. Székyné-Fux, Z. Pécskay: **Covered Neogene Volcanic Rocks at the Eastern and Northern Areas of the Pannonian Basin, Hungary**, ibid.
23. V. Székyné-Fux, Cs. Ravasz, Z. Pécskay: **Tertiary Volcanism of the Pannonian Basin**, ibid.
24. L. Lénárt, J. Hakl, I. Hunyadi: **Barlangi vizek természetes eredetű radon break szintjének vizsgálata**, IV. Fejér megyei környezetvédelmi szeminárium, Székesfehérvár, Magyaro. 1990. okt. 15-17.
25. A. Várhegyi, I. Baranyi, J. Hakl: **Az új radonmigrációs elmélet alkalmazhatósága jelenkori geodinamikai események folyamatos vizsgálatára**, XIX. Geofizikai Vándorgyűlés. Pécs, Magyaro., 1990. máj. 24-25.

Biological and Medical Research

1. A.V. Bakulin, A.S. Rakhmanov, I. Uzonyi, J. Bacsó: **Svyaz' mezhdu makro- i mikro-elementami v sherstnym i kostnym obraztsak obez'yan v eksperimente gipokinezii (abstr.:pp.11-12)**, XXIII Soveshchanie postoyanno dejstvuyushchej rabochej gruppy po kosmicheskoj biologii i meditsine programmy interkosmos, Kosice, Czechoslovakia, 20-26 May 1990.
3. F. Szelecsényi, Z. Kovács, F. Tárkányi, Gy. Tóth: **Production of ^{110}In for PET Investigation via Cd(^{3}He,xn)^{110}Sn-^{110}In Reaction with Low Energy Cyclotron**, (abstr.: Princeton University, Princeton, New Jersey, pp. 95-96), Eighth International Symposium on Radiopharmaceutical Chemistry, Princeton, USA, 24-29 June, 1990.
4. A.V. Bakulin, A.S. Rachmanov, I. Uzonyi, J. Bacsó: **Nyomelemek közötti kapcsolat vizsgálata hypokineziás és normál körülmények között tartott majmok szőr és csontmintáiban**, (A MÉT LV. Vándorgyűlésének előadás és poszter kivonatai, p. 9.), A Magyar Élettani Társaság LV. Vándorgyűlése, Budapest, 1990. július 4-6.
5. P. Mikecz, Gy. Tóth, F. Szelecsényi: **Separation of Indium-111 from Cadmium Target**, VIIIth International Symposium on Nuclear Chemistry, Radiochemistry and Radiation Chemistry, Toluca, Mexico, 9-13 July, 1990.
6. F. Tárkányi: **Excitation Functions and Yields Relevant to Radioisotope**, Conference on Methods of Production of Cyclotron Radioisotopes for Medical Purposes, Debrecen, Hungary, 8-12 Oct. 1990.
7. F. Tárkányi, L. Andó, F. Szelecsényi, F. Ditrói, S. Takács, A. Fenyvesi, T. Molnár, I. Mahunka: **The Use of the Debrecen Cyclotron for Applied Research and Practice**, ibid.
8. F. Szelecsényi, F. Tárkányi, Z. Kovács, Gy. Tóth: **Production of ^{110}In for Medical Purposes**, ibid.
9. P. Mikecz, Gy. Tóth, Z. Szűcs, L. Sarkadi, Z. Kovács: **Recent Developments in the ATOMKI Radiochemistry**, Methods of Production of Cyclotron Radioisotopes for Medical Purposes, Debrecen, Hungary, 8-12 Oct. 1990.
10. P. Mikecz: **Vegyületek és prekurzorok előállítása PET-tel történő vizsgálatokhoz**, Pozitron emissziós tomográfia (PET) és orvosi kutatási alkalmazásai, Debrecen, 1990. dec. 12.
11. F. Tárkányi: **Pozitron emittáló izotópok előállítása a debreceni ciklotronon**, ibid.
12. A.M. Dám, M. Rétlaki, L.G. Gazsó, A. Fenyvesi, T. Molnár, I. Mahunka: **Measurement of Oer and Rbe for P (18MeV)+Be Fast Neutrons**, Seventh Tihany Symposium on Radiation Chemistry, Balatonszéplak, Magyarország, 1990. szept. 9-14.
13. J. Kispéter, L. Horváth, I. Borbély-Kiss, L. Kiss: **The Investigation of Milk Power and Milk Protein as a Function of Additional Iron Concentration and Ionizing Gamma Radiation by Physical Methods**, (abstr.: Biophysics for the 90's p.523) 10th International Biophysics Congress, Vancouver, Canada, 29 July - 3 August 1990.

Development of Instruments and Methods

1. I. Csige, I. Hunyadi, J. Charvat: **Alpha Response of Cr-39 in Vacuum and Aair**, Rabotsego soveshchaniya "tverdotel'nye trekovye detektory yader i ikh primeneniya", Dubna, USSR, 6-8 Febr. 1990.
2. E. Hertelendi, P. Márton: **Fizikai módszerek a régészetben**, (abstr. p.29), XV. Sugárvédelmi továbbképző tanfolyam, Balatonkenese, 1990. május 2-4.
3. I. Csige, I. Hunyadi, J. Hakl: **Cr-39 nyomdetektoros személyi radon dozimméter fejlesztése**, (abstr.: p. 10), ibid.
4. K. Jansson, P. Carlson, C. Fuglisang, K. John-And, A. Kerek, S. Szilágyi: **Comparison of Physics Data with Monte-Carlo Calculation in the CPLEAR Experiment**, CPLEAR Collaboration Meeting No. 27, Paris, France, 19-21 March, 1990.
5. C. Fuglisang, P. Carlson, K. Jansson, John-And, A. Kerek, S. Szilágyi: **Status Report of the PID in the CPLEAR Experiment**, ibid.
6. S. Szilágyi, *et al.*: **The Detector Technics Used at the CPLEAR Experiment**, Stockholm Physics Days'88, Stockholm, Sweden, 12-16 Sept. 1988.
7. P. Mikecz, Gy. Tóth, F. Szelecsényi: **Separation of Indium-111 from Cadmium Target**, VIIIth International Symposium on Nuclear Chemistry, Radiochemistry and Radiation Chemistry, Toluca, Mexico, 9-13 July, 1990.
8. S. Bohátka, H. Deng: **The Influence of Water Activity on Enzyme Reactions in Organic Media** (abstr.: p. 242), 5th European Congress on Biotechnology, Copenhagen, Denmark, 8-13 July, 1990.
9. F. Lauritsen, S. Bohátka, H. Deng: **A Simple Tandem Mass Spectrometer for On-Line Process Control of Fermentors**, (abstr.: p. 315), ibid.
10. S. Bohátka: **Mass Spectrometer System for Monitoring Fermentation Processes**, 1st All-Union Workshop on Mass-Spectrometric Monitoring of Fermentation Processes. Puschino, Soviet Union, 22-26 Oct. 1990.
11. L. Kövér: **Novel Methods for Calibration of Electron Spectrometers**, Novel Methods for Calibration of Electron Spectrometers, Quantitative Surface Analysis, Sixth International Conference. London, 13-16 Nov. 1990.
12. S. Bohátka, S. Fekete, I. Futó, I. Gál, J. Gál, G. Langer, A. Paál, G. Pintér, M. Simon, J. Szádai, G. Székely: **Fermentation Monitoring and Control with Quadrupole Mass Spectrometer**, 2nd International Symposium on Applications of Analytical Techniques to Industrial Process Contrl. Noordwijkerhout, Holland. 3-5 April, 1990.
13. A. Valek: **Beszámoló az ATOMKI ciklotron laboratóriumának munkájáról**, (abstr. ATOMKI, Debrecen, 1990. p. 40.) X. Magyar Magfizikus Találkozó, Sárospatak, Magyaro. 1990. aug. 21-24.
14. K. Turek, J. Bednar, G. Dajkó, F. Spurny: **Study of Parameters Including the Internal Heating Effect During Electrochemical Etching at Room Temperature**, 15th International Conference on Particle Tracks in Solids, Marburg, FRG, 3-7 Sept. 1990.
15. A. Várhegyi, I. Baranyi, J. Hakl: **Az új radonmigrációs elmélet alkalmazhatósága jelenkori geodinamikai események folyamatos vizsgálatára**, XIX. Geofizikai Vándorgyűlés, Pécs, Magyaro., 1990. máj. 24-25.

16. G. Dajkó: **Nekotorye osobennosti travleniya detektora Cr-39 Na komnatnoj temperature**, T'erdotel'nye trekovye detektory, yader i ikh primeneniya, Dubna, SSSR, 6-8 Fevr. 1990.

17. Z. Kormány, A. Valek: **Recent Developments at the MGC of the ATOMKI**, Trudy xi vsesoyuznogo soceshchaniya po uskoritelyam zaryazhennykh chastic, Dubna, 25-27 Okt. 1988. D9-89-52. Red. B.B. Kolesova, E.V. Ivashkevich, Dubna, 1989. Akademiya Nauk SSSR, Gos. Komitet po Ispol'z. Atomnoj Energii, SSSR, OIYAI, **2** 359 (1989)

Theses Completed

DOCTORAL DEGREES:

A. Fenyvesi, **Neuton Sources at the MGC-20 Cyclotron and their Applications**, (in Hungarian); supervisor: I. Mahunka.

G. Halász, **Study of Current Conduction Properties of high-T_c Superconductors**, (in Hungarian); supervisor: S. Mészáros.

G. Lévai, **Study of Exactly Solvable Potentials Using the Methods of Supersymmetric Quantum Mechanics**, (in Hungarian); supervisor: J. Cseh.

DIPLOMA WORKS:

J. Dominguez, **Calculation and Measurement of the Stopping Power of Foils**, (in Hungarian); supervisor Á. Z. Kiss.

M. K. Mácsainé Tóth, **Lead Contamination and its Environmental Effects**, (in Hungarian); supervisors: I. Gaál, J. Bacsó.

Hebdomadal Seminars

January 11
Perspectives of the Technical Park
L. Szabó, I. Molnár

January 18
Anomalous internal conversion coefficients in high multipole orders
Zs. Németh, Isotope Institute, Budapest

January 25
Superdeformation and shape-coexistence in nucleus ^{152}Dy
B. Nyakó

February 1
Science policy in Hungary now and in the future
K. Balázs, Sociology Institute, Budapest

February 8
Neutron sources at the MGC-20 cyclotron and their applications
A. Fenyvesi

February 15
(n,t) cross sections in discrete and diverse neutron fields
S. Sudár, Kossuth University, Debrecen

February 22
Low energy charged particle induced reactions on ligth targets
J. Szabó, Kossuth University, Debrecen

March 22
(n,2n) reactions on ^{238}U, ^{232}Th and ^{237}Np nuclei
P. Raics, Kossuth University, Debrecen

March 29
Investigation of exactly solvable potential problems by methods of supersymmetric quantum mechanics
G. Lévai

April 4
The task and perspectives of the institute
D. Berényi

April 19
Modernization of the cyclotron controll system
A. Valek

April 25
Possibility of ECR ion source developments and applications at the institute
J. Pálinkás, T. Fényes, F. Tárkányi, L. Zolnai, S. Biri, A. Valek

April 26
Heavy-ion source in an MGC cyclotron
S. Biri, A. Valek

May 9
Ion traps
J. Pálinkás

May 17
Quark atoms, quarkchemistry
I. T. Lentei, Kossuth University, Debrecen

May 24
Hadronization of quark-gluon plasma
Z. Árvay, T. Csörgő, J. Zimányi, Central Research Institute for Physics, Budapest

May 31
Low energy alpha scattering
Z. Máthé

June 7
Microscopic study of nucleus-nucleus interaction
H. Horiuchi

June 12
Science policy questions
D. Berényi, R. Lovas

June 20
Computer codes for electron and X-ray spectrum analysis
J. Végh

June 27
Heavy-ion projects in Dubna for 1990-1995
T. Fényes

September 6
Symbolic programming (REDUCE, LISP) for cluster-model calculations
A. Kruppa

September 12
Conductive properties of weak-coupling superconductive junctions
S. Mészáros

September 13
Conductive properties of high-temperature superconductive materials
G. Halász

September 27
Production and application of medical radionuclides
G. Stöcklin

October 3
Trace elements in atmospheric aerosols
E. Koltay

October 10
Quadrupole mass spectrometer analysis of gases dissolved in liquids
G. Langer

October 11
40 years in Oak Ridge
F. Kertész, Oak Ridge National Laboratory

October 17
Development of research instruments
D. Varga

October 25
Economic status of the institute
D. Berényi and M. Józsa

November 7
Galaxy distribution in Universe
S. A. Szalay, Eötvös University, Budapest

November 8
Computer controlled quadrupole mass spectrometer system
I. Szabó

November 15
Instruments and methods for isotope analytics
E. Hertelendi

November 22
Possibility of heavy-ion beam acceleration at the institute
J. Pálinkás, E. Somorjai

November 29
Six new methods for determination of counting loss using different number of radiactive sources
Cs. Újhelyi

December 6
Investigation of low energy nuclear reaction with solid state nuclear track detectors
I. Hunyadi

December 20
Solid state nuclear track detectors in space- and radon dosimetry
I. Csige

Author Index

Allart *K. 15
Amemiya *S. 77,79
André *S. 29
Andó L. 14, 100
Agoston A. 61
Arva-Sós E. 90

-

Bacsó J. 95
Bakulin *A.V. 95
Balogh K. 90
Barci*V. 29
Bartha L. 128
Berényi D. 49, 51
Bergman*J. 5
Béres*Cs. 8
Bibók Gy. 123
Biswas*S.K. 79, 82, 110
Blokhin*S.M. 59
Bohátka S. 97
Bonsignori*G. 15
Borbély-Kis I. 77, 79, 81, 110
Bucurescu*D. 29
Burgdörfer*J. 69

-

Cata-Danil*G. 29
Curien*D. 29
Curutchet*P. 30

-

Csatlós M. 112
Cseh J. 40, 42, 44
Cserny I. 71, 117
Csige I. 121
Csótó A. 33

-

Ditrói F. 75
Dombrádi Zs. 16, 17, 19, 23, 25, 27

-

El-Ghawi*U.M. 110

-

Fekete S. 97
Fenyvesi A. 8, 99, 109
Fényes T. 12, 16, 17, 19, 23, 25, 27
Foin*F. 29
Fülöp Zs. 3, 81, 82

-

Gácsi Z. 15, 16, 17
Gál I. 97
Gál J. 97, 123
Genevey*J. 29
Gesztelyi*T. 81
Gizon*A. 29
Gizon*J. 29
Gömöri*J. 88
Gulyás J. 19,21
Gulyás L. 49,69

-

Hakl J. 84,109
Halász G. 73
Hegman N. 73
Hertelendi E. 86,92
Hildingsson*L. 29
Hock G. 63,65
Horváth F. 86
Hunyadi I. 84,121

-

Julin*R. 12,21
Jurney*E. T. 15

-

Kahane*S. 15
Kato*K. 40
Katoh*T. 77,79
Katona G. 73
Kavanagh*R. W. 1
Kádár I. 51,61,67
Keinonen*J. 3
Kibédi T. 19
Kiss Á. Z. 5, 102
Kiss L. 97
Kis-Varga M. 88
Klamra*W. 29
Koltay E. 77,79,81,82,110,128
Kopeczky*P. 7,14
Kovács P. 125
Kovács Z. 5,102

Kövér Á. 49,57
Kövér L. 71,117
Krasznahorkay A. 10,12
Kruppa A. T. 33
Kumpulainen*J. 12,21
-
Lakatos T. 105,125
Langer G. 97
Lévai G 37,40,44
Lindbad*Th. 107
Liotta*R. J. 30,35
Lovas R. G. 33,35
-
Mahunka I 5,75,99,100
Marton*L. 92
Máthé G. 119
Medveczky L. 109
Merdinger*J. C. 29
Mészáros*E. 77
Mészáros S. 73
Mikecz P. 7,14,100,102
Mikó*L. 92
Molnár J. 103
Molnár*N. 77
Molnár*T. 8,99,109
Montemayor*V. C. 67
-
Nagy A. 128
-
Nyakó B. M. 29
-
Oganov*V. S. 95
-
Paar*V. 16
Paál A. 103,107,114
Pál K. F. 33
Pálinkás J 51,59
Papp T. 51,59
Pethukov*V. 59
Pécskay Z. 90
-
Quang T. X. 10,12
-
Rachmanov*A. S. 95
Raman*S. 15
Ricz S. 51,53,55,67
Rolfs*C. 1
Rosengärd*U. 107
Rydl*A. 14
-
Sa*J. 15
Sarkadi L. 53,57,59
Schiwietz*G. 67
Schröder*U. 1
Schulte*W. H. 1
Sepsy K. 97
Seuthe S. 1
Shriner*J. F. jr. 15
Simon M. 112
Solin*O. 5
Somorjai E. 1,3,82,128
Stolterfoht*N. 67
Sulik B. 51,53,55,59,61,67,103
Suvorov*I. A. 100
-
Szabó I. 97
Szabó Gy. 49,69,77,79,81,110,128
Szádai J. 97,114,125
Székely G. 107,114,125
Szelecsényi F. 7,8,14,101,102
Szűcs Z. 8,101
-
Takada*N. 55
Takács E. 51,53,55,59
Takács S. 75
Tárkányi F. 5,7,8,14
Tcheltsov*N. 100
Tikkanen*P. 3
Tímár J. 10,12
Tóth B. 51
Tóth*Gy. 14
Tóth J. 71,117
Tóth L. 53,55
Tóth-Szilágyi M. 84
Török I. 51,53,55,59
Tőkési K. 55,63,65,71,117
Trajber Cs. 97,112
Trautwetter*H. P. 1
-
Uzonyi I. 95

Vad K. 73
Vajnai*T. 49,57
Valek A. 127
Varga D. 71,117
Varga*M. 77
Varga K. 33,35
Vasváry L. 75
Vatai E. 46
Végh J. 51,57
Vertse T. 30,35

-

Walkiewicz*T. A. 15
Weil*J. L. 15

-

Zolnai L. 29

(* denotes author from other establishment)

Kiadja a
Magyar Tudományos Akadémia Atommag Kutató Intézete
A kiadásért és szerkesztésért felelős
Dr. Pálinkás József, az Intézet igazgatója
Készült a Bogáti vállalkozás nyomdájában
Törzsszám: 51786
Debrecen, 1991. március.